ADDIS ABABA UNIVERSITY

ADDIS ABABA INSTITUTE OF TECHNOLOGY

SCHOOL OF CIVIL AND ENVIROMENTAL ENGINERING

LAKE TANA VOLUME MONITORING BY INTEGRATING *In-situ* AND SATELLITE DATA

A Thesis Submitted To the Graduate School of Addis Ababa University in Partial Fulfillment of the Requirements for the Degree of Master of Science in Geodesy and Geomatics (Specialization in Geodesy)

Prepared by

Sintayehu Abie

Advisor

Tulu Besha Bedada (Ass. Prof.)

November 2018

ADDIS ABABA UNIVERSITY

ADDIS ABABA INSTITUTE OF TECHNOLOGY

SCHOOL OF CIVIL AND ENVIRONMENTAL ENGINEERING

LAKE TANA VOLUME MONITORING BY INTEGRATING *In-situ* AND SATELLITE DATA

BY

SINTAYEHU ABIE

November 2018

Approved by board of examiners:

____________________	____________________	____________________
Advisor	Signature	Date
____________________	____________________	____________________
Internal Examiner	Signature	Date
____________________	____________________	____________________
External Examiner	Signature	Date
____________________	____________________	____________________
School dean	signature	Date

DECLARATION

I, the undersigned, declare that this thesis work is my original work carried out under the supervision of Ass. Prof. Tulu Besha Bedada. It has not been presented for a degree in any other universities and all sources of materials used for the thesis work have been properly acknowledged.

____________________	____________________	____________________
Name	Signature	Date

Place: Addis Ababa

ACKNOWLEDGEMENT

First of all, I express my greatest gratitude to God; no success would have been achieved without his grace and mercy.

I would like to express my sincerest gratitude to my great advisor Ass. Prof. Tulu Besha Bedada for his valuable guidance, help and encouragement during the progress of this thesis. He was the one encourage me to work on this title. I enjoyed working with him, because of not only his encyclopedic knowledge and his brilliant works on Chaos Theory but also for a far greater matter, his humble personality, which I tried to learn from and the passion he gave me and his wonderful data analysis course where I learned critical thinking.

My deepest appreciation extended to Mr. Andenet Ashagrie (Phd candidate at Entoto Observatory and Research Center), Dr. Berhan Gessesse (staff at Entoto Observatory and Research Center), Mr. Eshetu Setegn (Phd candidate at Entoto observatory and Research Center) and Dr. Ing. Elias Lewi (staff at Addis Ababa University IGSSA) for their depth constructive critics, encouragement and support throughout my lecture and in the progress of the thesis.

I am indebted to Ministry of Water, Irrigation and Electricity, Abay Basin authority deeply thank for their material and idea support.

My deepest appreciation extended to my friends and classmates who have been very cooperative and supportive with different materials and ideas.

Last, but definitely not least, I would like to heartily and deeply thank my greatest parents, my mom, my beloved brothers; Abewa Abie, Alemu Abie and my sister Hana Atersaw for bearing with me in all the ups and downs in my chaotic life and for their continuous love, patience, presence, and support which mean the world to me. I am nothing without you.

Sintayehu Abie

November 2018

ABSTRACT

Lakes are integrator of environmental changes occurring at a regional to global scale and present a high variety of behaviors on a variety of time scale. In addition, their crucial importance as water stocks and retaining given the significant environmental changes occurring worldwide at many anthropocentric levels has increased the necessity of monitoring all its morphodynamic characteristics i.e. water level, surface area and volume. In this thesis, we used satellite altimetry data from Jason and TOPEX to analyze fluctuation in water level of Lake Tana. Our analysis also combined optical satellite imagery and satellite altimetry to determine the volume fluctuation of the lake. The use of GRACE gravity data makes it possible to determine local water storage changes and to assess the water budget on monthly to multi-annual time scales. The Mann-Kendall trend tests, Sen Slope estimate and simple linear regression were utilized to detect trends in annual and seasonal extremes. Altimetry data showed insignificant positive trend detected during the entire study period (1960 to 2017). The water level of the lake has been increasing at a rate of 0.00574m/year. The lake exhibited insignificant increasing trend during summer and significant positive trend during winter, spring and autumn. Water level variations as the eco-hydrological indicator of the lake are compared for the two periods of natural and anthropogenically intervened .i.e. 1960 to 1996 and 1997 to 2017. The result of Mann-Kendall trend test shows that there is a unique insignificant increasing trend of about 0.00243m/year in average during the recent period of 1960 to 1996 and decreasing trend of about 0. 00225m/year during the period 1997 to 2017. Moreover, combined analysis of altimetry and remotely sensed satellite imageries indicated insignificant increasing trend in the volume of the Lake Tana for the period spanning from 1984 to 2017. However, the volume of the lake has been decreasing at an alarming rate of 0.612 km^3/year starting from the year 2012 to the present. From alarmingly low value for the remaining water volume in the lake, the lake will completely disappear within twelve thousands of years if no countermeasures are taken. Geo-observatory products such as the GRACE can provide an accurate estimate of changes in total terrestrial water storage at a coarser, regional resolution. The change in storage fluctuation of the 15-year monthly data, from 2002 to 2016 of the Lake Tana sub Basin reveals total water storage of the basin has declined by 0.0375mm of equivalent water thickness. a correlation coefficient of 0.73 and 0.75 is observed between the GRACE estimates TWSC and lake volume change and TWSC and rainfall respectively.

Keywords: Satellite altimetry, Mann Kendell test, Sen Slope estimate, Tana basin.

CONTENTS

LIST OF TABLES

LIST OF FIGURES

ABBRIVATIONS

ANN	Artificial Neural Network
CSR	Center for Space Research
DEM	Digital Elevation Model
DLR	Germany Eurospace Center
ECMWF	European Center for Medium Weather Forecast
ETM+	Enhanced Thematic mapper plus
FEWS-NET	Famine Early Warning System Network
GPS	Global Positioning System
GLEAM	Global Land surface Evaporation from Amsterdam Metrology
GRACE	Gravity Recovery And Climate Experiment
ISDC	Integrated System Data Center
JPL	Jet Proposal Laboratory
MIR	Middle Infrared
MK	Mann Kendall
MNDWI	Modified Normalized Differential Water Index
MoWIE	Ministry of Water Irrigation and Electricity
MSS	Multi Spectral Sensor
NASA	National Aeronautic
NCEP	National Center for Environmental Prediction
NDWI	Normalized Differential Water Index
NIR	Near Infra-Red
RMSE	Root Mean Square Error
SLC	Scan Line Error
SVM	Support Vector Machine
TFPW	Trend Free Pre Whitening
TS	Theil Slope
TWS	Total Water Storage
USA	United States of America
USDA-FAS	U.S. Department of Agriculture's Foreign Agriculture Service
WLALL	Water Level Above Lowest Level
WMO	World Metrology Organization
WVALL	Water Volume Above Lowest Level

CHAPTER ONE: INTRODUCTION

1.1. Background

Terrestrial water is critical to sustaining life on Earth and it contribute to a global water cycle. Terrestrial water is usually stored in rivers, lakes, manmade reservoirs, wetlands, and episodically inundated areas. It interact with the ocean and atmosphere through evaporation and surface runoff (Papa et al., 2008). Assessing spatio-temporal variation of water resources is important for sustainable water resource management practice (Anteneh et al., 2017).

This study focuses on spatio-temporal variation of Lake Tana water level and hydrological mass variability within its sub basin. Lake Tana has significant ecological service and socioeconomic benefit (Chebud et al., 2012). It is a source of Blue Nile Water head (Yirgalem et al., 2009) and widely used for agriculture, serving over 2 million population residing within the basin (Chebud et al., 2012). Some studies indicated that decline in wells productivity and stream discharges within the Lake Tana catchment due to over exploitation of ground water (Anteneh et al., 2017). Historical records showed the variation of Lake water level as a function of hydrological alterations within its basin (Yirgalem et al., 2009).

Soil moisture and groundwater storage showed a declining trend as recovered from time varying GRACE gravity data (Anteneh et al., 2017). However, the water level of the lake is observed to be less sensitive to variation in rainfall (Kebede et al., 2005). While Deganovsky et al. (2008) observed cyclic pattern of lake level fluctuation in response to climate change with a repeat period of 11 years. Seasonal variability of 1.6m in the lake water level detected from combined analysis of satellite altimetry and remote sensing data until the period 2013 (Duan et al., 2013). Beside, Chebud et al., (2013) showed that the lake water level has decreased in 1972, 1984, 2002/2003 and has increased in 1987. Temporal variations of Lake water level did not well matched with variation of El Nia (1972, 2002, 1978) and La Nina (1984).

The hydrological balance of the lake was also simulated by Wale (2009), giving emphasis on the contribution of ungauged catchment on the water balance of the lake. Nigatu (2016) has investigated the impact of climate change on the hydrological water mass balance of the basin. Different methodologies were also used to quantify the water mass balance of the lake Tana (Yirgalem et al., 2008, 2009; Rientjes et al., 2011; Duan et al., 2013; Tegegne et al., 2013; Duan et al., 2014; Dessie et al., 2014).

Recently, Studies also used similar method to estimate water mass balance of the surface water in large river basins such as the Negro river basin (Frappart et al., 2005) and Syrdarya river basin (Cretaux et al., 2014). Few studies attempted to derive water volume variations in lakes and reservoirs using the combination of satellite altimetry and imagery data. Duan et al., (2013) estimated water volume variations in Lake Mead (U.S.A.), Lake Tana (Ethiopia) and Lake IJssel (The Netherlands) from four operational satellite altimetry databases and satellite imagery data. Baup et al. (2013) employed satellite altimetry and remote sensing to estimate volume fluctuation of small lakes in France. Tourianet et al. (2014) uses satellite altimetry and satellite imagery data to monitor the desiccation of Lake Urmia in Iran. Muala et al. (2014) drive Estimation of Reservoir Discharges from Lake Nasser and Roseires Reservoir in the Nile Basin Using Satellite Altimetry and Imagery Data. Zhu et al. (2014) applied satellite altimetry and ICESAT altimetry data to monitor volume fluctuation of Lake Qinghai. Gao et al. (2012) computed water storage changes in five large lakes of the USA using altimetry water levels and remotely sensed surface areas. Sichangi et al. (2017) estimated volume variation of Lake Victoria using bathymetric map and remote sensing data. Zhang et al. (2011) estimated the Water level variation of Lake Qinghai from satellite and in-situ measurements. All of these studies demonstrated the capabilities of satellite radar altimeters and passive and active microwave sensors to monitor river and lake level and its extent.

Moreover, the GRACE satellite gravimetry has been used in combination with satellite altimetry and optical imagery data to study the water volume variations in the very large inland water bodies e.g. Lake Victoria (Swenson, 2009), Ganges basin in India (Khan et al., 2012), Poyang Lake Basin (Zhou, 2016). However, the characteristics of GRACE restrict its meaningful application to study areas not smaller than 200,000 km^2 (Duan et al., 2013). Which is a big limitation for hydrological study of many lakes and reservoirs with relatively smaller surface areas.

This research unique due to, it is conducted during the emerging of natural and artificial problems in the area expected having an impact on the water balance of the lake and its catchment. Moreover, there is no any coordinated method to control the water balance of the lake. Therefore, this research quantify the existing water balance of the lake and surrounding area and also proposes a new method for estimating water volume changes in lakes and catchment. Despite our growing knowledge regarding the quantity of the lake water, studying long-term temporal variability of water mass balance of the lake is important for exploring new scientific thoughts as well as help for effective water management.

1.2. Statement of the problem

Most accessible water resource available for human consumption and the ecosystem are contained in lakes and rivers. These water bodies corresponds to 0.27% of the global fresh water and only 0.008% of the earth water budget (Ayana, 2007). Being a scarce resource strained by competing demands it has become crucial to develop robust, consistent and reliable method of water management infrastructures for effectively monitor the water balance.

However, Lake Tana suffer different problems in the present context. Water hyacinth is a serious problem in the water balance of lake and the surrounding catchment (Asmare et al., 2016, Tewabe et al., 2016). The lake and its catchment also expose to clearing of wetland, canalization of tributaries, toxigenic cyano bacteria, improper damming, construction of buildings in the Lake Shore areas and poor waste management problems (Goshu et al., 2017). The sediment inflow towards the lake increase from time to time (Moges et al., 2016). Climate change is the other problem (Asmare et al., 2016). Because the health of the lake affects so many people, the ability to routinely observe the lake and make those observations publically available is important. Hence, any information that would be relevant to water resources study is scarce. Due to lack of information on how the water system behaves, the use of the resources is based on traditional methods. This calls for an urgent understanding of the water reserve in the area. Therefore, reliable information derived from emerging technology options, such as remote sensing products in combination with ground based measurements, is mandatory to evaluate and understand the water quantity and spatiotemporal distribution of the lake.

Therefore, the outcome of this research provides a clear input to understand water level trend of lake Tana like previous studies done on Urmia Lake (Khatami, 2013), lake Orta (Saidi, 2015), quantify the volume fluctuation of the lake like studies done on lake La Bure (Baup et al., 2014), Lake Nasser (Ebaid et al., 2017). It also analysis of TWS change of Lake Tana sub basin from a free available satellite mission called GRACE.

1.3. Objectives of the research

1.3.1. Main objective

Lake Tana is an important asset for both Ethiopia and the downstream countries. It is essential to understand long-term spatio-temporal variation of the water balance of the lake and its catchment in order to derive policy briefs that could be used for future water resource management options. Therefore, the general objective of the thesis is to analyze the morphodynamic characteristics of the lake and surrounding catchment.

1.3.2. Specific objectives

This research has the following specific objectives:

- ✓ To characterize temporal trend of lake water level fluctuation.
- ✓ To analyze trend in volume fluctuation of the lake.
- ✓ To analyze the correlation between lake water balance with mass flux of the entire Tana basin.

1.4. Scope of the study

The following study was conducted in the Lake Tana and the Lake Tana sub Basin. The study has been carried out to determine and analyze the mean monthly, seasonal and annual water level trend of Lake Tana. It also proposed to evaluate a method that combines operational satellite altimetry databases with satellite imagery data to estimate water volume variations in lakes Lake Tana and to correlate with mass flux of the entire Tana.

1.5. Significant of the study

The results of this study could provide information on the status and dynamics of the water balance of Lake Tana, which used as an input for government policy makers, stakeholders, natural resources managers, environmental experts and other concerned bodies for their decision-making processes related to sustainable management and utilization of the resource. It also shows the capabilities of satellite radar altimeters and passive and active microwave sensors to monitor the morphodynamic characteristics of water bodies. In addition to this, it can be a reference or initial step and use as input for coming researchers based on the analysis of the study.

1.6. Thesis structure

The study is organized in to six chapters. The first chapter concerned on introduction part of the study that contains background of the study, problem statement, objectives to be achieved in the thesis and significance and scope of the thesis are discussed. The second chapter is literature review on application of space-based techniques (satellite altimetry, remote sensing and GRACE) in for lake water resources monitoring. The third chapter describes the study area such as geographic settings, topography, climate, geological setting, socio-economic situation of the lake and the land-use soil types of the study area. In the fourth chapter, materials, research design and method used in the research are discussed. Chapter fifth presents results and discussion of the study. The sixth chapter highlights the main conclusion of the study and points out future recommendations.

CHAPTER TWO: LITRACTURE REVIEW

2.1. Introduction

Water management will become even more relevant in the future as urbanization, industrialization, and climate change exert greater pressures on water use (OECD, 2012). Water resources can be monitored on a global scale using three approaches: in situ measurements, modelling and remote-sensing observations (Baup et al, 2014). Measuring water stages by remote sensing and especially by satellite has become a major goal in hydrology for the coming decades.

Comprehensive monitoring of surface resources also requires knowledge of the extent of the surface water and the water volume. Previous studies combined satellite observations of either water level or extent with bathymetry or in situ measurements of water storage to determine the water volume variations of lakes and inland seas.

Water balance components of lakes are the direct rainfall over the lake surface, inflow from the gauged rivers, inflow from unmonitored rivers, outflow from the lake, lake evaporation and the change in water balance or the closure term. Ideally, in-situ measurements of each water balance component should provide a complete understanding of inflow, storage changes and outflow of a lake. In reality, I) direct measurements are not performed at all; II) in-situ data are incomplete and inadequate to represent the areal average values over a lake and surrounding catchments (e.g. precipitation); (iii) data are of poor quality; (iv) data are available but are not shared with the public.

A robust, consistent and reliable method of water quantity measurement infrastructure is required to effectively monitor the spatial and temporal variation of surface water resources. Since the mid-eighties a decline of hydrological stations can be observed in many developing countries mainly due to political and institutional instability as well as economic problems to support adequate networks (Dost, et al., 2006).

2.2. Satellite Altimetry

The first satellite altimeter to be launched was GEOS-III in 1975, followed in 1978 by Seasat. The first use of satellite altimetry for hydrology was with GEOSAT launched in 1985. However, thanks to substantial progress in orbit determination from geodetic systems such as Doris, the use of GPS and laser started with the launch of the US/French TOPEX/Poseidon (T/P) satellite in 1992 (J.-F. Cre´taux1, R. Abarca-del-Rı´o, et al, 2016).

Since 1993, the satellite altimetry data have been used to monitor the water level variations of many large inland water bodies including wetland zones, reservoirs, lakes and river channels. The U.S. Department of Agriculture's Foreign Agricultural Service (USDA-FAS) in co-operation with the National Aeronautics and Space Administration and the University of Maryland has been monitoring the water height variations of 75 major lakes worldwide[1]. The time series of water level variations in the largest lakes (such as the Laurentian Great Lakes, Lakes Victoria and Tanganyika in Africa) are expected to have the accuracy better than 10 cm in terms of the root-mean-square (RMS). Smaller lakes (such as Lake Chad) or those that experience more sheltered conditions are typically less accurate with the expected RMS of better than 20 cm (Kaba, 2007).

Satellite altimetry measure the time required for pulse to travel from the satellite antenna to the earth surface and back to the satellite receiver. The time required by the microwave to illuminat

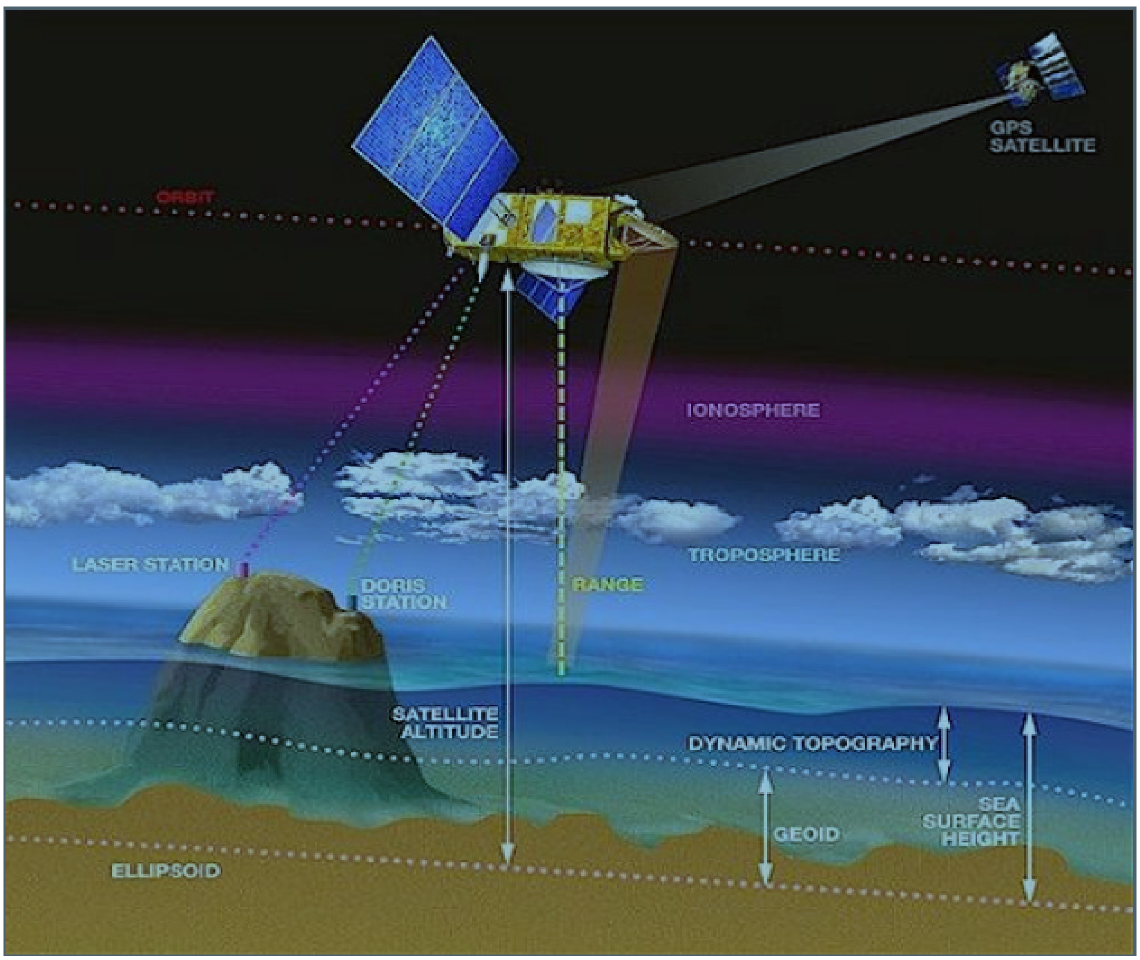

Figure 2.1: working principle of altimetry sea level measurement (modified from Kaba, 2007, Msc thesis)

[1] *http://www.pecad.fas.usda.gov/cropexplorer/global_reservoir*

a target and reflect back to the receiver antenna used to calculate the range. The speed of electromagnetic wave multiplied by half of the total time gives the range from the satellite to the ocean surface. An important quality of radar altimetry therefore is its accuracy with which it measures range. The limit of the range resolution of a radar system defined as the ability to distinguish in time the return pulse from two idealized point targets (Coe et al., 2004).

Microwave pulses are sent to the nadir of the satellite at a frequency of about 1 kHz. These pulses reflected on the ground (water, land…) and part of the transmitted signal goes back towards the satellite. The shape and arrival time of the returned signal gives information about the characteristics of the reflecting surface.

The difficulty of measuring surface topography is a combination of knowing exactly where the instrument is at the time of the measurement and being able to characterize all the other variables that influence the delay time of the echo. Therefore, various correction have to be applied before using the altimetry data.

Orbital determination: The accurate determination of ocean height is made by first characterizing the precise height of the spacecraft above the center of the earth. This achieve through a technique called precise orbital determination(POD) and basically involves satellite tracking information.

Sea-state bias: Sea state effect are an intrinsic property of the large footprint radar measurements. Ocean waves crests scatter the radar waves outward away from nadir while the troughs of the waves focus the energy back toward radar. Characteristics of the sea state bias are depend on significant wave height and wave age. The SWH is the average of the one third highest wave valid for the intended 12 month period. Wave height vary seasonally and hence can easily introduce a 5-10cm bias (Rees, 2005). The shift referred to as the electromagnetic bias, causes the altimetry to overestimate the range (Rosmorduc et al., 2006).

Atmospheric effect: The earth atmosphere exhibit considerable variability and consequence affects microwave signal accordingly. In the troposphere that extend from the surface of the earth to a height of about 6km the north pole or the south pole and 18 km at the equator temperature decrease rapidly with altitude and hence much turbulence because of variations in temperature, density and pressure. Moreover, clouds form in the region of the earth atmosphere. These conditions have a greater effect on the propagation of radar waves.

Inverse barometer effect: This is the effect caused by variation in atmospheric pressure at sea surface height. An increase in atmospheric pressure cause a depression of the sea surface, a phenomenon refers to as the inverse barometer effect. The instantaneous inverse barometer effect on sea surface height is computed from the surface atmospheric pressure.

Instrumental error: There are error due to a drift in oscillator onboard the satellite, shift in satellite center of gravity (due to a fuel consumption, solar panel orientation and other factors) and filters applied to eliminate certain frequencies in the return radar signal.

2.3. Trends in water level

In addition to long-term, climate-driven fluctuations or trend, three other types of fluctuations in lake levels can be distinguished. The first type is a short period fluctuation caused by precipitation associated with extreme storms that can last from a few hours to a few days. The second type is a regular seasonal fluctuation from summer and spring highs to winter and autumn lows specific to Lake Tana. The third type is the fluctuation that results from artificial regulation of lake levels by control works at the outflow dam. The seasonal and inter-annual fluctuations of lake level are a normal and essential component of the Lake Tana basin hydrological cycle (Saidi et al., 2015).

A number of statistical tests are available to identify and quantify monotonic trends in a way that is defensible and repeatable. The tests are further divided in to parametric, nonparametric and mixed types. Parametric tests are considered more powerful and/or sensitive to detect significant trends than nonparametric tests, especially with a small sample number. However, unless the assumption of normal distribution for parametric statistics is met (Meals et al., 2011).

Parametric test: The parametric test is the hypothesis test, which provides generalizations for making statements about the mean of the parent population. The t-statistic rests on the underlying assumption that there is the normal distribution of variable and the mean in known or assumed to be known. The population variance is calculated for the sample. It is assumed that the variables of interest, in the population are measured on an interval scale.

Non-parametric test: hypothesis test which is not based on underlying assumptions, i.e. it does not require population's distribution to be denoted by specific parameters. The test is mainly based on differences in medians. Hence, it is alternately known as the distribution-free test. The test assumes that the variables are measured on a nominal or ordinal level. It is used when the independent variables are non-metric.

2.3.1. Mann–Kendall (MK) trend test

The Mann–Kendall (MK), commonly known as the Kendall's tau statistic, is a non-parametric test used for trend analysis. Mann (1945) first used this test and Kendall (1975) derived the test statistic distribution. The test has been suggested by the World Meteorological Organization (WMO) to assess trends in environmental data time series (Rustum et al., 2017) as the test is suitable for cases where the trend may be assumed monotonic and therefore no seasonal aspects are presented in the data. A major advantage of the Mann-Kendall test is that:

- It is not a presupposition method in terms of data distribution i.e. there are no necessary assumptions about the data distribution as the prerequisite of this method known as nonparametric method. Therefore, there is no uncertainty associated with the data distribution.
- It is directly applicable to climate data for a given month or season.

The Mann-Kendall, as a hypothesis test, is a nonparametric, rank-based. The data is ranked according to measurement epoch in order to evaluate the presence of trends in time series data. The MK test has been widely used to test stationary statistics against trend statistics in hydrology and climatology. This test evaluates whether y values tend to increase or decrease over time through what is essentially a nonparametric form of monotonic trend regression analysis. The Mann-Kendall test analyzes the sign of the difference between later-measured data and earlier-measured data. A serious problem in detecting and evaluating trends in hydrological data is the effect of serial dependence. If an autocorrelation exists in a time series, the MK test tends to reject the null hypothesis of no trend more often than the specified level of significance (Zelenáková et al., 2017).

2.4. Remote sensing

Remote sensing is a technique to observe the earth surface or the atmosphere from out of space using satellites (space borne) or from the air using aircrafts (airborne). Remote sensing uses a part or several parts of the electromagnetic spectrum. It records the electromagnetic energy reflected or emitted by the earth's surface. The amount of radiation from an object (called radiance) is influenced by both the properties of the object and the radiation hitting the object (irradiance). The human eyes register the solar light reflected by these objects and our brains interpret the colors, the grey tones and intensity variations.

Remote sensing imagery has many applications in mapping land-use and cover, agriculture, soils mapping, forestry, city planning, archaeological investigations, military observation, and geomorphological surveying, land cover changes, deforestation, vegetation dynamics, water quality dynamics, urban growth, etc. Digital image analysis is usually conducted using raster data structure-each image is treated as an array of values. It offers advantages for manipulation of pixel values by image processing system, as it is easy to find and locate pixels and their values.

Resolution is an important term commonly used to describe remotely sensed imagery. There are four distinct types of resolution. These are spatial, spectral, radiometric, and temporal. These resolution characteristics help to describe the functionality of both remote sensing sensors and remotely sensed data (ERDAS Field Guide, 2002).

Spatial resolution: is the measure of the smallest object that can be resolved by the sensor or the smallest area on the ground represented by each pixel. It tells the degree of detail of the earth surface feature recorded by the sensor. The finer the spatial resolution in remote sensing refers to imagery in which each pixel represents a small area on the ground and the detail the recorder. Small scale refers to imagery in which each pixel represents a large area on the ground.

Spectral resolution: refers to the specific wave length intervals in EM spectrum sensor can record. Wide intervals in the electromagnetic spectrum are referred to as coarse spectral resolution, and narrow intervals are referred to as fine spectral resolution.

Radiometric resolution: refers to the dynamic range, or number of possible data files value in each band. This is referred to by the number of bits into which the recorded energy is divided. The total intensity of the energy, from 0 to the maximum amount, the sensor measures is broken down, for example, into 256 brightness values for 8-bit data. The data file values range from 0, for no energy return, to 255, for maximum return, for each pixel.

Temporal resolution: is a measure of how often a given sensor system obtains imagery of a particular area, or how often an area can be revisited or the frequency at which satellite data is recorded about an earth surface feature. Temporal resolution is an important factor to consider in change detection studies.

2.4.1. Image processing

Image processing is a mathematical manipulation and interpretation applied on the pixel value and/or its geometry. Is broadly classified in to preprocessing and post-processing. Pre-processing operations, which are also called image restoration and rectification, are essential for prior to image classification and change detection analysis. It involves correction of sensor- and platform-specific radiometric and geometric distortions of data.

Radiometric corrections: removes errors related with variation of illumination and viewing geometry, atmospheric conditions, and sensor noise and response. Radiometric preprocessing influences the brightness values of an image to correct for sensor malfunction or to adjust the value to compensate for atmospheric degradation. Absolute radiometric calibration techniques require ground reflectance data and information about the sensor and atmosphere for the date of image acquisition, which are often difficult or impossible to obtain.

Geometric distortions: can be caused by several factors, including: the perspective of the sensor optics; the motion of the scanning system; the motion of the platform; the platform altitude and velocity; the terrain relief; and, the curvature and rotation of the Earth. The sources of geometric distortions are classified in two categories: Observer and Observed. Geometric corrections are intended to compensate for these distortions so that the geometric representation of the imagery will be as close as possible to the real world.

Image enhancement: is basically improving the interpretability or perception of information in images for human viewers and providing `better' input for other automated image processing techniques. The principal objective of image enhancement is to modify attributes of an image to make it more suitable for a given task and a specific observer. During this process, one or more attributes of the image are modified. The choice of attributes and the way they are modified are specific to a given task.

2.5. Integrating satellite image with radar altimetry

The ability of radar altimetry to measure lake level could further be extended by integrating it with satellite image. The relation between the three parameters, namely lake level, lake surface and lake storage volume is the basis to integrate information from satellite image in to altimetry measurements. The elevation-storage-area characteristics of a lake can be mathematically described using the bathymetric characteristics of the lake. Similarly, the surface area of the lake can be determined from satellite image using digital image processing methods.

The surface area of the lake from satellite imagery can thus be to calculate the lake level using the storage characteristics of the lake established from bathymetric survey. Once the accuracy of this method is validated using temporarily installed gauges it can be used to validate altimetry measurement based on lake surface area from satellite image that corresponds to the altimetry measurement. The potential use of this approach is to monitor lakes with little or no accessibility of gauging and even to fill data gaps in gauges lakes.

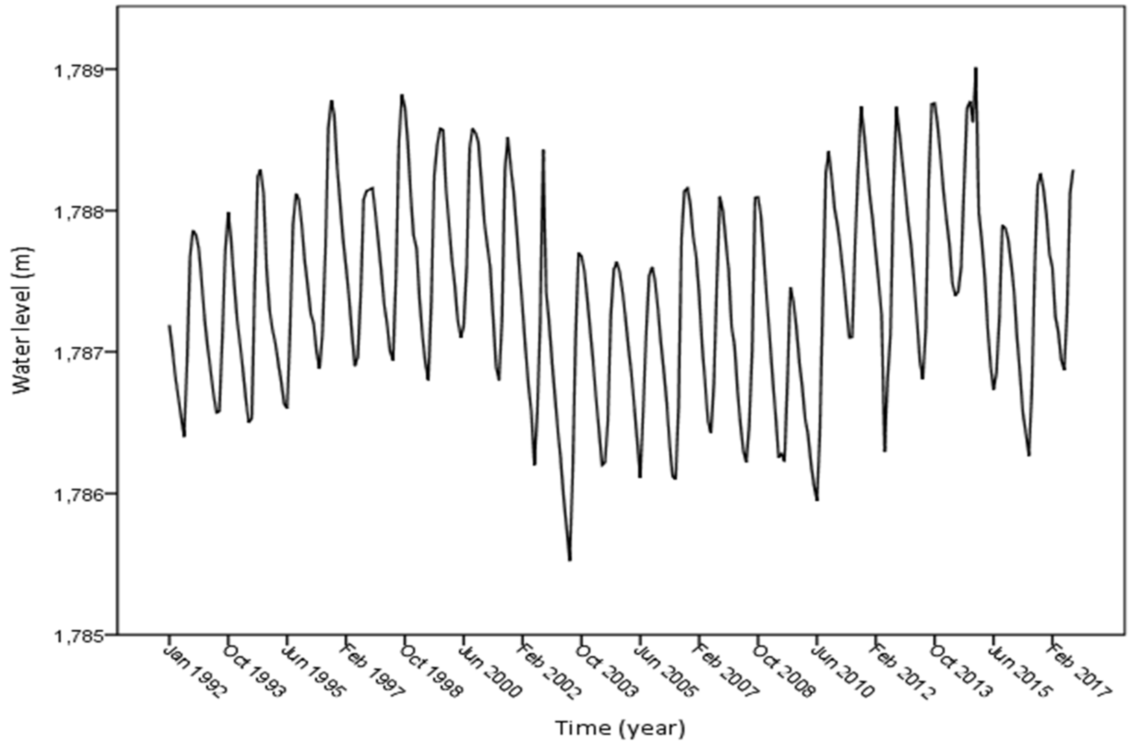

Figure 2.2: Lake Tana stage variation from historical 16-year average as measured (TOPEX and Jason Altimetry)

2.6. GRACE twin satellites

GRACE is a satellite mission jointly managed by the US National Aeronautics and Space Administration (NASA) and the German Aerospace Center (DLR). Its goal is to map Earth's gravity field with high precision, approximately on a monthly basis (Rodell et al., 2006). Although it was originally planned to be a 5 year mission it still runs today (2017). Obtained monthly observations of the Earth's gravity field which has a spatially correlated with water on the Earth's surface and in subsurface layers, allowing estimations of total water storage (TWS). TWS is the sum of all water stored in a GRACE cell regardless of how or where it is stored, i.e. surface water, soil water, groundwater and vegetation-bound water are all together in one TWS value (Andrew et al., 2017).

The primary objective of the GRACE mission is to obtain accurate estimates of the mean and time-variable components of the earth's gravity field variations. This objective is achieved by making continuous measurements of the change in distance between a twin spacecraft, co-orbiting at ~ 500 km altitude, in a near circular, polar orbit, spaced 220 km apart, using a microwave ranging system. In addition to this range change, the non-gravitational forces are measured on each satellite using a high-accuracy electrostatic, room-temperature accelerometer. The satellite orientation and position (and timing) are precisely measured using twin star cameras and a GPS receiver, respectively. Spatial and temporal variations in the earth's gravity field affect the orbits (or trajectories) of the twin spacecraft differently. These differences are manifested as changes in the distance between the spacecraft, as they orbit the earth. This change in distance is reflected in the time-of-flight of microwave signals transmitted and received nearly simultaneously between the two spacecraft. The change in this time of flight is continuously measured by tracking the phase of the microwave carrier signals. The so-called dual-one-way range change measurements can be reconstructed from these phase measurements. This range change (or its numerically inferred derivatives), along with other mission and ancillary data, is subsequently analyzed to extract the parameters of an earth gravity field model.

2.6.1. Terrestrial water storage estimation from GRACE

The changes in terrestrial water storage result in mass redistribution in the Earth's system, thereby causing changes in the gravity field. For a fixed continental region, the changes in water storage (including soil water and surface snow) come from rainfall, evapotranspiration, river transportation, and deep underground infiltration. Except the rainfall, which can cause increased water storage, the remaining three processes all reduce it (Jiang et al., 2014). The Earth's gravity field can be expressed as geoid:

$$N(\vartheta, \lambda) = a \sum_{n=0}^{\infty} \sum_{m=0}^{n} [\bar{C}_{nm}(m\lambda) + \bar{S}_{nm} sin(m\lambda)] \bar{P}_{nm}(cos\vartheta) \quad [2.1]$$

Where n and m are spherical harmonic degree and order of the gravity field, respectively; a is the Earth's equatorial radius (about 6,371 km); θ and λ are colatitudes (the difference between 90∘ and latitude) and longitude; C_{nm} and S_{nm} are spherical harmonic coefficients (dimensionless); P_{nm} is the normalized associated Legendre functions. The maximum value N of the order n of ideal gravity field should be infinite ($N \sim \infty$), while the actual order of spherical harmonic coefficients obtained by the gravity satellite has a finite value ($N < \infty$) and the spatial resolution of gravity field data is estimated approximately to be $\pi a/N$.

For ocean and atmosphere mass variations are removed based on Parallel Ocean Program (POP) model, the above equation is the basic equation for the retrieval of surface mass variations based on spatiotemporal changes gravity field. The Earth's surface density changes can be derived from the changes of gravity field coefficients obtained from GRACE satellites.

In this paper GRACE total water storage (TWS) data from The University of Texas Centre for Space Research (CSR)[2]. The model is already corrected for the influence of the lunar solar gravitational effect, atmospheric tide, pole tide, Earth tide and ocean tide and other effects. The terrestrial mass variations recovered from GRACE thus comprise mainly the hydrological signal, i.e. the TWS variations (Zhou et al., 2016).

2.6.2. Gaussian smoothing in the spectral domain

Spectral analysis has shown that the reliability of the GRACE spherical harmonic coefficients C_n^m and S_n^m decreases rapidly at larger degree, *n*, with some additional increase for larger order, *m*. Seo and Wilson (2005) have used the ratio of signal to signal plus noise variance at each degree and order, a least square optimum weight. However, their approach requires knowledge of both signal and noise variance at each degree and order, which both may only be known approximately. Han et al. (2005a) used non-isotropic weighting with Gaussian-type operators that suppress high order terms. This is effective, but not a well-defined optimization strategy. In this thesis, the noise has been suppressed with a smoothing filter but only an isotropic one.

For practical applications, it is better to suppress the noise by applying a filter that decreases smoothly to zero as *n* increases rather than truncating the spherical harmonic series at some particular degree. An appropriate filter is one that corresponds to convolving the space-domain gravity signal with a Gaussian curve. The smoothing increases as the Gaussian half width increases. In this thesis, the noise has been suppressed with Gaussian filtering that convolves a function $f(\theta,\lambda)$ with the filter $\mathcal{W}(\Psi)$. For plane geometry the Gaussian filter has the form

$$w(s) \propto \exp\frac{1}{2}(\frac{s}{\sigma})^2 \quad [2.2]$$

Where, s is the distance between two points and σ is area of the plane. Convolution is computationally slow but an equivalent operation is commonly done in the spectral domain because it corresponds to multiplication. The theory is well known for plane Cartesian

[2] *http://grace.csr.nasa.-gov/data/get-data/*

geometry, where multiplication of Fourier transforms has the same effect as convolution of space-domain data.

If the points are on a sphere at positions (θ, λ) and (θ', λ'), rather than on a plane, their separation is represented by the geocentric angle ψ given by

$$\cos(\psi) = sin\theta sin\theta' + cos\theta cos\theta' \cos(\lambda - \lambda') \quad [2.3]$$

Following Jekeli (1981), Wahr et al. (1998) give a spatial averaging filter appropriate to a spherical surface that has properties like a Gaussian function

$$w(\psi) = \frac{b\ \exp(-b(1-cos\psi)}{2\pi(1-e^{-2b})} \quad [2.4]$$

Where ψ to be an angle between 0 and π and,

$$b = \frac{ln2}{1-(\cos(r_{1/2}/R))} \quad [2.5]$$

The parameter R is the radius of the Earth and $r_{1/2}$ denotes the half width radius of the Gaussian averaging function that is when $\psi = r_{1/2}/R$, $w(\psi)$ has decreased to half its value at $\psi = 0$. The data are computed using models complete up to degree and order 120 derived by the CNES group.

Bedada, (2007) showed that a Gaussian half-width filter of 650 km can effectively eliminate or suppress ripple errors that contaminate the gravity signal with a north-south orientation. Filter of this size was used for further analysis.

CHAPTER THREE: STUDY AREA

3.1. General

The Lake Tana basin is a source of headwater for the Blue Nile and it has of prime importance to management of the Nile basin. Lake Tana is located in the north-western part of Ethiopia between latitudes 10°58` to 12°47`N and longitudes 36°45` to 38°14`E. It occupies a total drainage area of 15,077 km^2 of which the lake covers 3057.4km^2. Lake Tana is situated at approximately 1800m above mean sea level (Figure 3.5) with mean and maximum depths of 8 and 14 m respectively (Wale 2008). The lake is approximately 84 km long and 66 km wide (Zemede et al, 2017) and it is the largest lake in Ethiopia and the third largest in the Nile Basin. It serves as a temporary storage for the Blue Nile River flow. It is sourced by more than 40 rivers (Kebede, 2005).

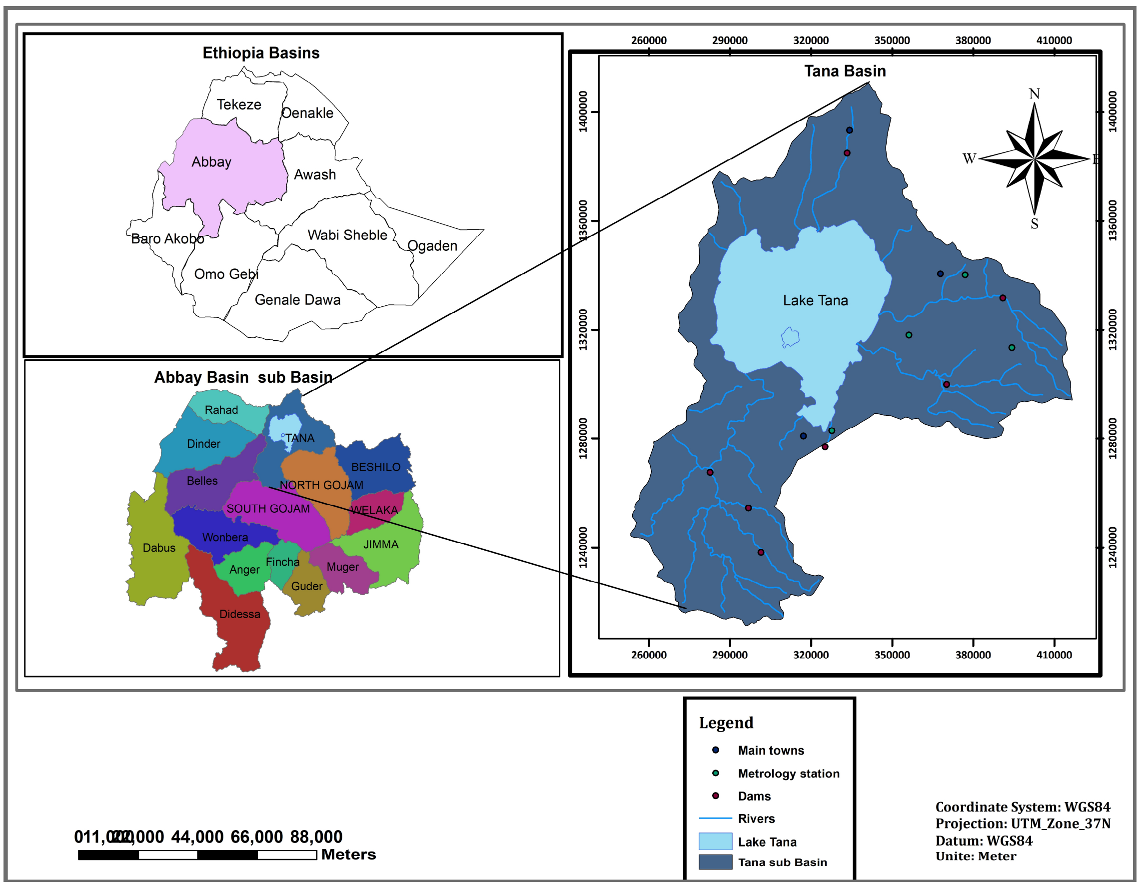

Figure 3.1: Location map of Lake Tana Basin

Major rivers producing the lion share of the annual inflow to the lake are Gilgel Abay from the south, Rib and Gumara from the east and Megech River from the north. According to Kebede et al. (2006), these four major rivers contribute 93% of the inflow and only 7% of the lake inflow is from ungauged catchments. The outflow from the lake is controlled manually by gates at the outlet to the Blue Nile (natural surface outflow at the southern shore) and at a tunnel hydropower outlet (Tana Beles) on the southwestern side of the lake. Wale (2008) report that, the lake water level fluctuates seasonally as a function of rainfall and evaporation. Its water level reaches maxima around September and minima around June. Historical records showed that the lake's water level has raised to maximum and minimum heights of 1788.02 m (September 21, 1998) and 1784.46 m (June 30, 2003) respectively. The lake's water level dropped in 2003 due to the establishment of the Chara Chara regulator weir at the lake’s only outlet. Further development of at least seven irrigation schemes with an overall water demand greater than 600 million m^3/year have been proposed (table 3.1) within the watershed of Lake Tana (Kebede et al, 2005).

Table3.1. Planned irrigation development in the Lake Tana catchment (Source*:* McCartney et al., 2010)

Irrigation schema	Irrigable area(ha)	Estimated annual gross water demand(Mm^3)	estimated net water demand(Mm^3)	Large dam Storage (Mm^3)	stage of development
Gilgal Abay B	12852	104-142	88-121	563	Feasibility study ongoing
Gumara A	14000	115	98	59.7	Feasibility study ongoing
Ribb	19925	172-220	146-187	233.7	Feasibility study ongoing
Megech	7300	63-98	54-83	181.9	Feasibility study ongoing
Jema^{++}	7800	57	48	173	Feasibility study ongoing
kogal	6000	62	52	78.5	Under construction
Northeast lake Tana	5745	50-62	43-53	Withdraw from the lake	Prefeasibility study completed
Northwest lake Tana	6720	54	46	Withdraw from the lake	Identified
Southwest lake Tana	5132	42	36	Withdraw from the lake	identification

3.2. Climate of Lake Tana

The climate of the study area is tropical highland monsoon with one rainy season between June and September. The air temperature shows large diurnal but small seasonal changes (Kebede, 2005). It reaches maximum in May and minimum in November (Figure 3.3). Due to its altitude, the highest temperature of the water surface is 21.7°C. The estimated annual precipitation of the lake basin ranges from 1200 to 1600mm with a maximum and minimum rain in July and February respectively (Figure 3.2). Potential evaporation varies between 1160 and 1900 mm per year (Konnerth 2016) and water yield of the catchment is 392mm (setegn, 2008; Zemede, 2013). Annual actual evapotranspiration is 773 mm for the entire basin and 1675 mm for the lake surface (Konnerth, 2016). The mean annual relative humidity (1961 to 2004) at Bahr Dar gauge station is 0.65 (Setegn, 2008).

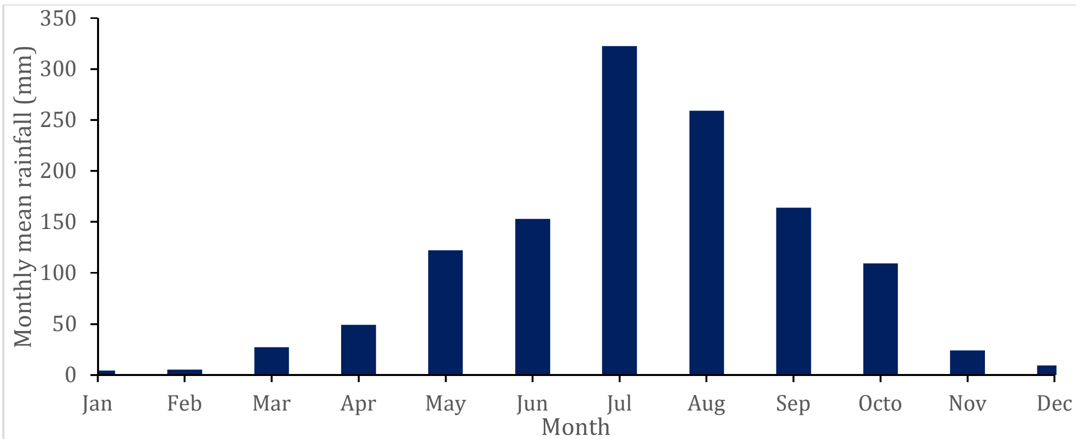

Figure 3.2: monthly average precipitation for Lake Tana at Adet gauge station (1986 to 2017)

3.3. Geology of Lake Tana

Lake Tana lies in a wide depression (graben) of the Ethiopian Plateau (Dessie et al., 2014). It was formed due to damming by lava flow during the Pliocene but the formation of the depression itself started in the Miocene (Kebede et al., 2005). The lake is shallow, oligotrophic

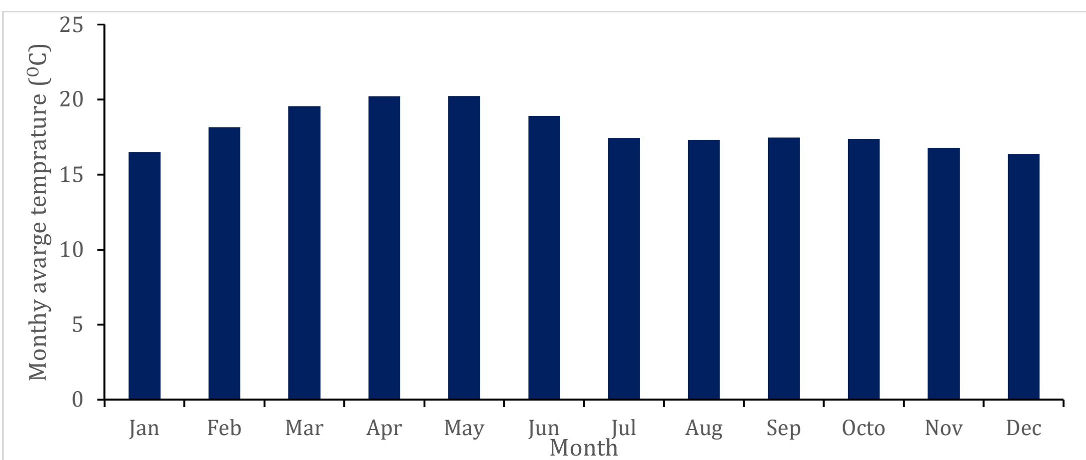

Figure 3.3: monthly average temperature for Lake Tana at Adet gauge station (1988 to 2017)

and fresh-water with weak seasonal stratification (Setegn, 2010). The lake is bordered by low plains (acting as floodplains) with mountain regions in the west and north-west. The largest area of the floodplain in the basin is located in the north and eastern parts of the basin (Zemede, 2013, Dessie et al., 2014). Because the lake is situated adjacent to the western topographic landmass steeply sloping downwards, its potential for electric power generation is evident. The increasing national demands for electricity would put more pressure on the lake water mass balance (Wale, 2008).

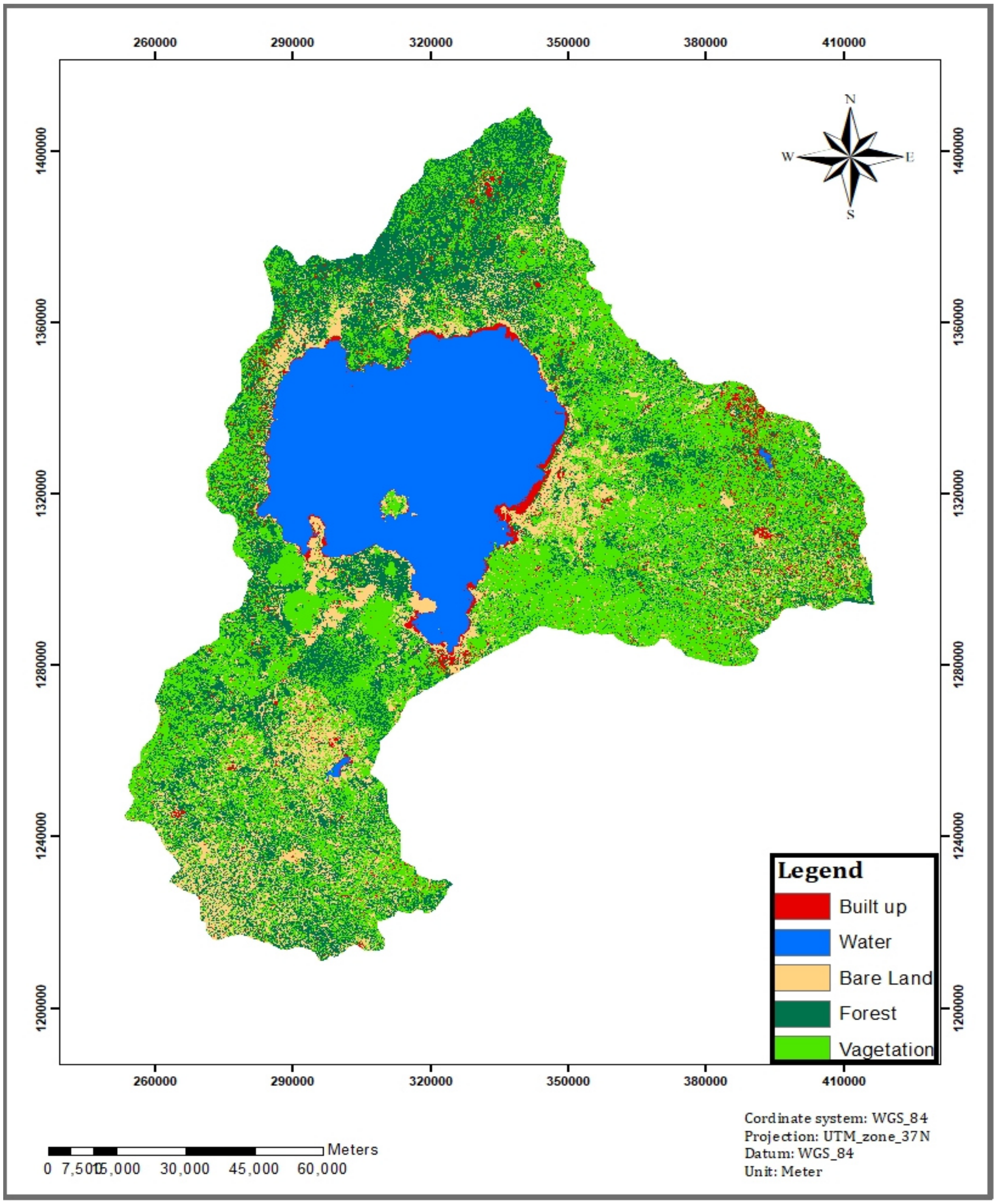

Figure 3.4: land use land cover map of Lake Tana Basin

3.4. Lake Tana sub Basin

Lake Tana basin is the second largest sub basin of the Blue Nile River basin and Lake Tana is the largest fresh water resource in Ethiopia. It is located within UTM zone 37 between 252788 and 396487m E longitudes and 1218577 and 1410176m N latitudes. The basin has an area of 15,077 km^2, of which Tana Lake occupies 3057.4 km^2.

Rugged mountainous volcanic terrain, moderate to gentle terrain in volcanic rocks with some isolated hills, escarpment and plain constitute the physiographic units of the area. Uniform and

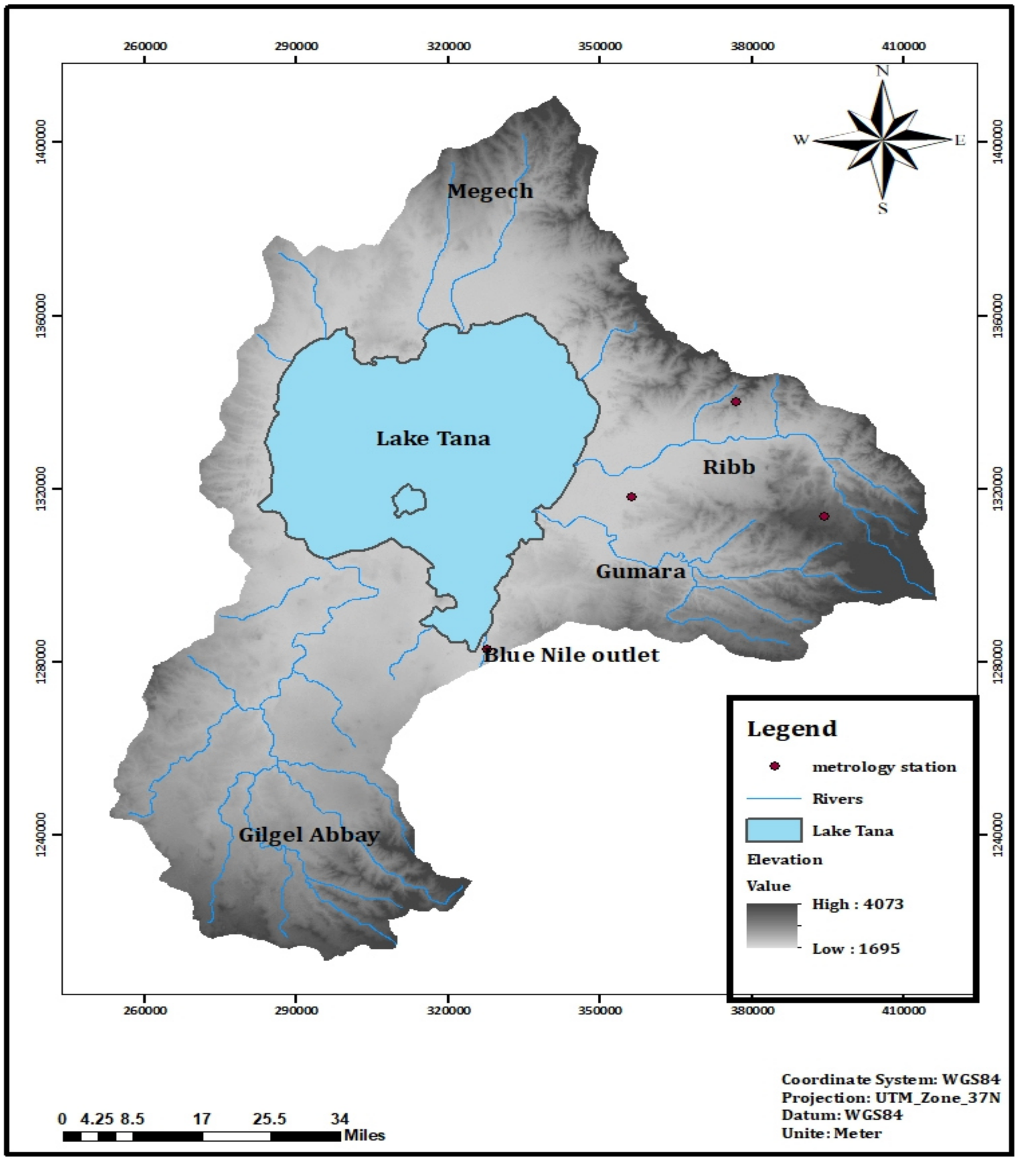

Figure 3.5: Location of major rivers, Metrological stations and elevation of Lake Tana basin

quite well adapted to irrigation development topography surrounds Lake Tana. The elevation ranges between 1695 m to 4073m above Mean Sea Level (Figure 3.5). There are two seasons; rainy and dry. The rainy season has two periods; the little rains, during April and May and the big rain, which last from mid to June to mid to September. In the basin, rainfall distribution has a mono-modal pattern i.e. one peak value observed during main rainy season.

The basin in its natural state has high potential for agriculture, livestock, water resource, forest and wildlife, tourism and fishery development besides too high biological diversity. There are animals, plants, fish, wet land and forest. The basin has also fertile soil and cultivable land for intensive agriculture. The agro-ecologies are also suitable to produce more than once per year.

3.5. Socio-economic factor of Lake Tana basin

Lake Tana basin is home to about 3 million people. Bahir Dar city is the largest urban landscape that is located in the basin with about 200,000 residents. Approximately, 15000 people live on the 37 islands in the lake (McCartney et al., 2010). Agriculture is the major economic activities in the Lake Tana Sub-Basin. The cropping pattern and crop diversification are well known practices in the basin. More than 80% of the cultivated land during the base year is under rainfed system and the remaining are cultivated using irrigation and residual moisture respectively. Recession farming, mainly maize and rice cultivation is carried out in the wetlands adjacent to the lakeshore (Awulachew et al., 2009). The lake is an important source of fish for the people around the lake and elsewhere in the country (McCartney et al., 2010).

In addition, Lake Tana basin is endowed with historical, cultural and natural heritages. The lake has become an important place among main tourist attraction sites in Ethiopia. About 30,000 people (both domestic and foreign) visit the area each year (Awulachew et al., 2009). The livelihood of more than five hundred thousand people directly or indirectly depends on the lake and adjacent wetlands.

The Lake Tana region has become the main priority area for water resource development (Danbara, 2014). The Lake Tana basin is of critical national significance as it has great potentials for irrigation, hydroelectric power, high value crops and livestock production; ecotourism and others (Setegn, 2010). It is rich in biodiversity with many endemic plant species and cattle breeds, it contains large area of wetlands, it is home to many endemic birds and cultural and archaeological sites.

3.6. Soil type of Lake Tana basin

Most of the Lake Tana catchment area is characterized by cropland with scarce woodland while only few limited areas of the highland are forested (1% of the catchment area). Figure 3.4 shows land cover types of Lake Tana basin (cf. MoWIE). The major land cover types are croplands (45.2%), woody savannah (18%), water (20.6%), grassland (13%), bar land (2%), forest (1%) and urban and built-up areas (0.2%).

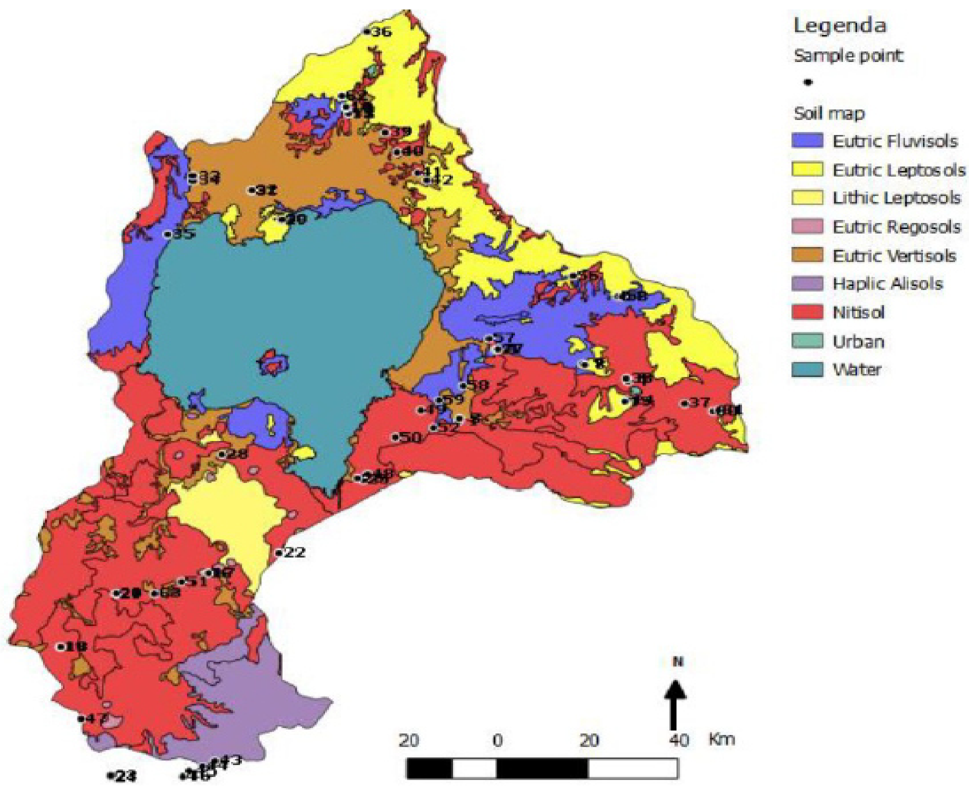

Figure 3.6: soil type map of Lake Tana basin (modified from Setegn (2008) by Miserez (2013)

The main soil types in the basin are Haplic Nitisols, Eutric Fluvisols, Eutric Leptosols, Eutric Vertisols, Haplic Alisols and Lithic Leptosols (Konnerth, 2016).

CHAPTER FOUR: METHOD AND MATERIALS

4.1. Data source

4.1.1. *In-situ* water level data

Lake level data from gauge stations should fulfill certain requirements. First, the gauge stations should be with in a very short distance from satellite ground track to help in minimizing measurement error due to location. Secondly, dates of gauge and altimetry measurement should match in order to make comparison. This is practically possible if the gauge data has higher temporal resolution than the altimetry satellite orbit's repeat cycle. For this study, daily measurement of lake Tana's water levels (from Bahir Dar station) were used for the period spanning from 1960 (January) to 2006 (December). This data was obtained from the Ministry of Ethiopia Minster of Water, Irrigation and Electricity.

4.1.2. Altimetry data

The primary aim of altimetry satellite missions is to map oceanic sea surface height. Altimetry satellites have also been used to detect water level changes in lakes and inland seas (Swenson et al., 2009). There are two ways of acquiring altimetry data. The first is a completely processed and corrected sea surface height anomaly which user can directly use for the intended application and the second one is unprocessed data altimetry height anomaly, which need preprocessing. ERS (ENVISAT), JASON-1 and TOPEX/POSEIDON (T/P) missions are the most common data sources that provide data on sea level anomalies, dynamic topography and surface wind speed.

Altimetry water level data are available for many large inland lakes from a global database. The United States Department of Agriculture/Foreign Agricultural Service (USDA/FAS) in cooperation with NASA and the University of Maryland prepares the GRLM database[3]. The database mainly utilizes data from T/P, Jason-1, Jason-2 and GFO and recent additional ENVISAT satellites to monitor time-series of water level variations for presently ~228 of the world's largest lakes and reservoirs in a near-real time manner (i.e. update on a weekly basis) for operational application. Currently GRLM provides a merger of T/P, Jason-1 and Jason-2 (TPJO.1 version) time-series relative water level variation with respect to the mean 9-year T/P level at 10-day intervals for 80 lakes/reservoirs including Lake Tana. For each lake/reservoir

[3] *http://www.pecad.fas.usda.gov/cropexplorer/global_reservoir/*

included in GRLM, there are two time-series of water level variations, i.e. the raw data and the smoothed data with a median type filter to eliminate outliers and reduce high frequency noise. However, smoothed data are only for visualization, they are not expected to be used for quantitative analysis. In this study, the raw data of TPJO.1 version including water levels and estimated errors for Lake Tana from GRLM has been used.

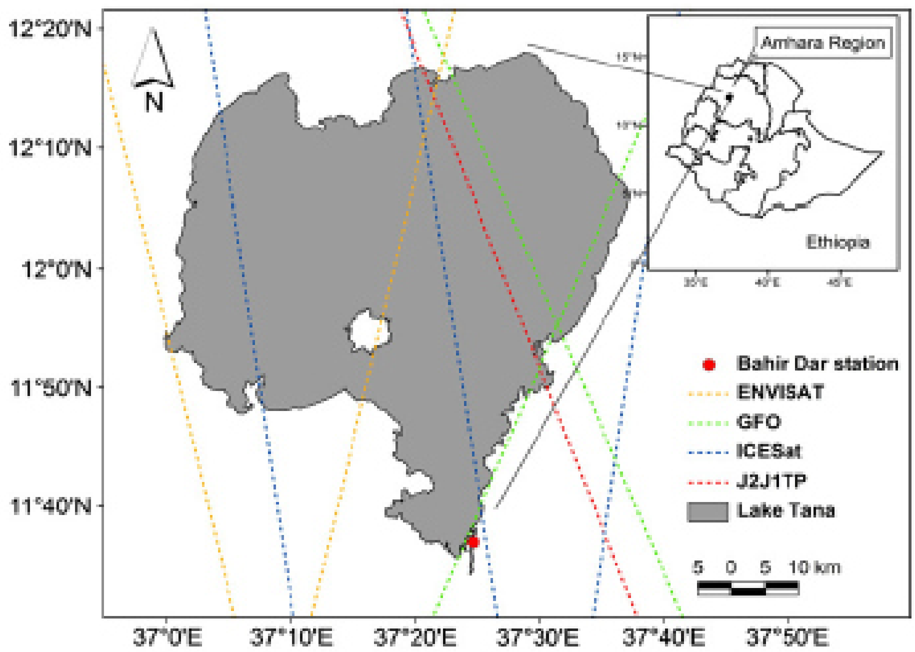

Figure 4.1: Location of Lake Tana gauge stations and ground tracks of satellite altimetry missions (modified from Duan et al., 2013)

4.1.3. Landsat TM/ETM$^+$ imagery

Time-series of Landsat TM/ETM+[4] data with spatial resolution of 30m were used to extract surface areas of lake Tana. The satellite imageries should coincide exactly with the dates of altimetry-derived water levels. However, most of the time this was not the case firstly because of the different crossover repeat cycles of Landsat (16-day) and altimeter satellites (10-campaign mode). Landsat TM/ETM+ imageries for the best 5 days before or after the dates of altimetry-derived water levels was used to derive water surface area corresponding to water level data.

[4] *http://glovis.usgs.gov*

4.1.4. GRACE data

Four processing centers, including the CNES[5], Center for Space Research (CSR), Austin, TX, Center for Space Research (CSR), Austin, TX, USA, GeoForschungsZentrum (GFZ), Potsdam, Germany, the Jet Propulsion Laboratory (JPL), Pasadena, CA, USA, and the Science Data Center (SDC) are in charge of the processing of the GRACE data and the production of Level-1 and Level-2 products. The GFZ's Integrated System Data Center (ISDC)[6] and the JPL's Physical Oceanography Distributive Active Data Center (PODAAC) distribute these products. Pre-processing of Level 1 GRACE data (*i.e*., positions and velocities measured by GPS, accelerometer data and KBR inter-satellite measurements) is routinely made by the SDC, as well as monthly global GRACE gravity solutions (Level 2). These latter solutions consist of time series of monthly averages of Stokes coefficients (*i.e*., dimensionless spherical harmonics coefficients of geopotential) developed up to a degree between 50 and 120 that are adjusted from along-track GRACE measurements. A dynamical approach, based on the Newtonian formulation of the satellite's equation of motion in an inertial reference frame, centered at the Earth's center, combined with dedicated modeling of the gravitational and non-conservative forces acting on the spacecraft, is used to compute the monthly GRACE solutions (Schmid et al, 2008). During the estimation process, atmospheric and ocean barometric redistribution of mass variations are removed from the GRACE coefficients using European Center for Medium-range Weather Forecasts (ECMWF) and National Centers for Environmental Prediction (NCEP) reanalysis for atmospheric mass variations and ocean tides, as well as global ocean circulation models. The GRACE coefficients are hence residuals that should represent mainly continental water storage, but also errors from the correction models and noise. The monthly GRACE solutions differ from one official provider to the other due to the differences in the data processing, the choice of the correction models and the data selection for computing the monthly average (Ramillien et al., 2014). This study has used GRACE data release from CNES as an input to estimate change in total water storage of Lake Tana Basin.

Therefore, by excluding the errors in gravity field model and the atmosphere and oceans models, GRACE time-varying gravity field reflects the non-atmospheric and non-ocean mass variations due to water mass variations on the continental area. On a seasonal or shorter time scale, it provides information on changes in terrestrial water storage in large river basin (Jiang et al., 2014).

[5] *http://grace.csr.nasa.-gov/data/get-data/*

[6] *http://isdc.gfz-potsdam.de*

Table 4.1: datasets used

variable	Dataset	version	resolution		Time period
			Spatial	Temporal	
Water level	TOPEX, Jason	-	5km	10day	1992 to 2017
Lake area	Landsat TM/ETM$^+$	-	30m x 30m	16day	1984 to 2017
In-situ water level	MoWIE	-	-	1day	1960 to 2006
Water storage ΔM	GRACE	RL03	-	1month	2002 to 2016
Precipitation	CHRIPS	2.0	0.05^0x0.05^0	1month	1981 to 2015

4.1.5. Satellite Precipitation data

Satellite rainfall data from the Climate Hazards group Infrared Precipitation with Stations (CHIRPS) was used for this study. CHIRPS was developed to support the United States Agency for International Development Famine Early Warning Systems Network (FEWS NET). It uses the Tropical Rainfall Measuring Mission Multi-satellite Precipitation Analysis version 7 (TMPA 3B42 v7) to calibrate global Cold Cloud Duration (CCD) rainfall estimates (Funk et al, 2015).

CHIRPS data is available from 6 hourly to 3 monthly aggregates. Almost all data has a 0.05° × 0.05° degree spatial resolution. CHIRPS data are provided in NetCDF, GeoTiff, and Esri BIL formats. The units are *mm* per time period, e.g., mm per day, mm per pentad, mm per month. Monthly rainfall estimates of CHIRPS-2.0 with spatial resolution of 0.05° × 0.05° was used for this study. The data covers time span from the 1981 to 2017[7].

4.2. Research design

In this study, qualitative data sets obtained from secondary data sources were used to achieve the required objectives. Some of these data sources are; space-borne data obtain from different satellite missions (Landsat image, satellite altimetry data, GRACE and CHIRPS data). Apart from the space-borne sources, we also used in-situ water level for a better analysis and interpretation of hydrological behavior over Lake Tana and Tana sub-basin. Table 1

7 *http://chg.geog.ucsb.edu/data/chirps/index.html for the year 1981 to 2017 products/CHIRPS-2.0"http://chg.geog.ucsb.edu/data/chirps/index.html for the year 1981-2017 products/CHIRPS-2.0.*

summarizes all datasets and sensors, which were used in this study. Different materials and software packages have been used for analyzing the data. Some of the software are: ERDAS imagine, GINS, GIS, matlab, ENVI etc. after analyzing those data sets by the above analysis tools, the results were presented in the form of table, figure and text.

4.3. Methodology

4.3.1. Analysis of water level variation of Lake Tana (1960 to 2017)

4.3.1.1. Principal Hypothesis & Assumptions

The principal hypothesis of this study is that 'during the recent years (1960 to 2017) there has been an intrinsic change in the dynamic of the lake water level mainly due to natural and anthropogenic activities, which has had deteriorating impacts on the lake. As it could be understood, there are 3 sub-hypotheses embedded; (1) there is a significant change in the water level of the lake for the entire study period (1960 to 2017) (hypothesis I) and (2) there is a seasonal and monthly trend in the water level of the lake (Hypothesis II) and (3) there is a uniquely significant change in the lake water level during the recent years (1997 to 2017) comparing to historical records (1960 to 1996) (Hypothesis III) The null hypothesis (H_O) is that there is no trend; each test has its own parameters for accepting or rejecting H_O. Failure to reject H_O does not prove that there is no trend, but indicates that the evidence is not sufficient to conclude with a specified level of confidence that a trend exists.

Because Lake Tana is a terminal lake, its water level can be seen as an eco-hydrological indicator and recorder reflecting the combination of all influencing factors. These factors influencing the lake water level could be categorized as natural (climate variability) and anthropogenic (e.g. dam construction, water diversion, climate change, groundwater withdrawals). Therefore, studying the lake water level fluctuations could be assumed reasonable approach in order to test the aforementioned hypotheses.

Having a 57-year daily water level time series, the period 1960 to 2017 of the lake water level fluctuations is divided into two distinct periods of 1960 to 1996 and 1997 to 2017. Such a division as another assumption of the principal hypothesis, is based on the facts that lake water level in this period is fluctuating quite distinctively from the period of 1996 to 2017 where there is an obvious declining trend in the water level. Moreover, a period of more than 30 years (1960 to 1996) is traditionally the standard period for climatic analysis as all possible climate variability could be seen in about 30 years (Khatami, 2013). Therefore, the first period, 1960 to 1996, period is assumed natural period of the lake. The period of 1996 to 2017 assumed the disturbed or anthropogenically intervened period. In this period, many dams were constructed across different inflowing rivers as well as surface water and groundwater were overexploited for meeting domestic, agricultural and industrial use (Anteneh et al., 2017). Especially, recent invasion of the Lake Tana by Water Hyacinth is assumed to reduce the lake's water level.

Table 4.2. Periods of different flow regulation from Lake Tana

Period	Description
May 1969 – April 1996	No regulation of outflow from the lake. Diversions to the Tis Abay-I power station, directly from the Abay river, commenced in January 1964.
May 1996 – December 2000	Two-gate Chara Chara Weir becomes operational in May 1996. Operated to regulate flow to the Tis-Abay-I power station.
January 2001 – December 2006	Five new gates constructed and become operational in January 2001. Operated to regulate flow to both Tis Abay-I and Tis Abay-II power stations.
January 2007 – December 2017	On May 11, 2010, the first 115 MW generator at Tana Beles the power plant began operation. The power plant was fully operational in February 2012.

4.3.1.2. Mann–Kendall (MK) trend test

In this study, Mann Kendall has been used for analysis of trend in the water level data available for the period spanning from 1960 to 2017 except data gap in the year 1963. The MK trend test is begun by computing the statistic S using the following Equation:

$$\mathrm{S} = \sum_{i=1}^{n-1} \sum_{j=i+1}^{n} sgn(x_j - x_i) \quad [4.1]$$

Where n is the number of data x_j and x_i are the sequential data values $sgn(.)$ is the sign function, which can be calculated by the following Equation:

$$sgn(x_j - x_i) = \begin{Bmatrix} 1\ x_j - x_i > 0 \\ 0\ x_j - x_i = 0 \\ -1\ x_j - x_i < 0 \end{Bmatrix} \quad [4.2]$$

A positive value of S indicates an upward trend, and a negative value indicates a downward trend. The statistical S is approximately normal distribution when n > 10. The mean of S is zero and the variance can be calculated as follow:

$$var(s) = \frac{n(n-1)(2n+5)-\sum_{i=1}^{m} t_i(t_i-1)(2t_i+5)}{18} \quad [4.3]$$

When m is the number of tied groups each with t_i tied observations. A set of data that has the same value is a tied group. The standardized test statistic (Z_{mk}) is calculated as:

$$Z_{mk} = \begin{bmatrix} \frac{S-1}{\sqrt{Var(S)}}, & S > 0 \\ 0, & S = 0 \\ \frac{S+1}{\sqrt{Var(S)}}, & S < 0 \end{bmatrix} \quad [4.4]$$

Thus in a two sided trends test, the null hypothesis should be accepted if at the level of significance (α). The positive value of Z_{mk} indicates an upward trend and the negative value of Z_{mk} indicates a downward trend. Where the value of Z_{mk} is the Mann-Kendall test statistic that follows a standard normal distribution with mean 0 and variance 1. The Z_{mk} value can be related to a p-value of a specific trend. A p-value is a measure of evidence against the null hypothesis of no change. The smaller the p-value the greater the strength of evidence against the null hypothesis. In a two-sided test for trend, the null hypothesis of no trend *H*o is accepted if $-Z1-\alpha/2 \leq Z_{mk} \leq Z1-\alpha/2$, where α is the significance level that indicates the trend strength.

4.3.1.3. Sen's slope estimation

The MK test does not provide an estimate of the magnitude of the trends themselves. In this research, another nonparametric method referred to as the Theil–Sen (TS) approach is used which is very popular among other techniques to quantify the slope of the trend (magnitude).

Sen's method assume a linear trend in the time series that has been widely used for determining trend magnitude in hydro-meteorological time series. In this method, the slopes (β) of all data pairs are first calculated by:

$$\beta = median((x_j - x_k)/(j-k)) \quad [4.5]$$

For $i = 1, 2, \dots, N$, where x_j and x_k are data values at times j and $k(k > k)$ respectively, and N is the number of all pairs x_j and x_k. A positive value of β indicates an upward (increasing) trend and a negative value indicates a downward (decreasing) trend in the time series.

Both the MK and the TS tests require time series to be serially independent, which can be accomplished using the pre-whitening technique. The trend-free pre-whitening (TFPW) procedure was applied to detect a significant trend in a serially correlated time series.

4.3.1.4. TFPW approach

According to Yue et al. (2002), the existence of serial correlation will increase the probability for significant trend detection. This leads to a disproportionate rejection of the null hypothesis of non-trend, whereas the null hypothesis is actually true. Therefore, the influence of serial correlation must be eliminated. In this study, all-time series data were first tested for the presence of a linear trend and autocorrelation at a 5% significance level, using a two-tailed test.

In order to limit the influence of existence of linear trend and serial correlation on the MK test, pre-whitening was proposed by Kulkarni and von Storch (1995). This procedure is intended to remove a serial correlation component such as a lag-one autoregressive (AR(1)) process from a time series. Before applying pre-whitening, the linear trend from the time series data must be removed. The overall analysis process is shown as below:

First: The slope b of a trend in sample data is estimated by the TSA. If the slope is Almost equal to zero, then it is not necessary to continue to conduct trend analysis. If it differs from zero, then it is assumed to be linear and the sample data are detrended by:

$$X_t' = X_t - T_t = X_t - bt \qquad [4.6]$$

Secondly: after computing the lag-1 serial correlation coefficient of the detrended series X_t', AR(1) is removed from X_t' by:

$$Y_t' = X_t' - r1X_{t-1}' \qquad [4.7]$$

This pre-whitening procedure after detrending the series is referred to as the trend- free pre-whitening (TFPW) procedure. The residual series after applying the TFPW procedure should be an independent series.

Third: The identified trend T_t and the residual Y_t' are blended by;

$$Y_t = Y_t' + T_t \qquad [4.8]$$

It is evident that the blended series T_t could preserve the true trend and is no longer influenced by the effects of autocorrelation.

The MK test is applied to the blended series to assess the significance of the trend.

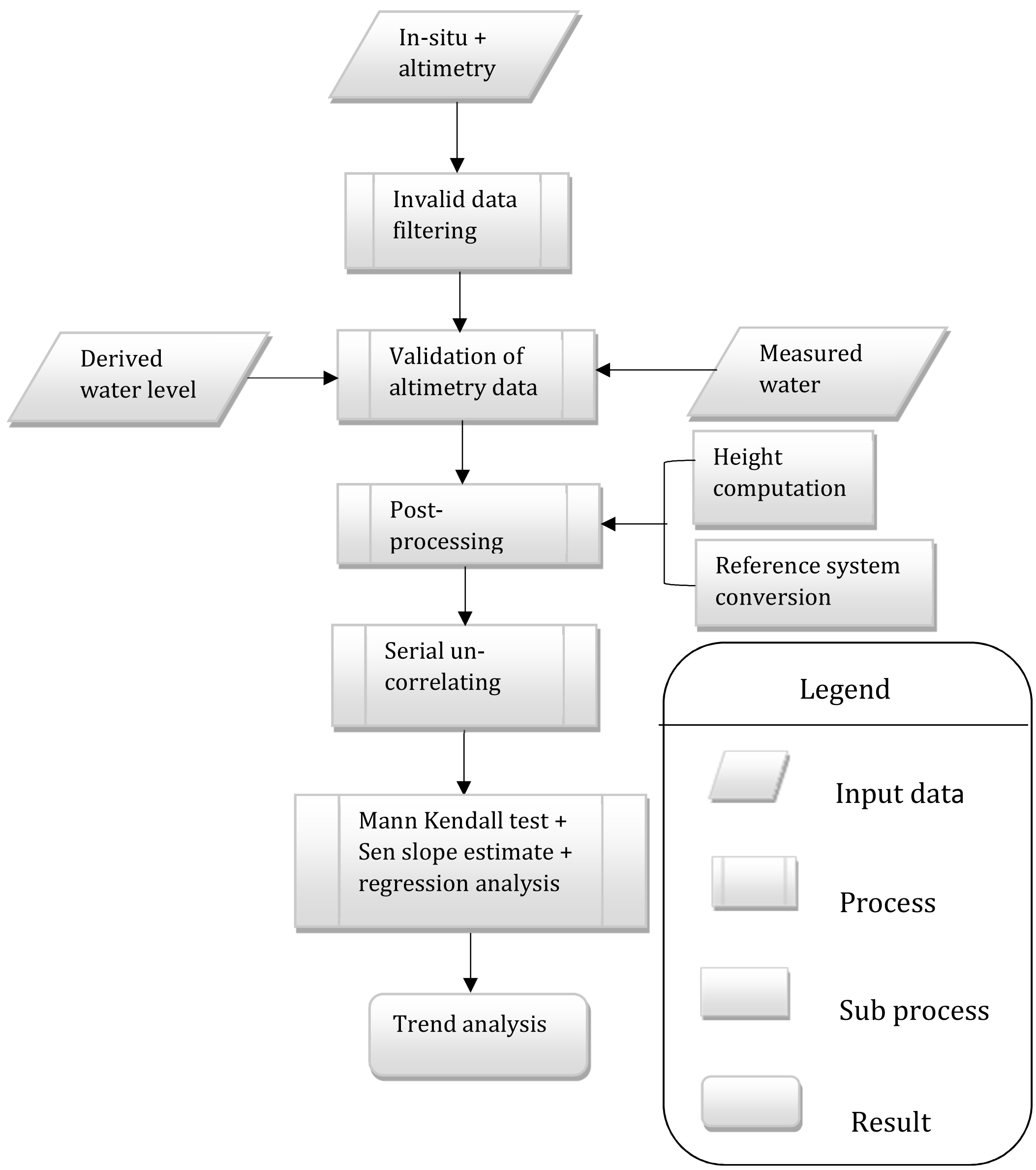

Figure 4.2: General flow chart of Lake Tana water level trend analysis

4.3.1.5. Linear regression

A simple liner regression analysis is the statistical process useful for estimating the relationship among single explanatory variables (Independent) and a predictor (Dependent variable). It is the generalization of linear regression to multiples, which can be expressed as:

$$Y_i = \beta_0 + \beta_1 X_{i1} + \beta_2 X_{i2} + \cdots + \beta_r X_{ir} + \varepsilon_i \qquad [4.9]$$

Where: we consider n number of observations of one predicator and r explanatory variables.

$Y\_i = ith$ Observation of the predictor

$X\_ij = ith$ Observation of the jth explanatory variable $(j = 1, 2, 3, \dots \dots r)$

β_j=Parameters to be estimated

$\varepsilon\_i = ith$ independent identically distributed normal error

In addition to the Sens slope estimation, the regression analysis has been applied between water level (dependent) and year (independent) to estimate the magnitude of change in water level within time.

4.3.2. Analysis for Water mass flux of Lake Tana (1984 to 2017)

4.3.2.1. Image pre-processing

The monthly time-series of Landsat TM/ETM$^+$/OLI imageries have been used to estimate temporal variability of the lake's aerial extent for the period spanning from 1984 (January) to 2017 (January). Two sets of Landsat imageries are required to cover the size of the lake. However, in every year, almost no interpretable imageries were available for 3 to 4 months (during summer season/June to August) due to the effect of cloud. These data gaps were filled by a SSM-based missing data modification method. In total, 196 mosaicked imageries were analyzed to recover the size of the lake in time scale (1984 to 2017).

Additional preprocessing is required due to that the Scan Line Corrector (SLC) compensating for the forward motion of the satellite in the ETM$^+$ sensor failed on May 31, 2003. Consequently, ETM$^+$ data acquired after the SLC failure (labeled as SLC-off data) have wedge-shaped gaps and missing pixels, which resulted in approximately 22% of missing imagery for each scene. For the selected SLC-off data, we used ENVI's gap-filling extension toolbox (landsat_gapfill.sav)[8] to fill the data gaps. Besides, atmospheric correction was applied to improve the interpretability of the imageries.

8 *http://www.exelisvis.com*

4.3.2.2. Modified normalized difference water index (MNDWI)

A number of studies have focused on applying different change detection methods for monitoring of inland water bodies (Tourian, et al., 2014 , F. Baup et al., 2014, Song et al., 2013, Crétaux et al., 2015, Sichangi et al., 2017) which range from conventional unsupervised methods to more advanced artificial neural networks (ANN) and support vector machine (SVM) classifiers. The MNDWI (Modified Normalized Difference Water Index) method proposed by Xu, (2006) has been widely used and proved better to extract area of water bodies (Duan, Bastiaanssen, 2013). We adopted the MNDWI method followed by a manual digitization. The MNDWI is calculated as the ratio of the Green band subtracted from the middle infrared (MIR) band to the sum of the Green band and the MIR band. The equation is expressed as follows:

$$MNDWI = \frac{Green - MIR}{Green + MIR} \qquad [4.10]$$

The difference between NDWI and MNDWI is that the latter uses the middle infrared band (MIR) instead of the near infrared band (NIR). Because of their high absorption in the MIR band and high reflectance in the Green band, water features usually have positive MNDWI values, while the MNDWI values of non-water features are usually negative. A proper definition of specific thresholds of MNDWI reclassification can be used to separate water from other land cover components. However, determining this threshold is the most critical part of classification (Klein et al., 2014). This is, in fact, crucial, as an appropriate threshold should be determined for every imagery separately. The subjective selection of the threshold value may lead to an over or underestimation of open water area. However, choosing the adequate threshold value to compute the water mask can be very tricky. Therefore, different MNDWI threshold values were tested and the resulting water feature/non-water feature separations, especially near the water body boundary, were visually checked. Finally, the water surface areas were calculated as the sum of the areas of the pixels identified as water bodies.

4.3.2.3. Validation of estimated lake area

Daily measurements of lake Tana's water levels (as observed at Bahir Dar station) for a period ranging from 1960 (January) to 2006 (August) were obtained from the Ethiopian Ministry of Water, Irrigation and Electricity. The relationship between water level (L) and surface areas (A) were derived based on Duan et al. (2013) by combining Landsat image and four operational satellite altimetry products (RLH, GRLM, ICESat-GLAS and Hydroweb). The L-A equations are:

$$A = -18.3098L^2 + 83.5395L + 2969.3014$$
$$A = -8.1353L^2 + 63.8015L + 2962.8856 \quad [4.11]$$
$$A = 1.2193L^2 + 24.6697L + 3019.8256$$
$$A = -11.8327L^2 + 76.1434L + 2960.8456$$

Respectively.

The daily surface areas were derived by converting daily measured water levels using Eqn. (4.10). In this research, these surface areas were used to validate the estimated surface areas.

4.3.2.4. Water level from satellite altimetry

The United States Department of Agriculture Foreign Agricultural Service (USDA/FAS) in cooperation with NASA and the University of Maryland prepares global Reservoir and Lake Monitor (GRLM) database[9]. The database is compiled from T/P, Jason-1, Jason-2 and GFO and ENVISAT satellites data. For each lake/reservoir included in GRLM, there are two time-series of water level variations, i.e. the raw data and the smoothed data with a median type filter to eliminate outliers and reduce high frequency noise. However, smoothed data are only for visualization, they are not expected to be used for quantitative analysis. The raw data of TPJO.1 version including water levels and estimated errors for Lake Tana from GRLM were used in this study. Water level value with a standard deviation more than 10cm are firstly filtered out. Then data also subjected to addition correction to remove the existence of serial correlation.

4.3.2.5. Validation of altimetry based water level

Validation of the GRLM altimeter-derived water level generally requires comparison with in situ measurements at gauge stations (Wu et al., 2014, Duan et al., 2013). The altimetry data were validated by directly comparing the altimetry-based water levels with the in situ water levels obtained from gauge measurements observed at Bahir Dar station over the period 1992 to 2006 (Fig. 2.2).

9 *http://www.pecad.fas.usda.gov/cropexplorer/global_reservoir/*

4.3.2.6. Estimation of Lake Water volume variation

The total volume (v) of water depends on a specific reference minimum volume of water contained in the lake(v_{con}), and a variable component that varies with the water levels(Δv):

$$v = v_{con} + \Delta v \qquad [4.12]$$

The lowest water level derived from satellite altimetry corresponding to a lowest monthly averaged perception over the study period was used as a reference level to separate v_{con} and Δv. The resulting water volume Δv is referred to as Water Volume Above the Lowest Water

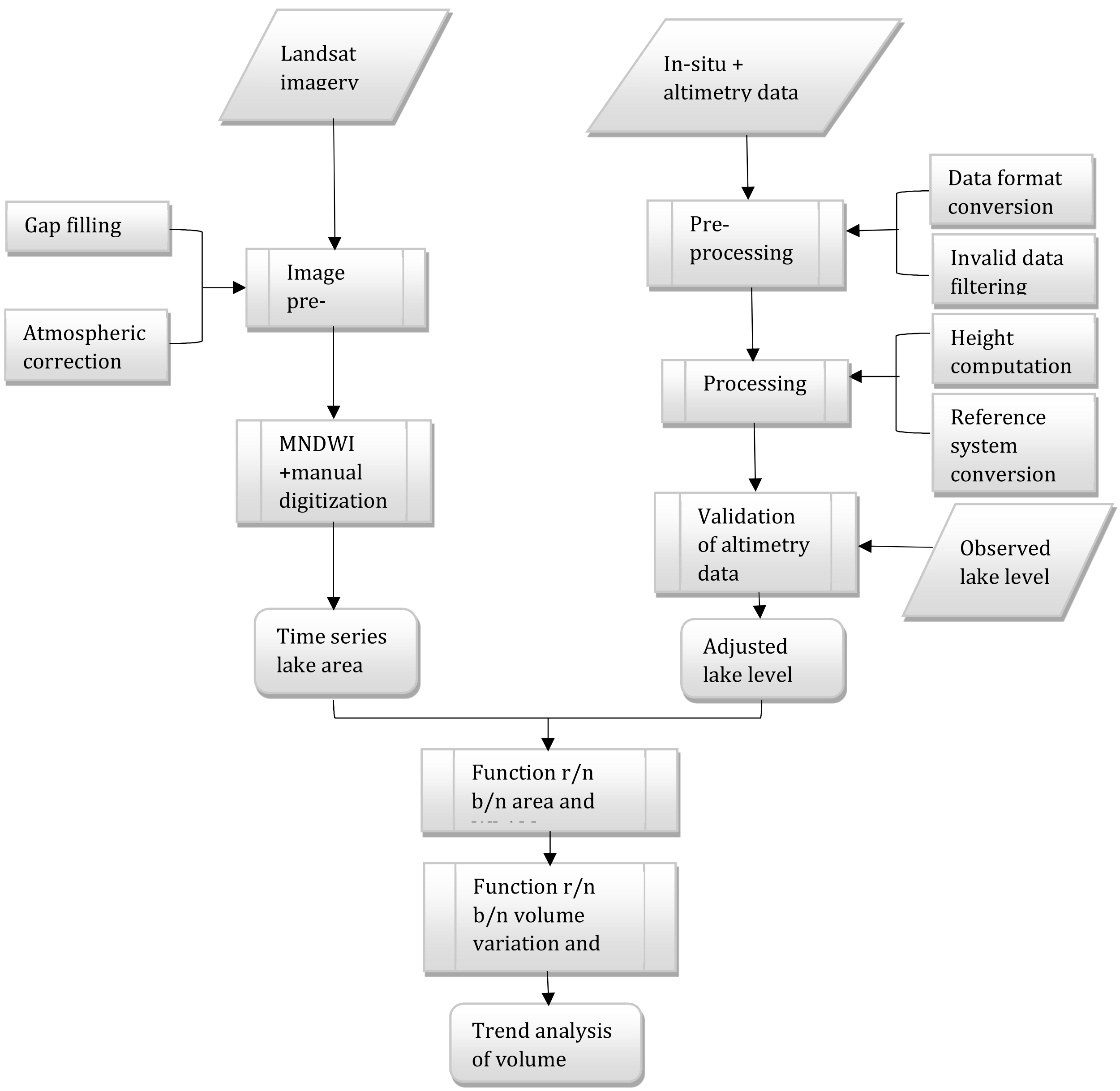

Figure 4.3: General flow chart of Lake Tana volume variation analysis

Level (WVALL). Considering that, the objective of this study is to estimate the relative water volume variations for the sake of water management rather than absolute values, values of v_{con} can be disregarded.

The lowest water level in the satellite altimetry product was determined first. Subsequently, the lowest water level was subtracted from all water levels obtained from satellite altimetry product to obtain the Water Level Above the Lowest Level (WLALL)/changes in volume of water in time scale/. The relationship between WLALL and corresponding surface area (area–WLALL) was established using regression analysis (Fig. 5.5). Because the water volume is the integration of the functional relationship between surface area and water level, the WVALL–WLALL relationship can be obtained by analytically integrating the function of area–WLALL with the condition that WVALL is equal to zero when WLALL is zero. Assume that the area–WLALL relation can be described as a second-polynomial function: $A = f(L) = aL^2 + bL + c$ where A is the surface area in km^2, L is WLALL in meter and a, b, c are coefficients determined by regression analysis. Then the WVALL–WLALL function which is the integration of $f(L)$ against dL can be written as $V = \int f(L)\, dL = aL^3/3 + bL^2/2 + cL + d$, where V means WVALL, and a, b, c and d are coefficients. a, b and c are the same values in area–WLALL function and d can be solved as 0 given the condition V = 0 when L = 0. The resulting equation can be used to convert the time-series of WLALL to WVALL for the analysis of water volume variations in lakes or reservoirs. Then simple linear regression and graphical interpretation area used to interpret the result. The result of the analysis is shown in Fig.5.6

4.3.3. Analysis of GRACE derived water storage variation of the Lake Tana basin (1992 to 2017)

4.3.3.2. Gravity anomalies to water layer thickness

The gravity potential described by a spherical harmonic coefficient δC_n^m or δS_n^m can be related to corresponding spherical harmonic coefficient describing the varying thickness of a water layer that is its source. The relation is different for each term of degree *n.*

$$V_n^m = \frac{GM}{R}\delta C_n^m = \frac{4\pi G(1+k_n)\rho_w R}{2n+1} h_n^m \qquad [4.13]$$

Where k_n is the load Love number of degree n and accounts for the extra potential created when the Earth is distorted elastically under the load of water; ρ_w is the density of water (1000kgm^{-3}).

The corresponding relationship between the coefficients of potential and the free air anomaly is

$$\Delta g_n^m = \frac{GM}{R}\frac{n-1}{R}\Delta C_n^m \quad [4.14]$$

So

$$\Delta g_n^m = 4\pi G\rho_w \frac{n-1}{2n+1} h_n^m \quad [4.15]$$

We used a plane version of this spherical formula where the ratio $(n - 1)/(2n + 1)$ tends to 0.5 for large n, while localizing the signal at a local scale (Bedada, 2007).

$$\Delta g_n^m = 2\pi G\rho_w h \quad [4.16]$$

This gives a relationship between gravity $mGal(milligal)$ and the thickness of the equivalent layer of water in $mm(millimeter)$ of

$$\delta h = 23.8\Delta g \quad [4.17]$$

This expression has been used throughout for hydrological interpretations of free-air gravity anomaly patterns. Then the resultant change in total storage of lake Tana basin presented in the form of graph.

4.3.3.4. Comparison of Mass flux of Lake Tana with the entire Tana sub basin

The hydrological balance of the lake is based on the mass conservation law or hydrological equation. Lake's water budget is computed by measuring or estimating all hydrological sources and sinks that cause variation in the lake's water level (Berehanu, 2016). In general, the hydrological equation is given by:

$$\frac{dW}{dt} = P(t) - R(t) - E(t) \quad [4.18]$$

Where P is the precipitation, ET is the evapotranspiration and R is the runoff. Neglecting R, the derivative of TWS is related to $(P - ET)$. The annual signal was removed and data were smoothed by applying a two-month smoothing without phase shift using the equation 5.2

$$\frac{dW_i}{dt} = \frac{W_{i+1} - W_{i-1}}{2} \quad [4.19]$$

In order to compare the terrestrial water balance from GRACE and satellite altimetry, we further plotted the TWS variations by the means of their volumes. The lake water volume of each month was computed by multiplying the equivalent water height obtained from GRACE by the basin area (15077 km^2). Similarly, the water level from satellite altimetry is multiplied by the average lake area (3057 km^2). The annual signal was removed and data were smoothed by applying the two-month window.

4.3.3.5. Ground water change of Lake Tana sub Basin

Groundwater storage variations can be isolated from GRACE-derived TWS change with auxiliary information. In case of Lake Tana sub basin GRACE ΔTWS is equal to the sum of change in groundwater storage (ΔGwS), change in soil moisture (ΔSoM) and change in surface water reserve (ΔSwR), assuming that the water mass flux contained in the biomass is assumed to be negligible over short time scale. Hence, the change in storage of the basin groundwater and soil moisture is the difference between the GRACE ΔTWS and the respective month change surface water storage.

$$\Delta GwS + \Delta SwR = \Delta TWS - \Delta SoM \quad [4.20]$$

The SwR is the sum of the change in storage from stream channels and Lake Tana storage. The Lake Tana water body is 3000km^2 area, accounting for 20% of the basin's total area so the lake level fluctuation is significant in the evaluation of the ΔTWS, the dominant SwR of the basin is driven from the change in storage of the Lake Tana water; whereas, the change in storage from stream channels is insignificant. In such cases, the SwR can be considered as the change in storage from surface water reservoirs only (Abiy et al., 2017). Therefore, the Lake Tana monthly changes in lake level corresponds to changes in SwR.

Catchment-average (including lake) time series of TWS were computed from GRACE data and changes in the water mass balance of the lake were removed using the altimetry data to determine the contribution of the Lake Tana's sub basin catchment to the hydrology of the basin.

At the catchment scale, changes in groundwater storage can be related to changes in groundwater levels by defining an effective drainage porosity

$$\frac{dS_{catchment}}{dt} = \eta \frac{dh_{groundwater}}{dt} \quad [4.21]$$

Where η is the effective drainage porosity.

On average groundwater levels occur at approximately the same rate as changes in lake levels

$$\frac{dS_{lake}}{dt} \simeq \frac{dh_{groundwater}}{dt} \tag{4.22}$$

Then η can be estimated by taking the ratio of the watershed and lake-only trends, i.e.

$$\eta = \frac{dS_{catchment}}{dt} / \frac{dS_{lake}}{dt} \tag{4.23}$$

CHAPTER FIVE: RESULT AND DISCUSSION

5.1. Water level variation of Lake Tana (1960 to 2017)

5.1.1. Hypothesis I

Fig. 5.1 shows the variability of the mean monthly lake level data for the entire period of study. The water level of the lake has an increasing trend. The lake has undergone a periodic trend until 1996. While the lake has experienced irregular and un-modelled trend between 1997 and 2017.

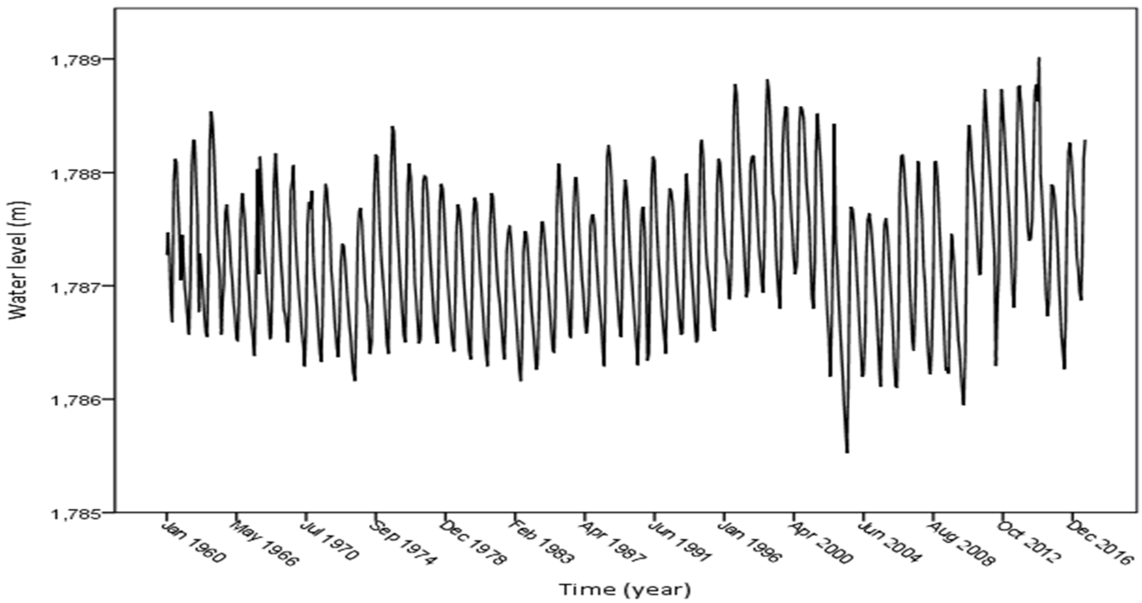

Figure 5.1: Linear tend of annual maximum lake level

Before 1970, the trends in Lake water level were mostly driven by seasonal variability of precipitation (Kebede et al., 2005). Impact of anthropogenic activities on the lake water level was negligible in a prior to 1996 (McCartney et al., 2010). Years before the 1996s were natural period for the lake, human-induced impacts on the lake water was minimal. However, from 1996 onwards, the Lake Tana sub-basin was extensively utilized to meet various needs of the society. For example, construction of hydro-dams have modified the natural lake-level regime, resulting in reduced seasonal but greater inter-annual variability. Water level trends show seven distinct phases of hydrological regime (Fig. 5.1). The first phase covers the period spanning from 1960 to 1973. During this period, the lake water level has decreased by a magnitude of 40 mm/yr. In the second phase (1974 to 1977), the lake water level has increased by 220 mm/yr. However, the lake water level has declined at a rate of 100 mm/yr in the third phase (1978 to 1984). While the lake water level has shown an increasing trend over an extended period from 1985 to 2000. During this period, the lake water level has increased by 55 mm/yr; in the latter years of the Millennium, variation in the lake water level was below this value.

Lake Tana has reached the lowest water level between 2002 (January) and 2003 (June). During this period, the lake water level has declined by 1.4 m. This an unprecedented reduction in the water level was unobserved since the advancement of satellite technology. Drought and initial filling of the newly constructed hydro-dams (e.g. Tana Beles) with water were thought to be the major causes for the sudden extreme decline of the Lake Tana's water level. However, the lake water level has steadily increased from 2003 (January) to 2013 (October) at a rate of 1040 mm/yr. On the other hand, the lake water level has decreased at a rate of 107.5 mm/yr between 2013 (November) and 2017 (September). This noticeable loss in the water level may be caused by anthropogenic factors (e.g. increased water usage for domestic, agriculture, industry and hydro- power generation), climate change and invasion of Water Hyacinth (Anteneh et al., 2017).

The results of Mann-Kendall test for trend analysis and Sen's slope estimation of data are presented in table 5.1. The Mann-Kendall test showed a significant increasing trend (at a significance level of 0.05) in the water level of the lake. The Sen's slope also indicated significant increment of the lake water level at a rate of 6.17mm/yr. The patterns of Lake water level variation over period ranging from 1960 to 2017 justified the validity of hypothesis I.

5.1.2. Hypothesis II

Monthly analysis

The Mann-Kendall (MK), Sen's slope estimation and linear regression were applied on a monthly scale to detect trends in the water level series at Bahir Dar station. Table 5.1 presents trends showing patterns of monthly variation of the Lake Tana's water level. Trend analysis was calculated based on the smallest significant level α, in which the trend is considered statistically significant at α confidence level.

The result showed that a generalized positive trend was observed from January to May and September to December during the study period, while no significant statistical trend is observed for the months of June, July and August at 95% confidence level (α = 0.05). Statistically insignificant positive trend was observed for the month of June while insignificant negative trends were observed for the months of July and August for the entire study period.

Table 5.1: Trend analysis of annual and monthly water level data (1960 to 2017)

Month	p-value	Sen's slope	Regression slope	Trend Nature	H_0 Rejected?
January	<0.0001	0.01	0.01	Positive	Yes
February	<0.0001	0.01	0.009	positive	Yes
March	0.001	0.009	0.008	positive	Yes
April	0.004	0.006	0.006	positive	Yes
May	0.04	0.004	0.005	positive	Yes
Jun	0.17	0.003	0.004	positive	No
July	0.833	-0.000526	0.00	Negative	No
August	0.827	-0.000864	-0.001	Negative	No
September	0.034	0.007	0.008	positive	Yes
October	0.003	0.009	0.008	positive	Yes
November	0.00	0.011	0.01	positive	Yes
December	<0.0001	0.012	0.011	positive	Yes
Annual	<0.0001	0.000432	0.000486	Positive	Yes

Long-term Sen's slope analysis indicated the existence of significant trends (> 0.5 m) at a monthly scale (Table 5.1). Most significant trend (~10 mm/yr) was detected from the Sen's slope for the month of December, compared to trends observed in other months. Throughout the study period, a decreasing statistically insignificant trend was observed in august and the water level of the lake had almost a constant trend in July.

Seasonal analysis

The MK and Sen's slope tests were also applied to study trend in the seasonal water level over the study period (1960 to 2017). Table 5.2 summarizes the results from the trend analysis at 95% confidence level.

Table 5.2: Trend analysis of seasonal water level data (1960 to 2017)

Season	p-value	Sen's slope	Kendall's tau	Trend Nature	H_0 rejected?
Winter	0.00	0.007	0.354	positive	No
Spring	0.004	0.009	0.263	Positive	No
Summer	0.396	0.002	0.079	Positive	No
Autumn	0.016	0.006	0.223	positive	No

On the basis of MK test, no significant trend was observed in the summer season. While positive trends (at 95% confidence level) were observed in the winter, spring and autumn seasons. The seasonal water level was lower in summer compared to other seasons. Whereas, the lake water level is relatively higher in winter compared with spring sand autumn (Fig. 5.2).

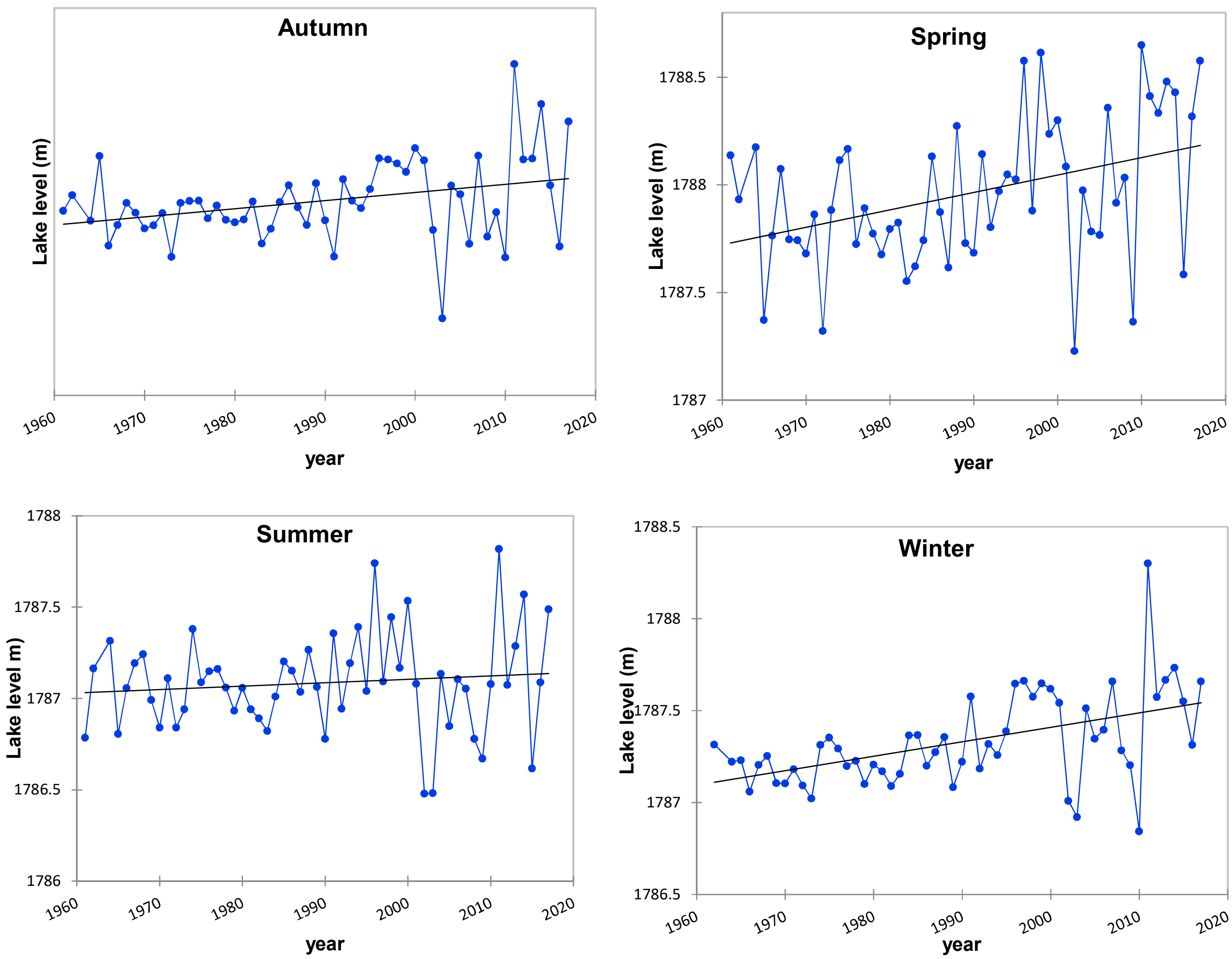

Figure 5.2: trend analysis of average monthly water level (1960 to 2017)

The results of the Sen's slope analysis showed significant trends at a monthly scale. Highest slope ($p<0.0001$) with a Sen’s slope of 8 mm/yr was observed in winter. The trend in spring ($p<0.01$ and 7 mm/yr) is significant compared to that of autumn ($0.01 < p < 0.05$, and 5 mm/yr). The summer season has insignificant trend accounting for 1.7 mm/yr.

5.1.3. Hypothesis III

In order to understand patterns of lake water level trend was analyzed for two district periods (1960 to 1996 and 1997 to 2017) using Mann-Kendall trend test and Sen's slope estimate (Figure 5.4).

Table 5.3: Results of Mann-Kendall trend test and Sen's slope estimate illustrating monthly water Level variation during two Periods (1960 to 1996 and 1997 to 2017)

month	**1960 to 1996**			**1997 to 2017**		
	P - value	Sen's slope	Slope magnitude	P - value	Sen's slope	Slope magnitude
January	0.044	0.005	0.180	0.526	0.006	0.144
February	0.009	0.006	0.213	0.717	0.004	0.120
March	0.055	0.005	0.185	0651	0.005	0.109
April	0.085	0.004	0.159	0.976	0.005	0.113
May	0.168	0.004	0.137	0.415	-0.003	-0.066
Jun	0.187	0.003	0.170	0.717	-0.005	-0.088
July	0.286	0.005	0.181	0.74	-0.006	-0.103
August	0.691	0.002	0.075	0.928	-0.008	-0.168
September	0.929	0.005	0.192	0.349	0.007	0.150
October	0.394	0.006	0.204	0.174	0.019	0.182
November	0.196	0.005	0.22	0.291	0.317	0.224
December	0.118	0.005	0.235	0.097	0017	0.267
Annual	0.955	0.002	0.085	0.526	-0.002	-0.0455

Figure 5.3 shows the MK trends of the lake water level for the two periods identified above. The lake water level showed an increasing trend between 1960 and 1996. Since 1996, the water level showed a downward trend; while the overall trend is negative, (both upward and downward trends are statistically insignificant at 95% confidence level). The Sen's slope was also positive from 1960 to1996 and negative between 1997 and 2017 see Table 5.3. In general, the lake water level has increased by 0.085m between 1960 to 1996 and declined by 0.0455m between 1997 and 2017

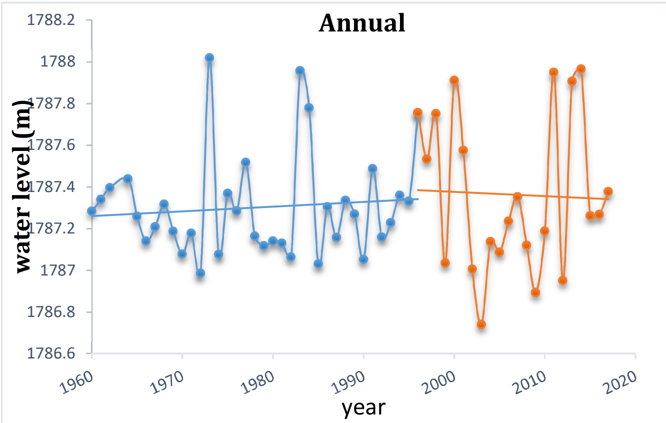
Annual
water level (m)
1788.2
1788
1787.8
1787.6
1787.4
1787.2
1787
1786.8
1786.6
1960 1970 1980 1990 2000 2010 2020
year

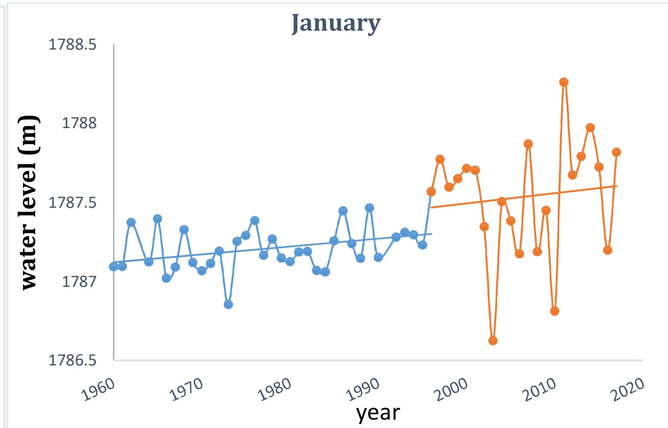
January
water level (m)
1788.5
1788
1787.5
1787
1786.5
1960 1970 1980 1990 2000 2010 2020
year

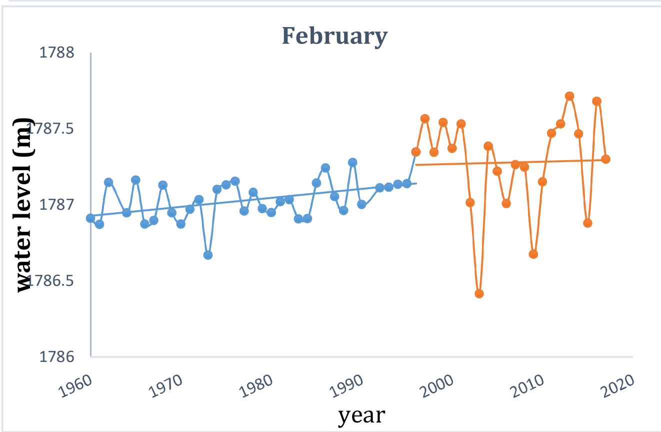
February
water level (m)
1788
1787.5
1787
1786.5
1786
1960 1970 1980 1990 2000 2010 2020
year

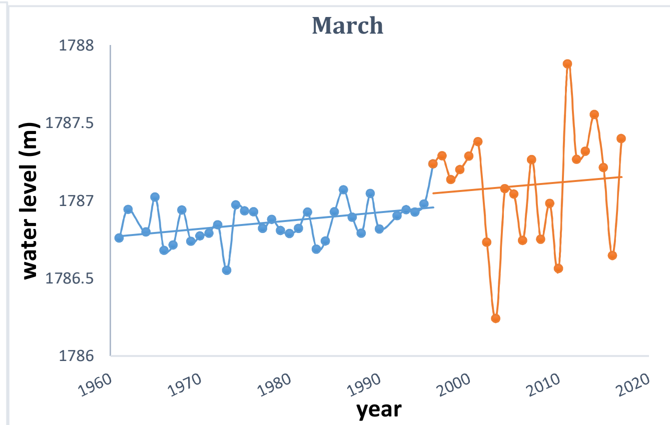
March
water level (m)
1788
1787.5
1787
1786.5
1786
1960 1970 1980 1990 2000 2010 2020
year

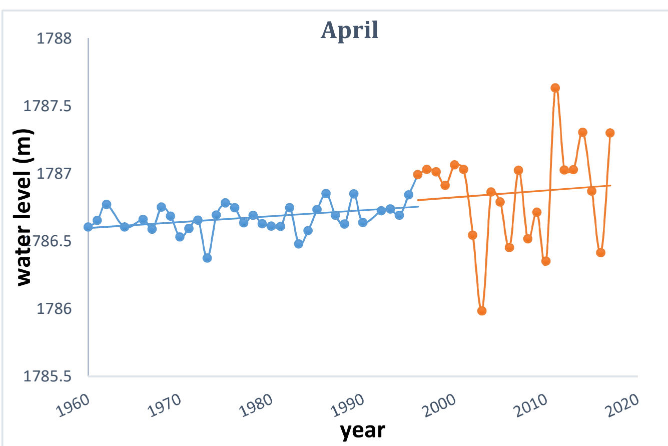
April
water level (m)
1788
1787.5
1787
1786.5
1786
1785.5
1960 1970 1980 1990 2000 2010 2020
year

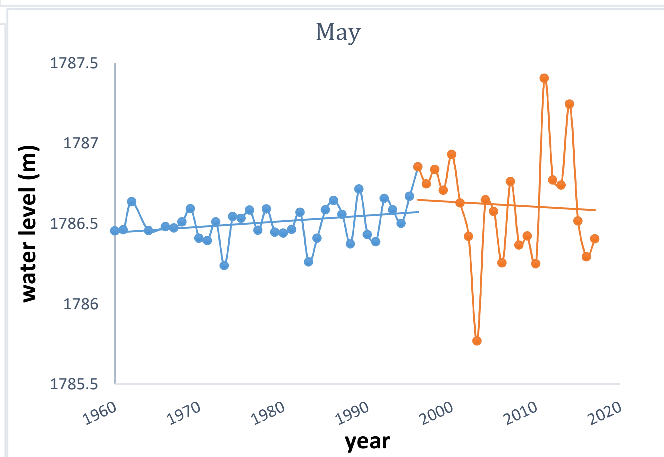
May
water level (m)
1787.5
1787
1786.5
1786
1785.5
1960 1970 1980 1990 2000 2010 2020
year

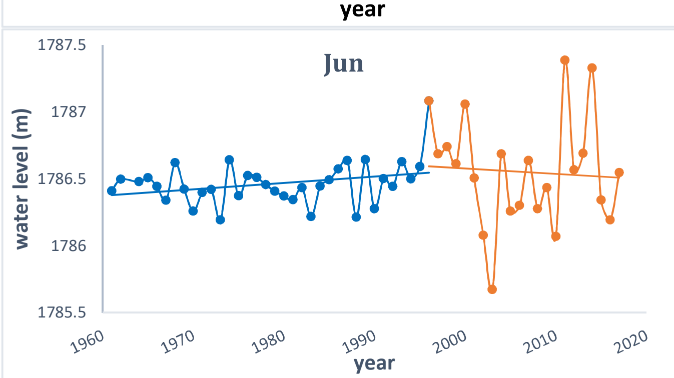
Jun
water level (m)
1787.5
1787
1786.5
1786
1785.5
1960 1970 1980 1990 2000 2010 2020
year

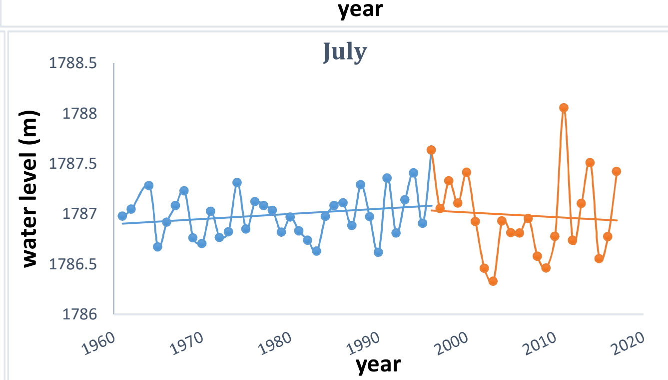
July
water level (m)
1788.5
1788
1787.5
1787
1786.5
1786
1960 1970 1980 1990 2000 2010 2020
year

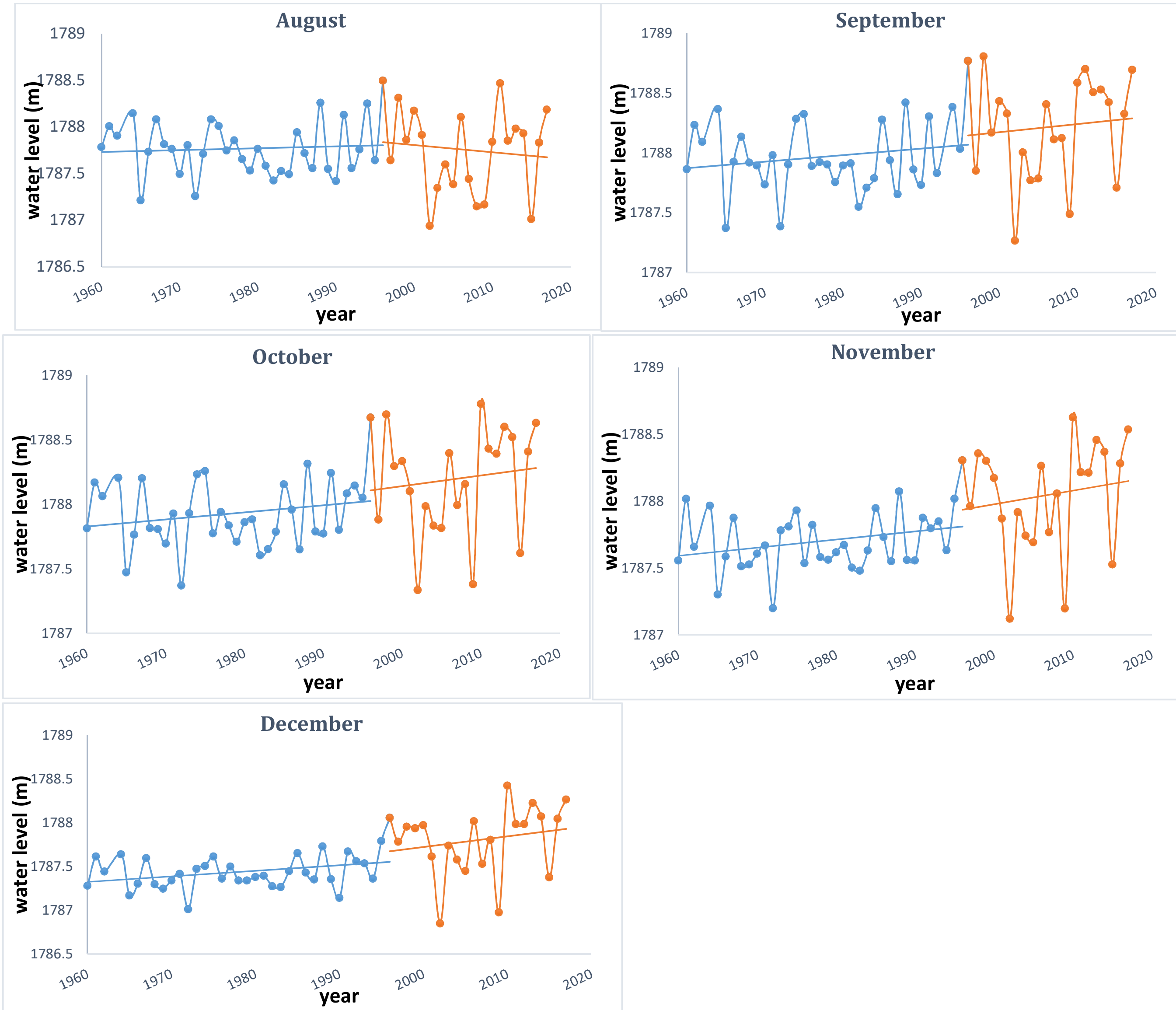

Figure 5.3: Results of Mann Kendall trend test and Sen's slope estimate illustrating monthly water level for two periods (1960 to 1996 and 1997 to 2017)

A monthly trend analysis (over the study period) showed insignificant upward trend for two periods: January to April, and September to December. However, for the specific period (May to August), a positive trend was observed between 1960 and 1996, and a negative trend was observed between 1996 and 2017 (both trends are statistically insignificant at 95% confidence level).

On the other hand, Sen's slope detected significant increasing trend in February, October, November and December for the first period with a magnitude of 213 mm, 204 mm, 220 mm and 235 mm in 36 years, respectively. From 1996 to 2017, the trend in the water level has increased by 224 mm and 267 mm for the month of November and December, respectively. However, no significant decreasing trend was identified for the first period but for the second period, statistically insignificant decreasing trend was observed for the period spanning from the month of May to August with a magnitude of -66mm, -88mm, 103mm and -168mm, respectively.

5.2. Mass flux of Lake Tana (1984 to 2017)

5.2.1. General

The results obtained from satellite imagery and altimetry were used study temporal variations of the Lake water level and water mass balance flux. Estimates of lake surface area derived from Landsat imageries were validated against previous numerical results computed in situ and bathymetric measurements. Validation result showed good agreement of estimated lake surface areas (as measured from remotely sensed data) the corresponding values derived from in-situ and bathymetric measurements Duan et al. (2013), with a correlation range of 0.7 to 0.96. amplitudes between 2.65m (2007/2008) and 5.36m (2003/2004).

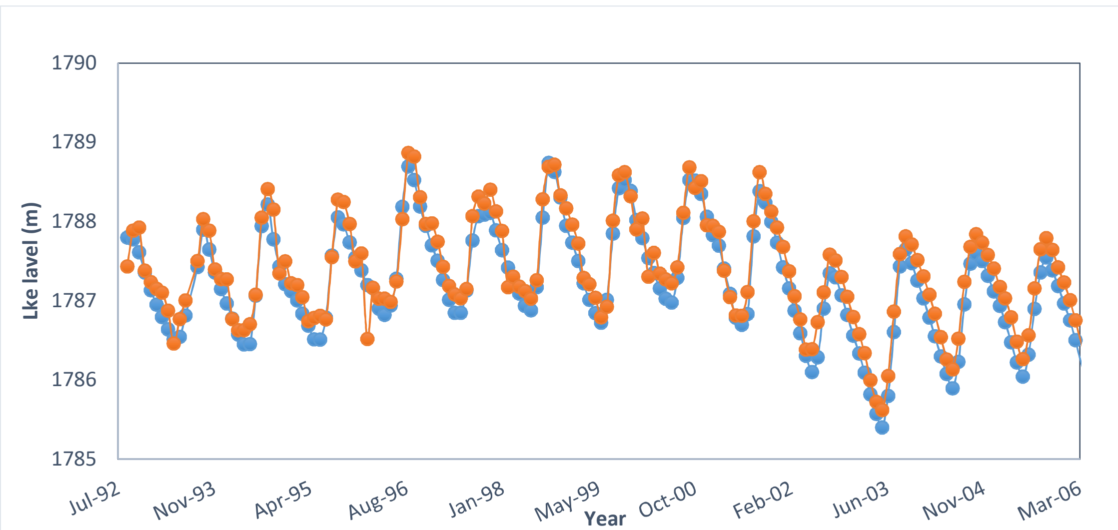

Figure 5.4: the correlation between *in-situ (blue)* and altimetry (red) water level from monthly average base

The altimetry data were validated by directly comparing the altimetry-based water levels with the in-situ water levels acquired from gauge measurements. Comparison was made for the period ranging from 1992 to 2006. Similarly, temporal variations were observed using both data sets (Fig. 5.4), in which the in-situ water levels exhibited annual (peak-to-peak) altimetric data detected seasonal and inter-annual variability of the lake water level. Patterns of seasonal lake-water level cycles showed maximum (September to October) and minimum (May to June) variability in water mass balance. The inter-annual variations in the lake's water level have detected the effect of drought on the water mass balance of the lake. The lake's water level was observed to be minimum during the 2003 drought year. The difference between in-situ and altimetry derived water levels is less than 0.3 m at 96.5% of the cases; the maximum range reached 0.681m. The RMSE and R^2 of the residuals between the two data sets were equal to 0.21m and 0.98, respectively. In general, the two data sets are in a very good agreement.

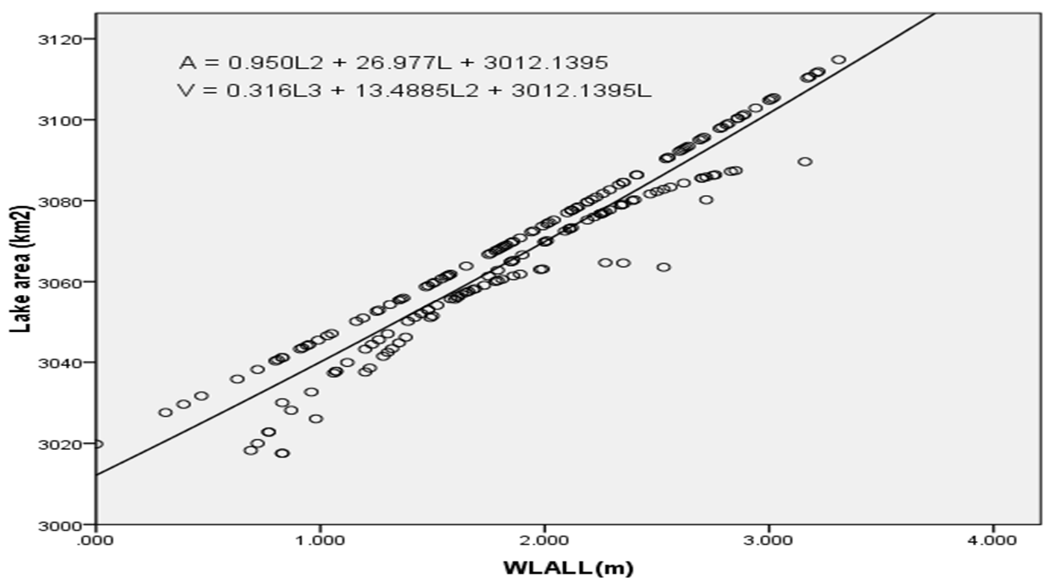

Figure 5.5: surface area (A)–WLALL (L) and analytical integrated WLALL (L)–WVALL (V) relationships for Lake Tana

Thus, altimetric data can be used to monitor lake's water level in cases where complete temporal coverage of *in-situ* gauge data is not available. In this study, we used altimetry data for the period from 2007 to 2017, during which in-situ gauge data were not recorded.

Based on the water level retrieved from GRLM and the corresponding surface extent extracted from Landsat, a second degree statistical relationship between water level (h) and surface area (A) of the Lake was established using linear regression method (Fig. 5.5). Also, the surface area corresponding to the water level retrieved from GRLM was estimated using this linear equation 4.9. Figure 5.5 shows strong correlation (> 0.94) between lake area and water level.

5.2.2. Water volume variation

The water volume variation in the Lake Tana was estimated from time-series of lake's water level and surface area extents. Figure 5.6 illustrates the variability in water volume of the lake over period from 1984 to 2017. The volume of the lake shows a positive trend with a minimum and maximum variation occurring in 2003 and 2013 respectively (Fig. 5.6). This is mainly due to the construction of the Chara Chara wair at the outlet of the lake (Chebud et al., 2009).

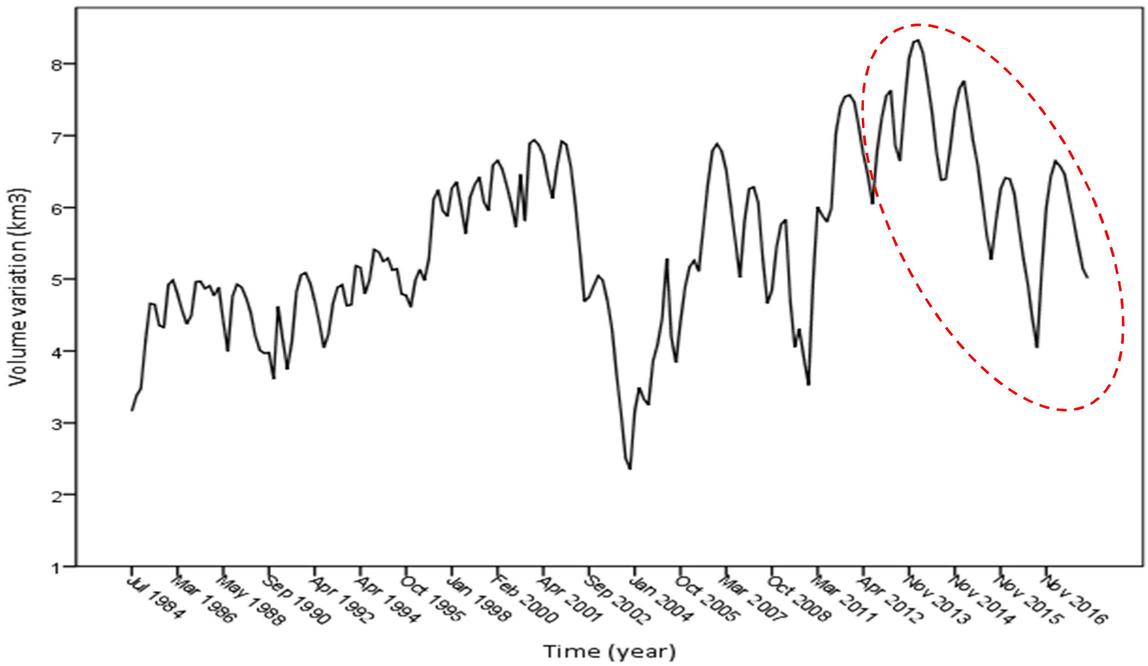

Figure 5.6: water volume variation of Lake Tana (1984 to 2017)

For the period 1984 to 2001, the water budget of the lake shows a positive trend. The volume of the lake increased by a magnitude of 0.155km^3/year. The lowest volume was recorded in 2003. During this time, the volume dropped by an amount of 4.412km^3. This was due to occurrence of drought. In an attempt to maintain electricity supplies, production at both Tis Abay power stations was maximized and as a result, lake levels dropped sharply (McCartney et al., 2010). However, for the year 2004 to 2012, the volume of lake show a positive trend with an immediate significant reduction in 2007/2008. The volume of water has increased by a magnitude of 0.326km^3/year. Nevertheless, for the period 2013 to 2017, the volume of the lake shows a continuous desiccation by a magnitude of 0.612km^3/year. Which may be related to, the construction of many hydropower stations, the water hyacinth and other natural and anthropogenic activities. Given the current negative trend in water volume loss, over the lake and the alarmingly low value for the remaining water volume in the lake, one can easily predict that the lake will completely disappear within twelve thousands of years if no countermeasures are taken. We acknowledge that there are uncertainties in our estimations and conclusions, which can be the scope of future works.

5.3. GRACE derived water storage variation of the Lake Tana basin (1992 to 2016)

5.3.1. General

154 monthly gravity solutions from August 2002 to May 2016 were extracted in units of equivalent water thickness (mm). 12-months missing data within this time range were filled by averaging and/or applying the corresponding month value from other times. For the sake of analyzing trend related to change in the water thickness of the catchment, firstly the driest season in the basin was taken as a reference gravity anomaly. In case of Lake Tana April 2003 was taken as reference epoch and the value of the reference gravity anomaly was subtracted from subsequent monthly values in order to obtain the gravity variation above the reference gravity anomaly. The resulting residual gravity anomalies are used to compute variable water thickness.

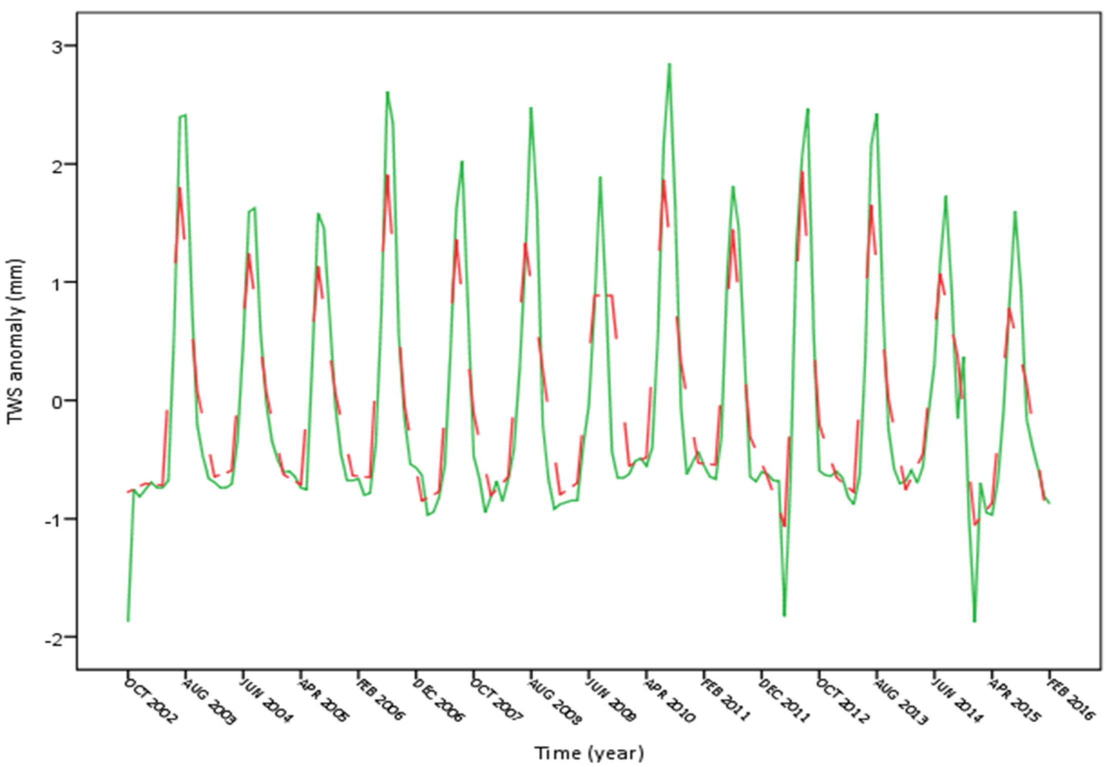

Figure 5.7: Time-series of the basin-averaged seasonal water change in TWS (red) and of monthly averaged change in TWS (green) for Lake Tana sub basin

Fig. 5.7 depicts the dynamics of basin-averaged monthly and seasonal total water storage anomaly plotted from GRACE data. The time-series plots do not only have striking similarities in especially the seasonal phases, but also indicate a small loss in the basin. According to the figure 5.7, there is excess water mass gain in summer and autumn and loss of water storage in winter and spring. Autumn is usually harvesting season, and a relatively high rainfall in the preceding summer augments storage in the autumn season. There is insignificant average annual depression in the basin. The total water storage of the basin depreciate with a magnitude of 0.0025mm/year.

The monthly averaged TWS of Lake Tana sub Basin for the period from 2000 (August) to 2016 (May) is shown in Fig. 5.8. it indicates the presence of enhanced seasonal pattern with the positive TWS values from May to September with a monthly maximum value of 38.8mm (in term of EWH) in July. Which may be due to an increase in inflow from tributaries and this is rainy season in the catchment. During this time, the TWS of Lake Tana sub Basin rise rapidly and reach its maximum peak.

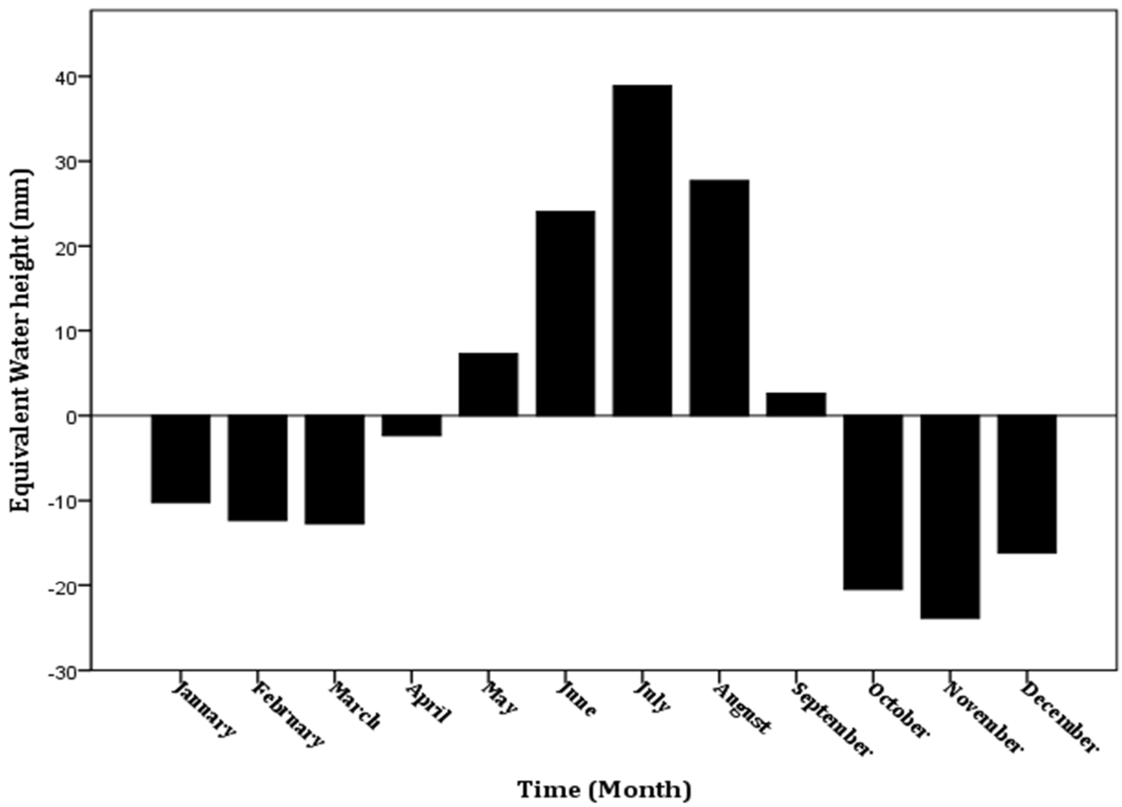

Figure 5.8: Monthly change in TWS of Lake Tana sub Basin

The TWS is negative during October to April with a minimum value of -23.8mm (in terms of EWH) in November. Due to the reduction in rainfall in the Lake Tana basin and decrease in the amount of inflow or recharge from four major tributaries, the TWS become decline reaching its minimum in April. Other previous studies also showed similar results. For example, Abiy et al. (2017) showed a consistent decreasing pattern of the total water storage of the basin in the driest season. Maximum precipitation occurs in July, while the GRACE change in total water storage reaches its maximum value in August to September. After September, the groundwater system gains at a decreasing rate until November.

5.3.2. Mass flux of Lake Tana with the entire Tana sub basin

As we can see in Figure 5.9, the variability of GRACE based volume of water is similar to the one derived from altimetry data. The correlation between the GRACE and satellite altimetry solutions is 0.73. Despite difference in the amplitude of the signal, the two data sets exhibit significant inter-annual and seasonal changes in the volume of water. The amplitude of TWSC rages from -0.63km^3 to 0.8km^3 from GRACE and -1.88km^3 to 2.85km^3 from satellite altimetry. The distinct decline of water quantity as inferred from GRACE in 2002 is associated with the occurrence of severe drought in the study area during the same time window.

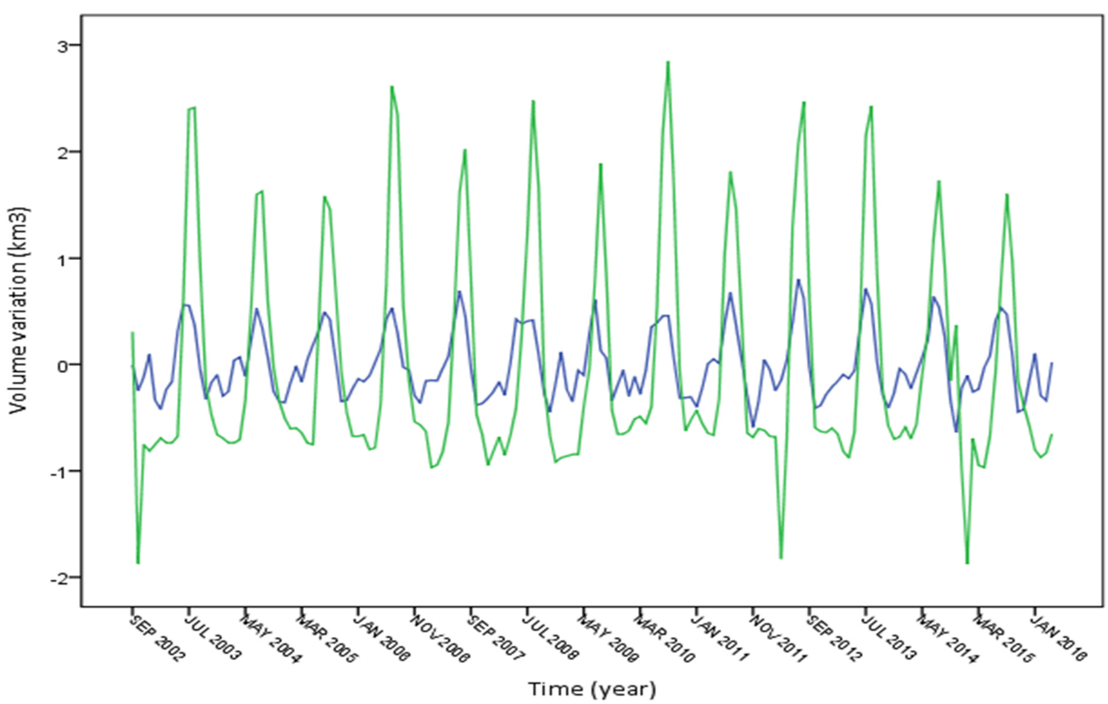

Figure 5.9: Comparison of water volume variation from GRACE (Blue) and satellite altimetry (Green)

5.3.3. Impact of rainfall on TWS variation

In this study, we used the Climate Hazards group Infrared Precipitation with Stations (CHIRPS). CHIRPS was developed to support the United States Agency for International Development Famine Early Warning Systems Network (FEWS NET). It uses the Tropical Rainfall Measuring Mission Multi-satellite Precipitation Analysis version 7 (TMPA 3B42 v7) to calibrate global Cold Cloud Duration (CCD) rainfall estimates.

Fig. 5.10 illustrates the amplitude of the annual signal for EWT from GRACE and the rainfall from CHIRPS. The amplitudes of the annual signal of the EWT and the rainfall show strong similarities. For the entire study area, the correlation coefficient between the EWT annual amplitudes and the rainfall annual amplitudes is about 0.65. This implies that, at annual scale, the precipitation can explain about the 65% of the EWT variations.

The rainfall ranges from-188.45 to 189.56 mm, while the TWS ranges from -42.448 to 53.15 mm (in terms of EWH). The rainfall reaches the maxima of 189 mm in Jun 2013 and the minimum of -188 mm occurs in September 2015 (in terms of EWH). There is a slight increment in TWS and rainfall during august 2002 to 2003 with a sudden reduction in august 2003 in both cases. Which is consistent with the drought occurred in this period. However,

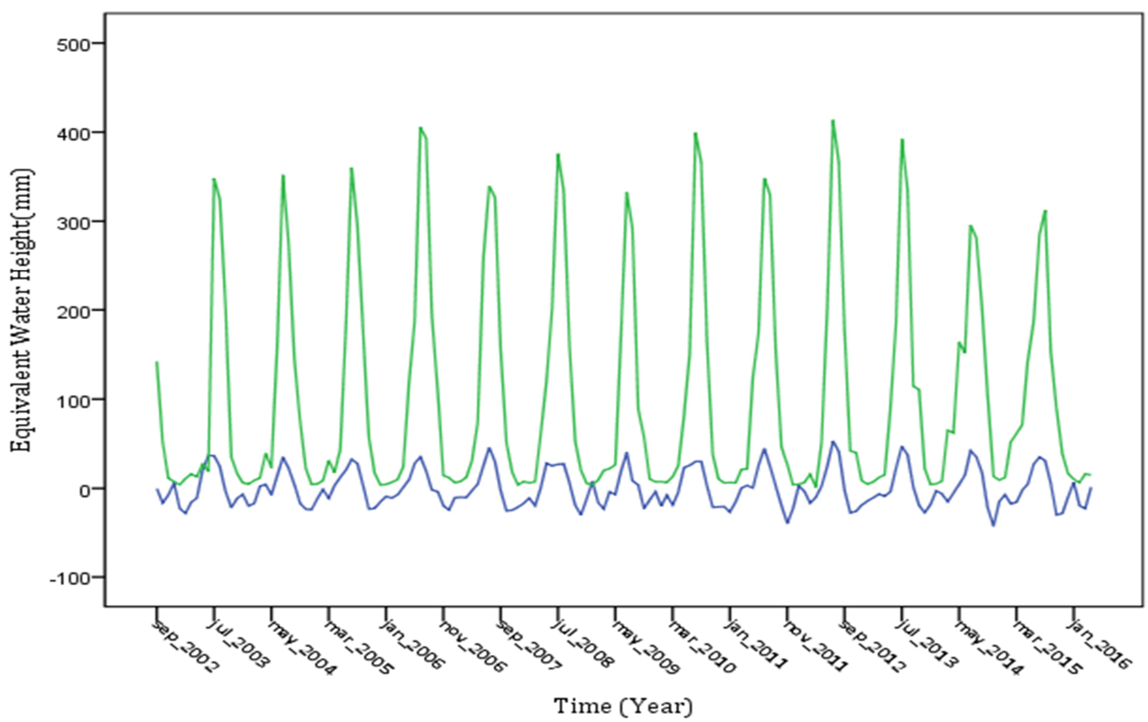

Figure 5.10: Comparison of rainfall variation from CHIRPS (green) and TWS variation from GRACE (blue)

during the period 2004 to 2005, trend of rainfall and TWS show a slight desiccation. A relatively conflicting trend occur during the period 2009, during this time TWS of the basin a slightly increasing trend but the precipitation of the basin show a significant decreasing trend. During the periods from 2010 to 2013, the trend shows no obvious change in TWS and precipitation. However, in 2014 a significant decreasing trend was observed which is consistent with reduction in rainfall in 2014. In 2015 to 2016, there is a slight decreasing trend in both cases.

The rainfall has large concentration during the period from Jun to August reaching its maximum peak in July while the TWS also increases during the period from May to august. Rainfall is relatively low during the period August to February, and it has minima in August while TWS shows a relatively lower record in the period from November to March. The lowest peak in total water storage is recorded in November. From this, we can concluded that, rainfall plays a primary role in governing the water mass balance of the Lake Tana sub basin, while other hydrological sink terms also controls the variability of water resource.

5.3.4. Ground water change of Lake Tana sub basin

Groundwater is one primary source of water in the region. Over exploitation of groundwater for irrigation, hydropower generation and other anthropogenic uses have posed challenge in water management. In-situ measurement of groundwater is limited as well as river gauge data are not available with complete spatial coverage so as to monitor the water mass balance in time scale.

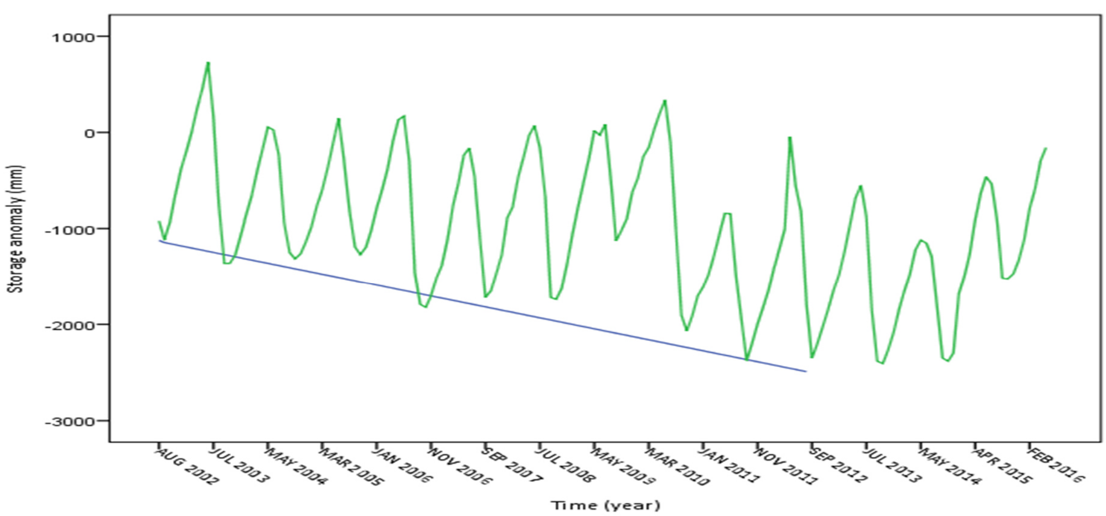

Figure 5.11: Time series of total catchment water storage from GRACE minus altimetry lake level for Lake Tana and best fitting line

Magnitude of change in groundwater depth is higher than that in the GRACE-derived total water storage anomaly. The trend of change in especially the groundwater depth data suggests that, the change in groundwater storage of the Lake Tana's sub-basin is predominantly in saturated storage.

CHAPTER SIX: CONCLUSIONS AND RECOMMENDATIONS

6.1. Conclusions

In this study, trend analysis of annual, seasonal and monthly water level for the period 1960 to 2017 were carried out for data measurement taken from a stations located at Bahir Dar city and data taken from satellite altimetry. Two non-parametric methods namely the Mann-Kendall test and the Sen's slope estimate were used for long-term trend analysis of hydrological signals.

The use of these methods allowed us to identify impact of anthropogenic activities on patterns of water quantity in time scale. The results of analysis pointed out that, at 5% significance level, the annual water lake trend of data has shown increasing trend while monthly analysis exhibited a highly increasing trend in the dry seasons (January, February, March, November and December) and slowly increasing trend in wet seasons of the area. The seasonal analysis of the lake level also shows a highly increasing trend in winter and spring seasons. While no trend was observed in summer seasons.

Comparative analysis of results of the two periods showed an increasing trend of the annual water level of the lake the period 1960 to 1996, but there is a statistically insignificant decreasing trend in the period (1997 to 2017). Results of the simulations indicate that anthropogenic activities are the major control now and increasingly will be in the future.

Knowledge of water volume variations in lakes and reservoirs is essential for water mass balance studies, water allocation, and water release strategies by the responsible agencies. This thesis aims to estimate water volume changes by combining water level data (satellite altimetry data + in-situ gauge measurements) and Landsat imagery. The study results demonstrate that, the time series of total water volume over the lake is obtained, whereby a positive trend with an average rate of 0.06km^3/yr is observed. However, the water volume variation of the lake shows different pattern when it was observed at different time phases. For the period spanning from 1984 to 2001, the water volume of the lake shows a positive and continuous trend by a magnitude of 0.148km^3/yr. This may be due less anthropogenic impact on the lake's water budget; the sub-basin was highly utilized since 1997. Prior to 1996, the hydrological cycles of the basin was predominately controlled by natural process: precipitation and evapotranspiration. The water volume of the lake has suddenly dropped of between 2002 and 2003 by an enormous amount than it has experienced ever. The volume of the lake water was reduced at a rate of 1.967km^3/yr. The loss of water in this particular case is thought to be caused by drought. On the other hand, for the period from 2000 to 2013, the water volume variation of the lake shows a slightly positive trend with a drastic decrement in 2010. A long term and continuous reduction of the water volume of the lake were recorded in the period 2013 to 2017, the water volume was reduced at a rate of 0.612km^3/yr.

We conclude, from our results that the drying up of the lake at the end of the study period has been occurring due to a chain of reasons, which are highly influenced by anthropogenic activities. Given the current negative trend in water volume loss, at 0.612 km^3/yr over the lake and the alarmingly low value for the remaining water volume in the lake, one can easily predict that the lake will completely disappear within twelve thousands of years if no countermeasures are taken. Approximately 3,400 Mm^3/yr of water will be diverted for hydropower and irrigation schemes if the likely future development (table 4.2) in the Lake Tana sub-basin is implemented. Consequently, the lake will be fall in danger and there will faster the disappearance of the lake. We acknowledge that there are uncertainties in our estimations and conclusions, which can be the scope of future works.

Total water storage change in Lake Tana sub basin was also successfully estimated for the period 2002 (August) to 2016 (May) using GRACE time varying gravity field. Total water storage derived from GRACE data was compared with satellite altimetry based derived volume variation of Lake Tana. We also try to compare GRACE change in total water storage with rainfall of the basin. We also estimate ground water change of the basin from auxiliary data obtained from GRACE. The result shows that, the TWS variation has a great seasonal behavior, and reach maximum in July and minimum in November. There is a correlation coefficient of 0.73 between GRACE and satellite altimetry, and 0.65 between GRACE and rainfall. From this, we concluded that the change in total water storage of the basin is dominated by the water volume change of the lake. Water volume variations of the lake and the sub-basin are highly dependent on precipitation. Moreover, the trend in the total water storage of the Tana sub basin is reduced at a rate of 0.0025mm/yr. Which is insignificant relative to the mass flux of the Lake Tana. The change in ground water of the sub basin also shows that, the basin loses its groundwater by a value of 101.3mm/yr. Which is statistically significant.

6.2. Recommendation

The time series analysis indicates an overall declining trend in water storage change in the lake and ground water storage in basin. Hence, the declining water reserve trend is evident. As a fact, a sustainable use of the water resource of the lake and the surrounding catchment should be based upon an informed decision on the overall aquifer storage and productivity. In addition, facilitation of water recharge mechanisms are highly recommended. For further application of the redistribution products to monitoring and evaluation of changes in water resources at local scale, it is recommended to evaluate the results using local ground based information on water balance of the lake.

In future, there is significant potential for further socioeconomic development based on increased utilization of water in the catchment. However, great care is needed to ensure that such development is sustainable and does not adversely affect those communities that depend on the natural resources of the lake and the rivers that feed into it. Any development should lay their base on Ethiopian law (through proclamation number 9/1995 passed in 2002) requires that, for all major development projects, an environmental impact assessment (EIA) is conducted and that environmental impacts should be minimized. Any development plan on the lake should consider its relation with the surrounding catchment. The response of lake in for increased discharge and sediment in flow should be further study from the perspective of change in storage of the lake.

Reference

Abebe, B., 1991 To Upgrade the Hydro-metrological Network in Ethiopia, 25th WEDC conference. Addis Ababa, Ethiopia.

Alexandra S. Richey, Brian F. Thomas2, Min-Hui Lo, John T. Reager, James S. Famiglietti, Katalyn Voss, Sean Swenson, and Matthew Rodell, 2015. Quantifying renewable groundwater stress with GRACE. Water Resour. Res., 51, 5217–5238, Doi: 10.1002/ 2015WR017349.

Alka Singh, Ujjwal Kumar and Florian Seitz, 2015. Remote Sensing of Storage Fluctuations of Poorly Gauged Reservoirs and State Space Model (SSM)-Based Estimation. Remote Sens. 2015, 7, 17113-17134; Doi: 10.3390/rs71215872.

Anteneh Z. Abiy, Assefa M. Melesse, 2017. Evaluation of watershed scale changes in groundwater and soil moisture storage with the application of GRACE satellite imagery data. Catena 153 (2017) 50–60.

Arkady Mikhailovich Deganovsky, Brook Abate Getahun, 2008. Water balance and level regime of Ethiopian lakes as integral indicators of climate change. The 12th world lake conference: 1093-1102.

Arthur W. Sichangi, Godfrey O. Makokha, 2017. Monitoring water depth, surface area and volume changes in Lake Victoria: integrating the bathymetry map and remote sensing data during 1993–2016. Model. Earth Syst. Environ. (2017) 3:533–538. Doi 10.1007/s40808-017-0311-2.

Asmare E, Sewmehon D, Dereje T, Mihret E, 2016. Impact of climate change and anthropogenic activities on livelihood of fishing community around Lake Tana, Ethiopia. J EC Cronicon Agric, 3(1): 548-557.

Behailu Berehanu, 2016. Hydrology of the Lake Tana Basin, Ethiopia: Implication to Groundwater-Surface Waters Interaction. Journal of Environment and Earth Science Vol.6, No.10, 2016.

Wale, T. H. M. Rientjes, A. S. M. Gieske, and H. A. Getachew, 2009. Ungauged catchment contributions to Lake Tana's water Balance. Doi: 10.1002/hyp.7284.

Chris Funk, Pete Peterson, Martin Landsfeld, Diego Pedreros, James Verdin, Shraddhanand Shukla2, Gregory Husak2, James Rowland1, Laura Harrison2, Andrew Hoell3 & Joel Michaelsen, 2015. The climate hazards infrared precipitation with stations new environmental record for monitoring extremes. Doi: 10.1038/sdata.2015.66.

Chunqiao Song, Bo Huang a, b, Linghong KeChunqiao Song, Bo Huang, Linghong Ke, 2013. Modeling and analysis of lake water storage changes on the Tibetan Plateau using multi-mission satellite data. Remote Sensing of Environment 135 (2013) 25-35. http://dx.doi.org/10.1016/j.rse.2013.03.013.

Cretaux, J.F., Birkett, S., 2006. Lake studies from satellite radar altimetry. Compt. Rend. Geosci. 338, 1098-1112.

Donald W. Meals, Jean Spooner, Steven A. Dressing, and Jon B. Harcum, 2011. Statistical Analysis for Monotonic Trends. Tech. Notes 6.

Dong Jiang, Jianhua Wang, Yaohuan Huang, 2014. The Review of GRACE Data Applications in Terrestrial Hydrology Monitoring. http://dx.doi.org/10.1155/2014/725131.

Dorothea Deus, Richard Gloaguen, Peter Krause, 2013. Water Balance Modeling in a Semi-Arid Environment with Limited in situ Data Using Remote Sensing in Lake Manyara, East African Rift, and Tanzania. Remote Sens. 2013, 5, 1651-1680; Doi: 10.3390/rs5041651.

Drolon, and Philippe Maisongrande, 2016. Lake volume monitoring from space Vol. 18, EGU2016-17964, 2016 EGU General Assembly 2016.

Dereje Tewabe, Erkie Asmare, Wondie Zelalem and Brehan Mohamed, 2016. Identification of impacts, some biology of water hyacinth (Eichhornia crassipes) and its management options in Lake Tana, Ethiopia. ISSN: 2315-9766.

Eric Muala, Yasir A. Mohamed, Zheng Duan and Pieter van der Zaag, 2014. Estimation of Reservoir Discharges from Lake Nasser and Roseires Reservoir in the Nile Basin Using Satellite Altimetry and Imagery Data. Remote Sens. 2014, 6, 7522-7545; Doi: 10.3390/rs6087522.

Essayas Kaba Ayana, 2007. Validation of radar altimetry lake level data and its application in water resource management. Msc Thesis.

F. Papa, A. Gu¨ntner, F. Frappart C. Prigent and W. B. Rossow, 2008. Variations of surface water extent and water storage in large river basins: A comparison of different global data sources. Doi: 10.1029/2008GL033857.

F. Baup, F. Frappart, and J. Maubant, 2014. Combining high-resolution satellite images and altimetry to estimate the volume of small lakes. Doi: 10.5194/hess-18-2007-2014.

Frappart, F., Seyler, F., Martinez, J. M., Leon, J. G., Cazenave, A., 2005. Floodplain water storage in the Negro River basin estimated from microwave remote sensing of inundation area and water levels. Remote Sensing of Environment, 99, 387-399.

GRDC, Temporal Distribution of Daily Data Stations, http://grdc.bafg.de/servlet/is/17/January 2017.

Getachew Tegegne, Dereje Hailu and Prof.Dr.S.Moses Aranganathan, 2013. Lake Tana Reservoir Water Balance Model. International Journal of Application or Innovation in Engineering & Management (IJAIEM), ISSN 2319 - 4847.

Goraw Goshu and Shimelis Aynalem, 2017. Problem Overview of the Lake Tana Basin. Doi 10.1007/978-3-319-45755-0_2.

Guillaume Ramillien, Frédéric Frappart, Lucia Seoane, 2014. Application of the Regional Water Mass Variations from GRACE Satellite Gravimetry to Large-Scale Water Management in Africa. Remote Sens. 2014, 6, 7379-7405; Doi: 10.3390/rs6087379.

Haris Hasan Khan, Arina Khan, Shakeel Ahmed, Marie-Claude Gennero, Kien Do Minh, Anny Cazenave, 2012. Terrestrial water dynamics in the lower Ganges estimates from ENVISAT and GRACE. Arab J Geosci (2013) 6:3693–3702, Doi: 10.1007/s12517-012-0629-z.

Helmi Saidi, Claudia dreSti, Marzia Cia Mpittiello, 2015. Fluctuations of Lake Orta water levels: preliminary analyses. J. Limnol., 2016; 75(s2): 86-92, Doi: 10.4081/jlimnol.2016.1230.

Hongbo Wu, Ninglian Wang, Xi Jiang, Zhongming Guo, 2014. Variations in water level and glacier mass balance in Nam Co Lake, Nyainqentanglha range, Tibetan Plateau, based on ICESat data for 2003–09. Annals of Glaciology 55(66) 2014 Doi: 10.3189/2014AoG66A100.

Huilin Gao, Charon Birkett, and Dennis P. Lettenmaier, 2014. Global monitoring of large reservoir storage from satellite remote sensing. Doi: 10.1029/2012WR012063, 2012.

Iris Konnerth, 2016. SWAT for Assessing Negative Impacts of Erosion in Lake Tana Basin. Msc thesis.

Jekeli C, 1980. Alternative method to smooth the Earth's gravity field, Dep. Of Geod. Sci. and Surv., Ohio State University, Columbus, Rep.327.

J.-F. Cre´taux, R. Abarca-del-Rı´o, M. Berge´-Nguyen, A. Arsen, V. Drolon, G. Clos, P. Maisongrande, 2016. Lake Volume Monitoring from Space. Surv Geophys (2016) 37:269–305, Doi: 10.1007/s10712-016-9362-6.

J. Wahr, S. Swenson, V. Zlotnicki and I. Velicogna, 2004. Time variable gravity from GRACE: first results," Geophysical Research Letters, vol. 31, no. 11, Article ID L11501, 2004.

Jean-François Crétaux, Sylvain Biancamaria, Adalbert Arsen, Murie Bergé-Nguyen and Mélanie Becker, 2015. Global surveys of reservoirs and lakes from satellites and regional application to the Syrdarya river basin. Environ. Res. Lett. 10 (2015) 015002, Doi:10.1088/1748-9326/10/1/015002.

Jean-Francois Crétaux, Rodrigo Abarca Del Rio, Muriel Berge-Nguyen, Adalbert Arsen, Vanessa Arthur W. Sichangi · Godfrey O. Makokha, 2017. monitoring water depth, surface are and volume changes in lake Victoria: integrating the bathymetry map and remote sensing data during 1993-2016. Model. Earth Syst. Environ. Doi: 10.1007/s40808-017-0311-2

Jun Magome, Hiroshiishidaira, Kuniyoshi Takeuchi, 2003. Method for satellite monitoring of water storage in reservoirs for efficient regional water management. IAHS Publ. no. 281, 2003.

Liu J, Wang Z, Gong T, Uygen T, 2012. Comparative analysis of hydro-climatic changes in glacier-fed rivers in the Tibet and Bhutan-Himalayas. Quat Int 282:104-112.

McCartney, M., Alemayehu, T., Shiferaw, A., Awulachew, S. B., 2010. Evaluation of current and future water resources development in the Lake Tana Basin, Ethiopia. Colombo, Sri Lanka: International Water Management Institute. 39p. (IWMI Research Report 134). Doi: 10.3910/2010. 204.

Mamaru A. Moges, Petra Schmitter, Essayas K. Ayana, Seifu A. Tilahun, Atikilt A. Ketema, Temesgen E. Nigussie, Teshale T. Danbera, Ahmed M. Hussien, Tammo S. Steenhuis, 2016. Water quality of Lake Tana by measuring and using Landsat 7 ETM+ Images, current and previous trends perspective. 4th International conference on the Advancement of Science and Technology ICAST, FCWRE, BIT, Bahir Dar University July 17th -18th 2016.

Martina Zele ˇnáková, Jaroslav Vido, Maria Manuela Portela, Pavol Purcz, Peter Blištán, Helena Hlavatá and Petr Hluštík, 2017. Precipitation Trends over Slovakia in the Period 1981-2013. Water 2017, 9, 922; Doi: 10.3390/w9120922.

Matthew Rodell, Jianli Chen, Hiroko Kato, James S. Famiglietti, 2006. Estimating groundwater storage changes in the Mississippi River basin (USA) using GRACE. Hydrogeology Journal (2007) 15: 159-166.

Melese Worku, 2017. Lake Tana as Biosphere Reserve: Review. Journal of Tourism & Hospitality, Doi: 10.4172/2167-0269.1000310.

Mekete Dessie, Niko E.C. Verhoest, Valentijn R.N. Pauwels, Enyew Adgo, Jozef Deckers, Jean Poesen, Jan Nyssen, 2014. Water balance of a lake with floodplain buffering: Lake Tana, Blue Nile Basin, Ethiopia. Journal of Hydrology 522 (2015) 174-86.

M.J. Tourian , O. Elmi, Q. Chen, B. Devaraju, Sh. Roohi, N. Sneeuw, 2014. A space borne multi sensor approach to monitor the desiccation of Lake Urmia in Iran. Remote Sensing of Environment 156 (2015) 349-360.

M. Shahzad Khattak, M. S. Babel1, M. Sharif, 2011. Hydro-meteorological trends in the upper Indus River basin in Pakistan. Vol. 46: 103-119, 2011 Doi: 10.3354/cr00957.

Michael Kizza, Ida Westerberg, Allan Rodhe, Henry K. Ntale, 2012. Estimating areal rainfall over Lake Victoria and its basin using ground-based and satellite data. Journal of Hydrology 464465 (2012) 401-411.

Michael T. Coe, Charon M. Birkett, 2004. Calculation of river discharge and prediction of lake height from satellite radar altimetry: Example for the Lake Chad basin, doi: 10.1029/2003WR002543, 2004.

René P. Mbanguka, Steve W. Lyon, Karin Holmgren, Marc Girons Lopez Jerker Jarsjö, 2016. Water Balance and Level Change of Lake Babati, Tanzania: Sensitivity to Hydro climatic Forcing. Water 2016, 8, 572; Doi: 10.3390/w8120572.

Robert Andrew, Huade Guan, Okke Batelaan, 2017. Estimation of GRACE water storage components by temporal Decomposition. Journal of Hydrology 552 (2017) 341-350.

Schmidt, R., Flechtner, F.; Meyer, U., Neumayer, K.-H., Dahle, Ch., Koenig, R.; Kusche, J. Hydrological signals observed by GRACE satellites. Surv. Geophysics. 200829, 319-334.

Sean Swenson, John Wahr, 2009. Monitoring the water balance of Lake Victoria, East Africa, from space Journal of Hydrology 370 (2009) 163-176.

Seleshi B. Awulachew, Teklu Erkossa, Vladimir Smakhtin and Ashra Fernando, 2009. Improved Water and Land Management in the Ethiopian Highlands: Its Impact on Downstream Stakeholders Dependent on the Blue Nile. Intermediate Results Dissemination Workshop February 5-6, 2009, Addis Ababa, Ethiopia.

Sen, P.K, 1968. Estimates of the regression coefficient based on Kendall’s tau. J. Am. Stat. Assoc. 1968, 63, 1379-1389.

Sheng Yue, Paul Pilon, Bob Phinne and George Cavadias, 2002. The influence of autocorrelation on the ability to detect trend in hydrological series. Hydrol. Process.16, 1807-1829, Doi: 10.1002/hyp.1095.

Sina Khatami, 2013. Nonlinear Chaotic and Trend Analyses of Water Level at Urmia Lake, Iran Does Climate Variability Explain Urmia Lake Depletion? Msc thesis.

Shimelis Gebriye Setegn, 2010. Modeling hydrological and hydrodynamic processes in Lake Tana basin, Ethiopia. Phd thesis.

Shin-Chan Han, Shum CK, Jekeli C, Chung-Yen Kuo, Clark Wilson and Ki-Weon Seo, 2005Non-isotropic filtering of GRACE temporal gravity for geophysical signal enhancement, Geophys. J. Int., 163, 18-25.

Shum CK, Han SC, Kuo C, Seo K., Wilson C, 2004. Assessment of GRACE time-variable gravity observable: a new filtering technique to enhance signal spatial resolutions, American Geophysical Union (AGU) Fall Meeting, San Francisco, USA.

S. Kebede, Y. Travi, T. Alemayehu, V. Marc. Water balance of Lake Tana and its sensitivity to fluctuations in rainfall, Blue Nile basin, Ethiopia, 2005. Journal of Hydrology 316 (2006) 233-247.

SPIE's, 1995. International Symposium on Optical Science, Engineering, and instrumentation, International Society for Optics and Photonics.

Tengfei Hu, Jingqiao Mao, Peipei Zhang, Diandian Xu, Weiyu Chen and Huichao Dai, 2017. Hydrological utilization of satellite precipitation estimates in a data-scarce lake region. Doi: 10.2166/ws.2017.223.

Teshale Tadesse Danbara, 2010. Deriving water quality indicator of Lake Tana, Ethiopia, from Landat 8. Msc thesis.

Tewabe D, 2015. Preliminary Survey of Water Hyacinth in Lake Tana, Ethiopia. Glob J Allergy 1(1): 103.

Tom H.M. Rientjes, Janaka B.U. Perera, Alemseged T. Haile, Ambro S.M. Gieske, Martijn J. Booij, and Paolo Reggiani, 2011. Hydrological Balance of Lake Tana, Upper Blue Nile Basin, Ethiopia. Doi: 10.1007/978-94-007-0689-7_3.

Tom H.M. Rientjes, Janaka B.U. Perera, Alemseged T. Haile, Ambro S.M. Gieske, Martijn J. Booij, and Paolo Reggiani, 2016. Hydrological Balance of Lake Tana, Upper Blue Nile Basin, Ethiopia. Doi: 10.1007/978-94-007-0689-7_3.

Wahr John M and Mery Molenaar, 1998. Hydrological and oceanic effects and their possible detection using GRACE time variability of the Earth's gravity field, J. Geophys. Res., 103 (B12), 30,205-30,229.

Wale, A., Rientjes, T. H. M., Gieske, A. S. M., & Getachew, H. A. (2009). Ungauged catchment contributions to Lake Tana's water balance. Hydrological Processes, 23, 3682-3693.

Wessel P, and Smith WHF, 1998New improved version of the Generic Mapping Tools Released, EOS Trans. AGU, 79, 579.

Xu, H. Q., 2006. Modification of normalized difference water index (NDWI) to enhance open water features in remotely sensed imagery. International Journal of Remote Sensing, 27, 3025-3033.

Yang Zhou, Shuanggen Jin, Robert Tenzer, Jialiang Feng, 2016. Water storage variations in the Poyang Lake Basin estimated from GRACE and satellite altimetry. Geodesy and geodynamics 2016, vol 7 no 2, 108-116.

Yirgalem A. Chebud and Assefa M. Melese, 2008. Hydrological water balance of Lake Tana, Ethiopia. https://www.researchgate.net/publication/281275226.

Yirgalem A. Chebud and Assefa M. Melesse, 2009. Modelling lake stage and water balance of Lake Tana, Ethiopia. Doi: 10.1002/hyp.7416.

Zeleňáková M., Blıšťan P., Hlavatá H, 2017. Rainfall distribution as a main factor influencing flood generation in the eastern Slovakia. CEST2017_00442.

Zemede Mulushewa Nigatu, Tom Rientjes, Alemseged Tamiru Haile, 2016 Hydrological Impact Assessment of Climate Change on Lake Tana's Water Balance, Ethiopia. American Journal of Climate Change, 2016, 5, 27-37.

Zemede Mulushewa Nigatu, 2013. Hydrological impact of climate change on Lake Tana water balance. Thesis.

Zheng Duan, W.G.M. Bastiaanssen, 2013. Estimating water volume variations in lakes and reservoirs from four operational satellite altimetry databases and satellite imagery data. Remote Sensing of Environment 134 (2013) 403-416.

Zheng Duan, 2014. Estimating Water Balance Components of Lakes and Reservoirs Using Various Open Access Satellite Databases. Phd thesis.

Appendix

Appendix A: Sample lake area estimated by MNDWI

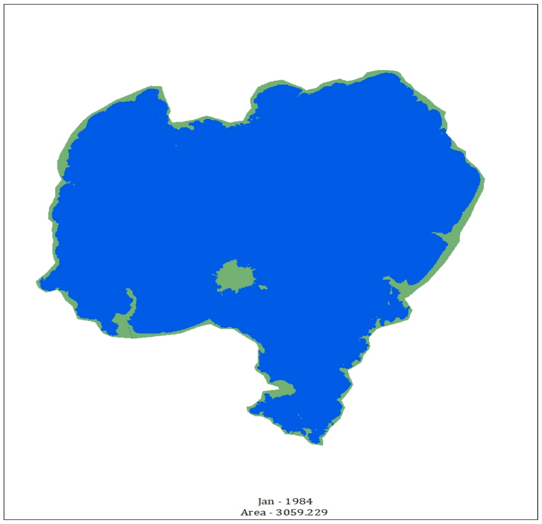

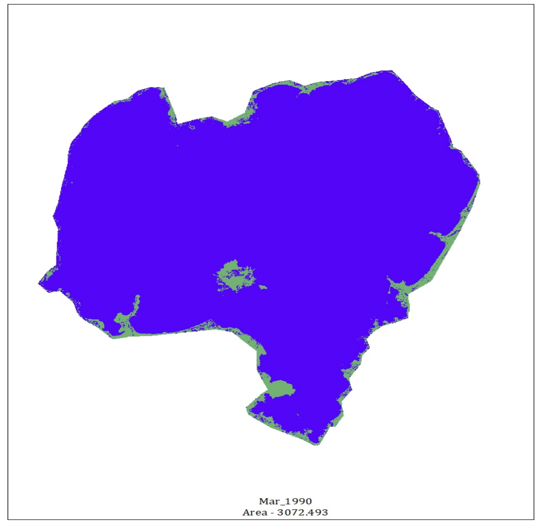

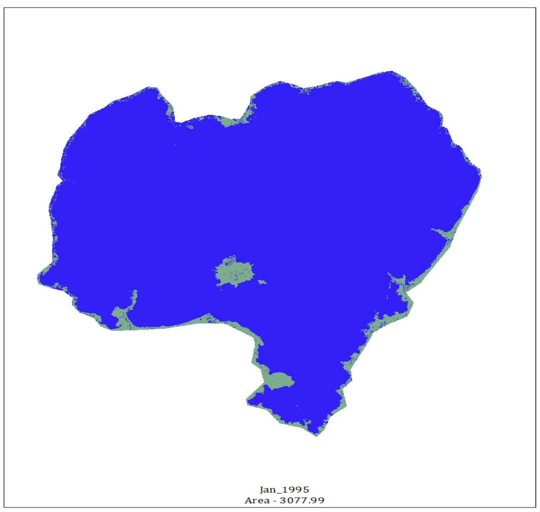

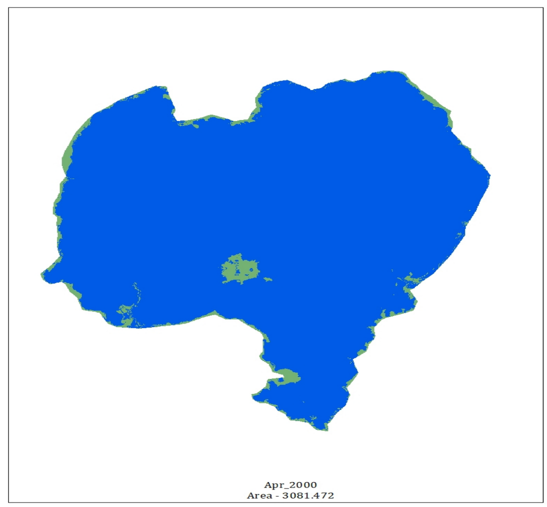

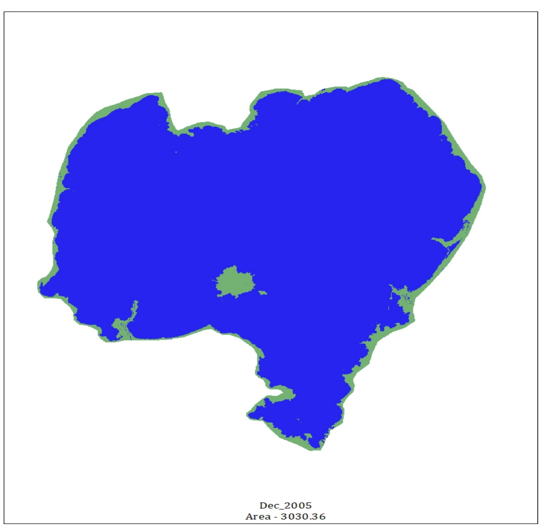

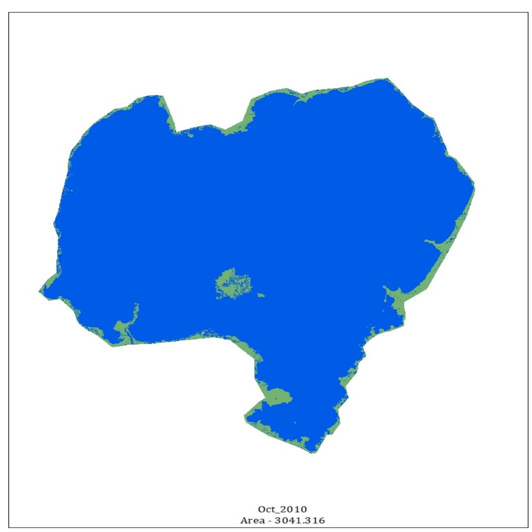

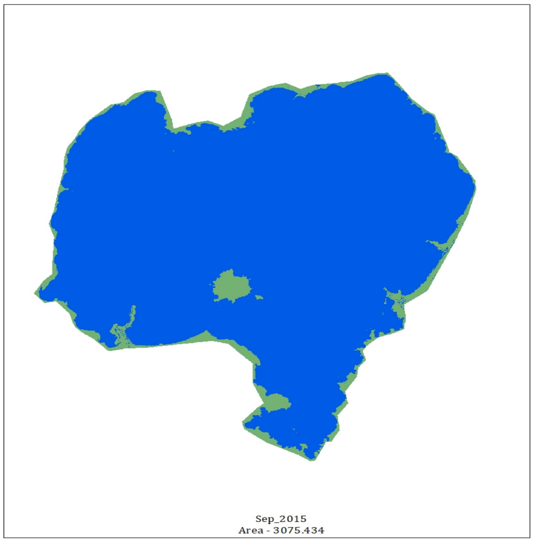

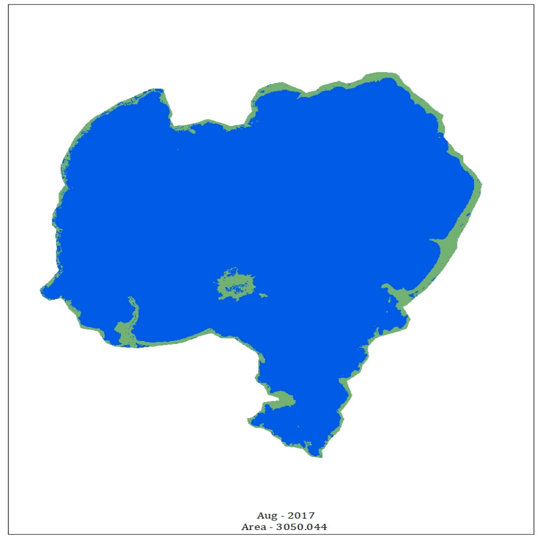

Appendix B: *In-situ* water level data for Lake Tana

year		Jan	Feb	Mar	Apr	May	Jun	Jul	Aug	Sep	Oct	Nov	Dec
	Mean	2.834	2.607	-	2.257	2.124	-	-	2.95	3.515	3.408	3.094	2.86
	Maximum	2.95	2.71	-	2.32	2.16	-	-	3.4	3.6	3.57	3.25	2.96
1960	Minimum	2.72	2.5	-	2.17	2.07	-	-	2.58	3.34	3.25	2.97	2.75
	Mean	2.638	2.476	2.318	2.141	1.954	1.827	2.212	3.112	3.753	3.626	3.308	3.067
	Maximum	2.75	2.53	2.41	2.25	2.06	2.05	2.53	3.56	3.82	3.77	3.6	3.19
1961	Minimum	2.53	2.41	2.23	2.07	1.83	1.78	2.02	2.56	3.57	3.47	3.1	2.94
	Mean	2.818	2.62	2.427	2.242	2.108	2.009	2.212	3.184	3.725	3.602	3.254	2.988
	Maximum	2.93	2.7	2.51	2.33	2.18	2.05	2.56	3.54	3.77	3.75	3.4	3.12
1962	Minimum	2.71	2.53	2.33	2.17	2.04	1.92	1.97	2.61	3.57	3.41	3.13	2.87
	Mean	2.681	2.508	2.304	2.119	1.985	1.939	2.305	3.373	3.935	3.765	3.421	3.113
	Maximum	2.76	2.59	2.41	2.2	2.06	2.03	2.81	3.77	4.02	3.88	3.61	3.28
1964	Minimum	2.59	2.42	2.2	2.04	1.92	1.89	1.99	2.83	3.78	3.62	3.29	2.96
	Mean	2.838	2.663	2.467	-	-	1.985	2.066	2.676	3.057	3.119	2.963	2.772
	Maximum	2.95	2.74	2.58	-	-	2.05	2.32	2.96	3.13	3.2	3.04	2.88
1965	Minimum	2.74	2.59	2.35	-	-	1.88	1.85	2.36	2.95	3.04	2.88	2.65
	Mean	2.575	2.41	2.247	2.076	1.936	1.878	2.056	2.683	3.208	3.122	2.924	2.704
	Maximum	2.66	2.53	2.32	2.19	2.02	1.99	2.33	3.06	3.3	3.19	3.05	2.82
1966	Minimum	2.48	2.34	2.14	2	1.84	1.78	1.86	2.29	3.08	3.05	2.82	2.6
	Mean	2.516	2.319	2.171	2.041	1.865	1.751	2.045	3.013	3.509	3.5	3.198	2.941
	Maximum	2.59	2.43	2.22	2.11	1.99	1.86	2.5	3.46	3.58	3.62	3.34	3.08
1967	Minimum	2.45	2.23	2.13	1.99	1.76	1.67	1.77	2.54	3.42	3.35	3	2.8
	Mean	2.704	2.499	2.319	2.118	1.954	1.966	2.375	3.075	3.393	3.265	3.002	2.785
	Maximum	2.79	2.6	2.39	2.23	2.01	2.08	2.73	3.4	3.48	3.42	3.11	2.9
1968	Minimum	2.61	2.4	2.22	2.01	1.9	1.91	2.07	2.76	3.3	3.12	2.91	2.67
	Mean	2.598	2.412	2.247	2.118	1.985	1.862	2.056	2.859	3.37	3.167	2.884	2.654
	Maximum	2.67	2.51	2.27	2.22	2.1	1.98	2.37	3.32	3.41	3.32	3.01	2.76
1969	Minimum	2.52	2.3	2.2	1.99	1.86	1.76	1.76	2.23	3.33	3.02	2.77	2.56
	Mean	2.467	2.317	2.156	1.967	1.806	1.677	1.859	2.599	3.159	3.117	2.91	2.668
	Maximum	2.56	2.38	2.24	2.06	1.96	1.77	2.14	3.01	3.22	3.16	3.04	2.78
1970	Minimum	2.38	2.25	2.07	1.86	1.71	1.57	1.64	2.16	3.04	3.04	2.78	2.56

	Mean	2.486	2.324	2.15	1.927	1.777	1.722	2.006	2.776	3.315	3.204	2.985	2.742
	Maximum	2.55	2.4	2.24	2.04	1.87	1.81	2.35	3.16	3.38	3.32	3.11	2.86
1971	Minimum	2.4	2.25	2.02	1.74	1.66	1.66	1.72	2.35	3.18	3.12	2.86	2.63
	Mean	2.545	2.377	2.2	2.007	1.847	1.714	2.025	2.471	2.793	2.754	2.577	2.393
	Maximum	2.62	2.47	2.29	2.09	1.94	1.85	2.19	2.69	2.85	2.83	2.67	2.49
1972	Minimum	2.48	2.29	2.1	1.88	1.76	1.59	1.78	2.22	2.7	2.67	2.49	2.31
	Mean	2.225	2.085	1.915	1.714	1.608	1.607	1.871	2.558	3.059	3.11	2.906	2.656
	Maximum	2.31	2.14	2.02	1.83	1.7	1.64	2.17	2.9	3.14	3.17	3.04	2.77
1973	Minimum	2.15	2.03	1.8	1.58	1.58	1.58	1.64	2.19	2.92	3.04	2.78	2.56
	Mean	2.476	2.304	2.134	1.939	1.842	1.897	2.311	3.052	3.585	3.443	3.082	2.824
	Maximum	2.56	2.38	2.3	2.02	1.88	1.99	2.65	3.38	3.64	3.62	3.24	2.93
1974	Minimum	2.39	2.23	2.03	1.86	1.81	1.86	1.98	2.67	3.38	3.26	2.94	2.72
	Mean	2.615	2.467	2.295	2.074	1.867	1.792	2.09	2.982	3.785	3.66	3.289	2.991
	Maximum	2.71	2.54	2.4	2.2	1.96	1.88	2.42	3.56	3.89	3.84	3.45	3.11
1975	Minimum	2.54	2.41	2.2	1.96	1.78	1.75	1.88	2.44	3.56	3.47	3.12	2.87
1976	Mean	2.754	2.554	2.351	2.16	2.018	1.938	2.224	3.068	3.509	3.305	3.059	2.825
	Mean	2.621	2.44	2.254	2.06	1.892	1.925	2.273	3.032	3.434	3.37	3.148	2.874
	Maximum	2.72	2.51	2.35	2.16	1.97	2.01	2.62	3.41	3.45	3.44	3.29	2.99
1977	Minimum	2.53	2.35	2.17	1.96	1.84	1.86	2.02	2.65	3.41	3.28	3	2.76
	Mean	2.655	2.46	2.275	2.105	2.003	1.909	2.238	2.952	3.328	3.246	2.975	2.742
	Maximum	2.75	2.55	2.36	2.17	2.06	1.97	2.59	3.22	3.38	3.33	3.11	2.85
1978	Minimum	2.56	2.37	2.18	2.05	1.93	1.88	1.99	2.63	3.25	3.11	2.86	2.65
	Mean	2.556	2.357	2.21	2.017	1.929	1.866	2.07	2.717	3.119	3.077	2.892	2.668
	Maximum	2.64	2.46	2.29	2.11	1.96	1.9	2.36	3	3.2	3.15	3	2.78
1979	Minimum	2.47	2.3	2.11	1.93	1.88	1.84	1.87	2.38	2.98	3.01	2.79	2.57
	Mean	2.48	2.303	2.131	1.984	1.826	1.762	2.053	2.817	3.211	3.148	2.89	2.676
	Maximum	2.56	2.38	2.23	2.06	1.9	1.83	2.4	3.12	3.26	3.22	3	2.78
1980	Minimum	2.38	2.23	2.06	1.92	1.76	1.74	1.83	2.42	3.12	3.02	2.79	2.59
	Mean	2.485	2.315	2.138	1.946	1.826	1.749	1.978	2.678	3.185	3.191	2.934	2.687
	Maximum	2.58	2.4	2.23	2.03	1.89	1.77	2.28	3	3.3	3.27	3.05	2.79
1981	Minimum	2.4	2.24	2.04	1.88	1.77	1.72	1.76	2.35	3.03	3.06	2.79	2.6
	Mean	2.506	2.331	2.259	2.055	1.916	1.794	1.897	2.509	2.893	2.969	2.784	2.559
	Maximum	2.59	2.42	2.33	2.15	1.99	1.83	2.13	2.78	2.95	3.01	2.9	2.67
1982	Minimum	2.43	2.25	2.17	1.97	1.83	1.76	1.79	2.15	2.79	2.91	2.67	2.47
	Mean	2.397	2.229	2.046	1.842	1.665	1.614	1.715	2.357	2.899	2.866	2.704	2.505
	Maximum	2.47	2.3	2.14	1.94	1.73	1.64	1.95	2.77	2.96	2.94	2.8	2.6
1983	Minimum	2.31	2.15	1.94	1.73	1.6	1.59	1.61	1.98	2.79	2.81	2.61	2.4
	Mean	2.316	2.168	2.008	1.838	1.689	1.692	1.96	2.528	2.939	2.98	2.818	2.648
	Maximum	2.4	2.23	2.09	1.93	1.74	1.78	2.21	2.73	3.04	3.04	2.9	2.74
1984	Minimum	2.24	2.11	1.93	1.75	1.65	1.64	1.78	2.24	2.75	2.9	2.68	2.58
	Mean	2.493	2.335	2.171	2.002	1.891	1.86	2.131	2.766	3.46	3.385	3.135	2.919
	Maximum	2.56	2.42	2.25	2.08	1.92	1.89	2.44	3.16	3.56	3.45	3.26	3.01
1985	Minimum	2.42	2.26	2.09	1.88	1.87	1.83	1.89	2.44	3.2	3.26	3.02	2.82
	Mean	2.716	2.548	2.378	2.179	1.978	1.899	2.244	2.887	3.338	3.332	3.053	2.813
	Maximum	2.82	2.62	2.47	2.27	2.07	2.02	2.58	3.16	3.44	3.43	3.21	2.91
1986	Minimum	2.62	2.46	2.29	2.08	1.88	1.86	2.04	2.6	3.16	3.22	2.92	2.74
	Mean	2.634	2.476	2.31	2.113	2.014	2.103	2.24	2.72	3.064	3.056	2.897	2.685
	Maximum	2.73	2.54	2.4	2.2	2.06	2.14	2.42	3	3.1	3.11	3	2.78
1987	Minimum	2.55	2.4	2.21	2.04	1.98	2.06	2.13	2.44	3	3	2.78	2.6
1988	Mean	2.498	2.321	2.155	1.974	1.81	1.755	2.122	3.245	3.687	3.559	3.267	2.965

	Maximum	2.59	2.4	2.26	2.1	1.87	1.77	2.75	3.62	3.72	3.63	3.42	3.09
	Minimum	2.4	2.26	2.07	1.87	1.75	1.74	1.76	2.8	3.62	3.38	3.1	2.85
	Mean	2.734	2.538	2.359	2.187	2.061	1.993	2.284	2.943	3.33	3.216	2.981	2.753
	Maximum	2.84	2.63	2.44	2.27	2.11	2.03	2.59	3.23	3.42	3.33	3.1	2.86
1989	Minimum	2.64	2.45	2.28	2.11	2.02	1.96	2.02	2.61	3.26	3.11	2.86	2.65
	Mean	2.563	2.394	2.22	2.041	1.863	1.737	1.894	2.557	3.084	3.083	2.831	2.435
	Maximum	2.64	2.48	2.3	2.14	1.95	1.78	2.16	2.9	3.16	3.18	2.94	2.53
1990	Minimum	2.48	2.31	2.13	1.94	1.78	1.68	1.71	2.18	2.91	2.96	2.72	2.34
	Mean	-	-	-	-	1.763	1.701	2.292	3.114	3.57	3.373	3.034	2.784
	Maximum	-	-	-	-	1.82	1.89	2.69	3.44	3.62	3.58	3.18	2.9
1991	Minimum	-	-	-	-	1.7	1.64	1.9	2.73	3.47	3.19	2.9	2.68
	Mean	2.582	2.415	2.233	2.07	1.955	1.834	2.032	2.755	3.275	3.253	3.091	2.837
	Maximum	2.67	2.5	2.31	2.16	2.02	1.88	2.4	3.15	3.34	3.31	3.21	2.96
1992	Minimum	2.5	2.32	2.16	2.01	1.89	1.8	1.86	2.31	3.16	3.22	2.97	2.7
	Mean	2.612	2.43	2.273	2.116	1.99	2.022	2.293	2.903	-	3.376	3.123	2.837
	Maximum	2.71	2.51	2.35	2.18	2.05	2.06	2.59	3.2	-	3.47	3.27	2.96
1993	Minimum	2.51	2.36	2.19	2.04	1.95	1.98	2.06	2.6	-	3.28	2.97	2.72
	Mean	2.626	2.444	2.255	2.052	1.927	1.93	2.543	3.419	3.694	3.252	2.911	2.686
	Maximum	2.71	2.53	2.35	2.14	1.98	2.01	2.95	3.72	3.77	3.6	3.08	2.78
1994	Minimum	2.55	2.36	2.14	1.97	1.86	1.85	2.14	2.88	3.56	3.08	2.78	2.57
	Mean	2.6	2.481	2.316	2.162	1.99	1.988	2.267	3.048	3.53	3.445	3.217	3.021
	Maximum	2.64	2.54	2.4	2.27	2.11	2.08	2.62	3.38	3.6	3.56	3.37	3.12
1995	Minimum	2.54	2.4	2.25	2.06	1.86	1.88	2	2.7	3.38	3.33	3.12	2.92
	Mean	2.863	2.676	2.639	2.378	2.3	2.416	2.755	3.663	4.174	4.002	3.667	3.424
	Maximum	2.94	2.75	2.68	2.48	2.36	2.6	3.19	4.06	4.26	4.16	3.79	3.54
1996	Minimum	2.75	2.61	2.51	2.34	2.25	2.27	2.32	3.16	4.04	3.82	3.56	3.3
	Mean	3.176	2.984	2.742	2.49	2.327	2.326	2.607	3.238	3.547	3.565	3.588	3.366
	Maximum	3.28	3.08	2.87	2.62	2.38	2.44	2.88	3.56	3.62	3.63	3.64	3.46
1997	Minimum	3.06	2.87	2.62	2.36	2.26	2.21	2.34	2.9	3.44	3.5	3.46	3.24
	Mean	3.116	2.895	2.722	2.568	2.414	2.356	2.649	3.526	4.218	4.106	3.782	3.424
	Maximum	3.26	3.04	2.81	2.67	2.48	2.42	3.01	3.97	4.3	4.21	3.96	3.59
1998	Minimum	3.02	2.82	2.62	2.48	2.35	2.29	2.36	3.03	4.06	3.96	3.61	3.25
	Mean	3.211	2.98	2.698	2.488	2.321	2.201	2.489	3.325	3.9	4.001	3.867	3.496
	Maximum	3.3	3.21	2.84	2.59	2.4	2.28	2.85	3.73	3.95	4.06	4.05	3.63
1999	Minimum	3.1	2.83	2.56	2.39	2.25	2.16	2.2	2.84	3.78	3.86	3.65	3.37
	Mean	3.268	3.019	2.826	2.635	2.504	2.457	2.766	3.523	4.002	3.994	3.829	3.539
	Maximum	3.38	3.13	2.94	2.7	2.58	2.66	3.08	3.92	4.06	4.03	3.96	3.68
2000	Minimum	3.16	2.94	2.72	2.56	2.4	2.34	2.5	3.13	3.92	3.95	3.66	3.39
	Mean	3.305	3.172	2.883	2.566	2.266	2.174	2.31	3.29	3.861	3.716	3.473	3.213
	Maximum	3.4	3.24	3.08	2.72	2.37	2.28	2.7	3.76	4	3.78	3.61	3.34
2001	Minimum	3.22	3.08	2.7	2.35	2.18	2.08	2.12	2.74	3.72	3.6	3.34	3.12
	Mean	2.899	2.635	2.351	2.067	1.783	1.577	1.765	2.38	2.823	2.775	2.545	2.298
	Maximum	3.05	2.78	2.5	2.24	2.05	1.68	2.05	2.7	2.91	2.9	2.69	2.41
2002	Minimum	2.77	2.5	2.24	1.93	1.63	1.5	1.56	2	2.64	2.67	2.42	2.16
	Mean	2.038	1.813	1.57	1.297	1.051	0.879	1.279	2.084	2.91	3.124	2.953	2.732
	Maximum	2.16	1.92	1.71	1.44	1.23	1	1.61	2.56	3.18	3.16	3.05	2.85
2003	Minimum	1.91	1.71	1.42	1.13	0.88	0.74	0.92	1.66	2.6	3.06	2.84	2.62
	minimum	2.509	2.265	2.03	1.776	1.553	1.374	1.708	2.431	2.944	3.074	2.979	2.792
	Mean	2.62	2.4	2.14	1.92	1.68	1.7	2	2.74	3.06	3.12	3.04	2.894
3004	Maximum	2.4	2.08	1.9	1.69	1.4	1.27	1.46	2	2.74	2.98	2.9	2.69

	Mean	2.595	2.415	2.209	1.953	1.699	1.521	1.797	2.376	2.835	3.027	2.863	2.666
	Maximum	2.71	2.5	2.321	2.08	1.84	1.59	2.07	2.62	3.02	3.08	2.98	2.78
2005	Minimum	2.48	2.33	2.1	1.82	1.58	1.43	1.53	2.02	2.64	2.98	2.76	2.54
	Mean	2.445	2.231	1.982	1.687	1.49	1.454	1.716	2.722	3.536	3.54	3.404	3.172
	Maximum	2.54	2.34	2.11	1.82	1.6	1.58	2.1	3.28	3.62	3.64	3.52	3.29
2006	Minimum	2.34	2.12	1.83	1.56	1.4	1.34	1.46	2.08	3.25	3.47	3.29	3.06

Appendix C: Altimetry data for Lake Tana

Mission	Date	Lake level	Mission	Date	Lake level
TOPEX	19920926	1.22	Jason	20050908	1.3
TOPEX	19921006	1.52	Jason	20050918	1.47
TOPEX	19921016	99.99 9	Jason	20050928	1.55
TOPEX	19921026	1.83	Jason	20051008	1.6
TOPEX	19921105	1.79	Jason	20051018	1.6
TOPEX	19921115	1.68	Jason	20051028	1.54
TOPEX	19921125	1.66	Jason	20051107	1.5
TOPEX	19921205	1.39	Jason	20051116	1.44
TOPEX	19921215	-0.54	Jason	20051126	1.35
TOPEX	19921225	0.95	Jason	20051206	1.28
TOPEX	19930103	0.91	Jason	20051216	1.2
TOPEX	19930113	1.24	Jason	20051226	1.15
TOPEX	19930123	0.92	Jason	20060105	1.05
TOPEX	19930202	0.73	Jason	20060115	1.04
TOPEX	19930212	1.09	Jason	20060125	0.97
TOPEX	19930222	1	Jason	20060204	0.84
TOPEX	19930304	0.95	Jason	20060214	0.84
TOPEX	19930314	0.9	Jason	20060224	0.71
TOPEX	19930324	0.82	Jason	20060306	0.65
POSDN	19930403	0.76	Jason	20060315	0.54
TOPEX	19930413	0.65	Jason	20060325	0.43
TOPEX	19930423	0.58	Jason	20060404	0.34
TOPEX	19930502	0.62	Jason	20060414	0.27
TOPEX	19930512	-0.05	Jason	20060424	0.16
TOPEX	19930522	0.18	Jason	20060504	0.12
TOPEX	19930601	0.54	Jason	20060514	0.05
TOPEX	19930611	0.64	Jason	20060524	0.02
TOPEX	19930621	0.49	Jason	20060603	0
TOPEX	19930701	0.68	Jason	20060613	0.05
TOPEX	19930711	0.84	Jason	20060623	0.06
POSDN	19930721	0.86	Jason	20060703	0.05
TOPEX	19930731	1.28	Jason	20060712	0.21
TOPEX	19930810	0.98	Jason	20060722	0.44
TOPEX	19930820	1.63	Jason	20060801	0.64
TOPEX	19930829	1.26	Jason	20060811	1.09
TOPEX	19930908	1.63	Jason	20060821	1.44
TOPEX	19930918	1.93	Jason	20060831	1.81
TOPEX	19930928	1.98	Jason	20060910	2.04
TOPEX	19931008	1.68	Jason	20060920	2.09
TOPEX	19931018	1.96	Jason	20060930	2.17
POSDN	19931028	99.99 9	Jason	20061010	2.13
TOPEX	19931107	1.74	Jason	20061020	1.97
TOPEX	19931117	1.73	Jason	20061030	2.02
TOPEX	19931127	1.55	Jason	99999999	99.99 9
TOPEX	19931207	1.45	Jason	20061118	1.95

TOPEX	19931217	0.73	Jason	20061128	1.81
TOPEX	19931226	1.37	Jason	20061208	1.75
TOPEX	19940105	0.83	Jason	20061218	1.72
TOPEX	19940115	1.24	Jason	20061228	1.65
TOPEX	19940125	1.12	Jason	20070107	1.58
TOPEX	19940204	1.09	Jason	20070117	1.46
TOPEX	19940214	1.1	Jason	20070127	1.34
TOPEX	19940224	0.98	Jason	20070206	1.26
TOPEX	19940306	0.92	Jason	20070216	1.21
POSDN	19940316	99.99 9	Jason	20070226	1.1
TOPEX	19940326	0.75	Jason	20070307	0.95
TOPEX	19940405	0.23	Jason	20070317	0.84
TOPEX	19940414	0.53	Jason	20070327	0.7
TOPEX	19940424	0.49	Jason	20070406	0.67
TOPEX	19940504	0.2	Jason	20070416	0.56
TOPEX	19940514	0.59	Jason	20070426	0.5
TOPEX	19940524	0.46	Jason	20070506	0.36
TOPEX	19940603	0.47	Jason	20070516	0.33
TOPEX	19940613	0.51	Jason	20070526	0.2
POSDN	19940623	99.99 9	Jason	20070605	0.21
TOPEX	19940703	0.71	Jason	20070615	0.21
TOPEX	19940713	0.84	Jason	20070624	0.24
TOPEX	19940723	1.04	Jason	20070704	0.38
TOPEX	19940802	99.99 9	Jason	20070714	0.59
TOPEX	19940811	1.69	Jason	20070724	0.75
TOPEX	19940821	1.54	Jason	20070803	1.03
TOPEX	19940831	2.28	Jason	20070813	1.3
TOPEX	19940910	2.3	Jason	20070823	1.49
TOPEX	19940920	2.1	Jason	20070902	1.74
TOPEX	19940930	99.999	Jason	20070912	1.97
TOPEX	19941010	2.16	Jason	20070922	1.96
TOPEX	19941020	1.89	Jason	20071002	1.89
TOPEX	19941030	1.77	Jason	20071012	1.84
POSDN	19941109	99.999	Jason	20071021	1.75
TOPEX	19941119	1.44	Jason	20071031	1.7
TOPEX	19941129	0.83	Jason	20071110	1.66
TOPEX	19941208	1.43	Jason	20071120	1.57
TOPEX	19941218	1.32	Jason	20071130	1.52
TOPEX	19941228	1.11	Jason	20071210	1.46
TOPEX	19950107	0.49	Jason	20071220	1.37
TOPEX	19950117	1.39	Jason	20071230	1.27
TOPEX	19950127	1.15	Jason	20080109	1.16
TOPEX	19950206	1.1	Jason	20080119	1.09
TOPEX	19950216	1.03	Jason	20080129	0.65
TOPEX	19950226	0.83	Jason	20080208	0.9
POSDN	19950308	0.94	Jason	20080217	0.88
TOPEX	19950318	0.67	Jason	20080227	0.73
TOPEX	19950328	0.89	Jason	20080308	0.67
TOPEX	19950406	0.34	Jason	20080318	0.51
TOPEX	19950416	0	Jason	20080328	0.39
TOPEX	19950426	0.72	Jason	20080407	0.33
POSDN	19950506	0.57	Jason	20080417	0.32
TOPEX	19950516	0.6	Jason	20080427	0.19
TOPEX	19950526	0.55	Jason	20080507	0.18
TOPEX	19950605	0.63	Jason	20080517	0.06
TOPEX	19950615	0.62	Jason	20080527	0.03
TOPEX	19950625	0.55	Jason	20080606	0.03

POSDN	19950705	0.62	Jason	20080615	-0.03
TOPEX	19950715	0.61	Jason	20080625	0.01
TOPEX	19950725	0.43	Jason	20080705	0.07
TOPEX	19950803	1.36	Jason	20080715	0.24
TOPEX	19950813	0.8	Jason	20080725	0.5
TOPEX	19950823	1.86	Jason	20080804	0.81
TOPEX	19950902	1.99	Jason	99999999	99.99 9
TOPEX	19950912	2.07	Jason	20080824	99.99 9
TOPEX	19950922	2.14	Jason	20080903	1.74
TOPEX	19951002	2.16	Jason	20080913	1.92
TOPEX	19951012	2	Jason	20080923	1.99
POSDN	19951022	1.94	Jason	20081003	1.97
TOPEX	19951101	1.78	Jason	20081012	1.87
TOPEX	19951111	1.76	Jason	20081022	1.82
TOPEX	19951121	1.73	Jason	20081101	1.79
TOPEX	99999999	99.999	Jason	20081111	1.77
TOPEX	19951210	1.16	Jason	20081121	1.69
TOPEX	19951220	1.14	Jason	20081201	1.57
TOPEX	19951230	1.56	Jason	20081211	1.51
TOPEX	19960109	1.42	Jason	20081221	1.39
TOPEX	19960119	1.39	Jason	20081231	1.33
TOPEX	19960129	1.34	Jason	20090110	1.27
TOPEX	19960208	1.28	Jason	20090120	1.14
POSDN	19960218	99.999	OSTM	20080715	0.28
TOPEX	19960228	-0.67	OSTM	20080725	99.99 9
TOPEX	19960309	0.87	OSTM	20080804	0.81
TOPEX	19960319	1.11	OSTM	20080814	1.27
TOPEX	19960328	0.87	OSTM	20080824	1.59
TOPEX	19960407	0.74	OSTM	20080903	99.99 9
TOPEX	19960417	1.1	OSTM	20080913	1.95
TOPEX	19960427	0.61	OSTM	20080923	1.97
TOPEX	19960507	0.85	OSTM	20081003	1.97
TOPEX	19960517	0.77	OSTM	20081012	1.9
TOPEX	19960527	0.83	OSTM	20081022	1.86
TOPEX	19960606	0.87	OSTM	20081101	1.71
POSDN	19960616	0.97	OSTM	20081111	1.74
TOPEX	19960626	0.48	OSTM	20081121	1.66
TOPEX	19960706	0.81	OSTM	20081201	1.58
TOPEX	19960715	0.93	OSTM	20081211	1.5
TOPEX	19960725	1.35	OSTM	20081221	1.41
TOPEX	19960804	1.44	OSTM	20081231	1.3
TOPEX	19960814	1.98	OSTM	20090110	1.23
TOPEX	19960824	2.04	OSTM	20090120	1.17
TOPEX	19960903	2.39	OSTM	20090130	1.05
TOPEX	19960913	2.82	OSTM	20090208	0.91
TOPEX	19960923	2.75	OSTM	20090218	0.92
TOPEX	19961003	2.76	OSTM	20090228	0.81
POSDN	19961013	2.58	OSTM	20090310	0.73
TOPEX	19961023	2.49	OSTM	20090320	0.65
TOPEX	19961102	1.99	OSTM	20090330	0.4
TOPEX	19961111	2.17	OSTM	20090409	0.45
TOPEX	19961121	2.13	OSTM	20090419	0.36
TOPEX	19961201	1.6	OSTM	20090429	0.18
TOPEX	19961211	1.58	OSTM	20090509	0.13
TOPEX	19961221	1.98	OSTM	20090519	-0.06
TOPEX	19961231	1.87	OSTM	20090529	-0.07
TOPEX	19970110	1.83	OSTM	20090607	-0.19

TOPEX	19970120	1.69	OSTM	20090617	-0.19
TOPEX	19970130	1.78	OSTM	20090627	-0.21
POSDN	19970209	1.57	OSTM	20090707	-0.14
TOPEX	19970219	1.5	OSTM	20090717	-0.03
TOPEX	19970301	1.46	OSTM	20090727	0.22
TOPEX	19970310	1.36	OSTM	20090806	0.4
TOPEX	19970320	1.2	OSTM	20090816	0.54
TOPEX	19970330	0.85	OSTM	20090826	0.85
TOPEX	19970409	1.05	OSTM	20090905	1.21
TOPEX	19970419	0.97	OSTM	20090915	1.28
TOPEX	19970429	0.9	OSTM	20090924	1.25
TOPEX	19970509	0.92	OSTM	20091004	1.19
TOPEX	19970519	0.81	OSTM	20091014	1.15
TOPEX	19970529	0.87	OSTM	20091024	1.1
TOPEX	99999999	99.99 9	OSTM	20091103	1.06
TOPEX	19970618	0.95	OSTM	20091113	0.94
TOPEX	19970628	0.69	OSTM	20091123	0.9
TOPEX	19970707	0.63	OSTM	20091203	0.84
TOPEX	19970717	1.1	OSTM	20091213	0.76
TOPEX	19970727	1.08	OSTM	20091223	0.56
POSDN	19970806	99.99 9	OSTM	20100102	0.6
TOPEX	19970816	1.87	OSTM	20100112	0.58
TOPEX	19970826	1.84	OSTM	20100121	0.5
TOPEX	19970905	2.13	OSTM	20100131	0.48
TOPEX	19970915	2.1	OSTM	20100210	0.39
TOPEX	19970925	2.14	OSTM	20100220	0.24
POSDN	19971005	2.08	OSTM	20100302	0.28
TOPEX	19971015	1.88	OSTM	20100312	0.16
TOPEX	19971025	2.09	OSTM	20100322	0.18
TOPEX	19971103	2.26	OSTM	20100401	0.05
TOPEX	19971113	2.23	OSTM	20100411	-0.01
TOPEX	19971123	2.08	OSTM	20100421	-0.05
TOPEX	19971203	2.02	OSTM	20100501	-0.14
TOPEX	19971213	1.94	OSTM	20100511	-0.13
TOPEX	19971223	1.79	OSTM	20100520	-0.2
TOPEX	19980102	1.78	OSTM	20100530	-0.25
TOPEX	19980112	1.65	OSTM	20100609	-0.25
POSDN	19980122	1.58	OSTM	20100619	-0.3
TOPEX	19980201	1.04	OSTM	20100629	-0.24
TOPEX	19980211	1.06	OSTM	20100709	-0.06
TOPEX	19980221	0.78	OSTM	20100719	0.15
TOPEX	19980302	1.34	OSTM	20100729	0.53
TOPEX	19980312	0.7	OSTM	20100808	0.82
TOPEX	19980322	1.24	OSTM	20100818	1.12
TOPEX	19980401	0.71	OSTM	20100828	1.52
TOPEX	19980411	1.18	OSTM	20100907	1.87
TOPEX	19980421	1.01	OSTM	20100916	2.09
TOPEX	19980501	0.97	OSTM	20100926	2.22
TOPEX	19980511	0.9	OSTM	20101006	2.23
POSDN	19980521	1.01	OSTM	20101016	2.24
TOPEX	19980531	0.76	OSTM	20101026	2.16
TOPEX	19980610	0.87	OSTM	20101105	2.1
TOPEX	19980619	0.76	OSTM	20101115	2.02
TOPEX	19980629	0.81	OSTM	20101125	1.95
TOPEX	19980709	1.18	OSTM	20101205	1.83
TOPEX	19980719	0.91	OSTM	20101215	1.84
POSDN	19980729	99.99 9	OSTM	20101225	1.74

TOPEX	19980808	1.55	OSTM	20110104	1.74
TOPEX	19980818	2.22	OSTM	20110113	1.67
TOPEX	19980828	2.44	OSTM	20110123	1.64
TOPEX	19980907	2.21	OSTM	20110202	1.61
TOPEX	19980917	2.84	OSTM	20110212	1.54
TOPEX	19980927	2.39	OSTM	20110222	1.42
TOPEX	19981007	2.8	OSTM	20110304	1.42
POSDN	19981016	99.99 9	OSTM	20110314	1.31
TOPEX	19981026	2.21	OSTM	20110324	1.24
TOPEX	19981105	2.1	OSTM	20110403	1.14
TOPEX	19981115	2.08	OSTM	20110413	1.14
TOPEX	19981125	2.18	OSTM	20110423	1.03
TOPEX	19981205	2.07	OSTM	20110503	0.92
TOPEX	19981215	1.77	OSTM	20110512	0.91
TOPEX	19981225	2.03	OSTM	20110522	0.84
TOPEX	19990104	1.82	OSTM	20110601	0.82
TOPEX	19990114	1.68	OSTM	20110611	0.92
POSDN	19990124	99.99 9	OSTM	20110621	0.94
TOPEX	19990203	1.68	OSTM	20110701	0.99
TOPEX	19990212	1.26	OSTM	20110711	1.01
TOPEX	19990222	1.59	OSTM	20110721	1.31
TOPEX	19990304	1.01	OSTM	20110731	1.41
TOPEX	19990314	1.1	OSTM	20110810	1.77
TOPEX	19990324	1.12	OSTM	20110820	2.16
TOPEX	19990403	0.97	OSTM	20110830	2.29
TOPEX	19990413	0.99	OSTM	20110908	2.44
POSDN	19990423	1.03	OSTM	20110918	2.59
TOPEX	19990503	0.88	OSTM	20110928	2.55
TOPEX	19990513	0.7	OSTM	20111008	2.49
TOPEX	19990523	0.9	OSTM	20111018	2.28
TOPEX	19990602	0.7	OSTM	20111028	2.24
TOPEX	19990611	0.68	OSTM	20111107	2.26
TOPEX	19990621	0.36	OSTM	20111117	2.03
TOPEX	19990701	-0.11	OSTM	20111127	2.03
TOPEX	19990711	0.98	OSTM	20111207	1.96
TOPEX	19990721	0.61	OSTM	20111217	1.88
TOPEX	19990731	1.37	OSTM	20111226	1.83
TOPEX	19990810	1.79	OSTM	20120105	1.79
TOPEX	19990820	1.81	OSTM	20120115	1.72
POSDN	19990830	99.99 9	OSTM	20120125	1.63
TOPEX	19990909	2.1	OSTM	20120204	1.52
TOPEX	19990919	2.57	OSTM	20120214	1.5
TOPEX	19990929	2.45	OSTM	20120224	1.44
TOPEX	19991008	2.09	OSTM	20120305	1.33
TOPEX	19991018	2.57	OSTM	20120315	1.26
TOPEX	19991028	2.57	OSTM	20120325	1.23
TOPEX	19991107	2.02	OSTM	20120404	1.13
TOPEX	19991117	2.04	OSTM	20120414	1.04
TOPEX	19991127	2.26	OSTM	20120423	0.96
POSDN	19991207	99.99 9	OSTM	20120503	0.88
TOPEX	19991217	2.01	OSTM	20120513	0.82
TOPEX	19991227	1.37	OSTM	20120523	0.71
TOPEX	20000106	1.87	OSTM	20120602	0.62
TOPEX	20000116	1.9	OSTM	20120612	0.54
TOPEX	20000126	1.71	OSTM	20120622	0.64
TOPEX	20000204	1.46	OSTM	20120702	0.7
TOPEX	20000214	0.92	OSTM	20120712	0.87

TOPEX	20000224	0.9	OSTM	20120722	1.18
TOPEX	20000305	1.47	OSTM	20120801	1.53
TOPEX	20000315	1.35	OSTM	20120811	1.8
TOPEX	20000325	1.36	OSTM	20120820	2.04
POSDN	20000404	99.99 9	OSTM	20120830	2.38
TOPEX	20000414	1.16	OSTM	20120909	2.48
TOPEX	20000424	1.1	OSTM	20120919	2.61
TOPEX	20000504	1.11	OSTM	20120929	2.48
TOPEX	20000514	0.97	OSTM	20121009	2.46
TOPEX	20000524	1.09	OSTM	20121019	2.33
TOPEX	20000602	0.93	OSTM	20121029	2.23
TOPEX	20000612	1.03	OSTM	20121108	2.21
TOPEX	20000622	1.07	OSTM	20121118	2.15
TOPEX	20000702	1.08	OSTM	20121128	2.05
TOPEX	20000712	1.22	OSTM	20121208	2.03
POSDN	20000722	1.33	OSTM	20121217	1.9
TOPEX	20000801	1.7	OSTM	20121227	1.86
TOPEX	20000811	1.86	OSTM	20130106	1.78
TOPEX	20000821	1.57	OSTM	20130116	1.72
TOPEX	20000831	2.46	OSTM	20130126	1.66
TOPEX	20000910	2.55	OSTM	20130205	1.61
TOPEX	20000919	2.39	OSTM	20130215	1.52
TOPEX	20000929	2.48	OSTM	20130225	1.49
TOPEX	20001009	1.92	OSTM	20130307	1.28
TOPEX	20001019	2.51	OSTM	20130317	1.31
POSDN	20001029	99.99 9	OSTM	99999999	99.99 9
TOPEX	20001108	2.47	OSTM	20130406	1.11
TOPEX	20001118	2.29	OSTM	20130415	1.03
TOPEX	20001128	2.13	OSTM	20130425	0.89
TOPEX	20001208	1.86	OSTM	20130505	0.8
TOPEX	20001218	1.66	OSTM	20130515	0.74
TOPEX	20001228	1.71	OSTM	20130525	0.63
TOPEX	20010107	1.46	OSTM	20130604	0.59
POSDN	20010116	1.85	OSTM	20130614	0.58
TOPEX	20010126	1.89	OSTM	20130624	0.62
TOPEX	20010205	1.72	OSTM	20130704	0.72
TOPEX	20010215	1.71	OSTM	20130714	0.9
TOPEX	20010225	1.55	OSTM	20130724	1.28
TOPEX	20010307	0.84	OSTM	20130803	1.65
TOPEX	20010317	1.39	OSTM	20130812	2.02
TOPEX	20010327	1.27	OSTM	20130822	2.31
TOPEX	20010406	0.91	OSTM	20130901	2.5
TOPEX	20010416	1.05	OSTM	99999999	99.99 9
TOPEX	20010426	0.54	OSTM	20130921	2.59
TOPEX	20010506	0.59	OSTM	20131001	2.49
TOPEX	20010515	0.46	OSTM	20131011	2.63
TOPEX	20010525	0.76	OSTM	20131021	2.58
TOPEX	20010604	0.73	OSTM	20131031	2.5
TOPEX	20010614	0.72	OSTM	20131110	2.48
TOPEX	20010624	0.35	OSTM	20131120	2.35
TOPEX	20010704	0.84	OSTM	20131130	2.34
TOPEX	20010714	0.88	OSTM	20131209	2.24
TOPEX	20010724	0.98	OSTM	20131219	2.19
TOPEX	20010803	1.41	OSTM	20131229	2.09
TOPEX	20010813	1.79	OSTM	20140108	2
TOPEX	20010823	2.18	OSTM	20140118	1.96
TOPEX	20010902	2.28	OSTM	20140128	1.84

TOPEX	20010911	2.45	OSTM	20140207	1.83
TOPEX	20010921	2.5	OSTM	20140217	1.68
TOPEX	20011001	2.11	OSTM	20140227	1.68
TOPEX	20011011	2.3	OSTM	20140309	1.59
TOPEX	20011021	2.1	OSTM	20140319	1.59
TOPEX	20011031	2.04	OSTM	20140328	1.47
TOPEX	20011110	1.99	OSTM	20140407	1.35
TOPEX	20011120	1.87	OSTM	20140417	1.33
TOPEX	20011130	1.88	OSTM	20140427	1.15
TOPEX	20011210	1.73	OSTM	20140507	1.17
TOPEX	20011220	1.71	OSTM	20140517	1.18
TOPEX	20011230	1.7	OSTM	20140527	1.21
TOPEX	20020108	1.59	OSTM	20140606	1.26
TOPEX	20020118	1.54	OSTM	20140616	1.19
TOPEX	20020128	1.27	OSTM	20140626	1.19
TOPEX	20020207	1.36	OSTM	20140706	1.28
TOPEX	20020217	1.09	OSTM	20140716	1.4
TOPEX	20020227	1.03	OSTM	20140725	1.49
TOPEX	20020309	1.01	OSTM	20140804	1.76
TOPEX	20020319	0.81	OSTM	20140814	2.04
TOPEX	20020329	0.71	OSTM	20140824	2.11
TOPEX	20020408	0.73	OSTM	20140903	2.34
TOPEX	20020418	0.4	OSTM	20140913	2.61
TOPEX	20020428	0.53	OSTM	20140923	2.6
TOPEX	20020507	0.2	OSTM	20141003	2.5
TOPEX	20020517	0.18	OSTM	20141013	2.63
TOPEX	20020527	0.14	OSTM	20141023	2.56
TOPEX	20020606	0.23	OSTM	20141102	2.54
TOPEX	20020616	0.11	OSTM	20141112	2.42
TOPEX	20020626	0.19	OSTM	20141121	2.29
POSDN	20020706	99.99 9	OSTM	20141201	2.17
TOPEX	20020716	99.99 9	OSTM	20141211	2.15
TOPEX	20020726	0.52	OSTM	20141221	2.08
TOPEX	20020805	0.59	OSTM	20141231	2.01
Jason	20020118	1.47	OSTM	20150110	1.82
Jason	20020128	1.36	OSTM	20150120	1.83
Jason	20020207	1.22	OSTM	20150130	1.67
Jason	20020217	1.2	OSTM	20150209	1.6
Jason	20020227	0.91	OSTM	20150219	1.56
Jason	20020309	0.97	OSTM	20150301	1.48
Jason	20020319	0.77	OSTM	20150311	1.41
Jason	20020329	0.75	OSTM	20150320	1.22
Jason	20020408	0.68	OSTM	20150330	1.17
Jason	20020418	0.61	OSTM	20150409	1.09
Jason	20020428	0.5	OSTM	20150419	0.95
Jason	20020507	0.4	OSTM	20150429	0.85
Jason	20020517	0.31	OSTM	20150509	0.74
Jason	20020527	0.18	OSTM	20150519	0.68
Jason	20020606	0.03	OSTM	20150529	0.65
Jason	20020616	0.12	OSTM	20150608	0.55
Jason	20020626	0.18	OSTM	20150618	0.52
Jason	20020706	0.19	OSTM	20150628	0.5
Jason	20020716	0.25	OSTM	20150708	0.54
Jason	20020726	0.46	OSTM	20150717	0.67
Jason	20020805	0.67	OSTM	20150727	0.72
Jason	20020815	0.96	OSTM	20150806	0.66
Jason	20020825	1.13	OSTM	20150816	1.13

Jason	20020903	1.32	OSTM	20150826	1.33
Jason	20020913	1.37	OSTM	20150905	1.57
Jason	20020923	1.42	OSTM	20150915	1.74
Jason	20021003	1.3	OSTM	20150925	1.75
Jason	20021013	1.36	OSTM	20151005	1.67
Jason	20021023	1.23	OSTM	20151015	1.72
Jason	20021102	1.14	OSTM	20151025	1.61
Jason	20021112	1.15	OSTM	20151104	1.61
Jason	20021122	0.97	OSTM	20151113	1.58
Jason	20021202	1	OSTM	20151123	1.56
Jason	20021212	0.9	OSTM	20151203	1.45
Jason	20021221	0.74	OSTM	20151213	1.43
Jason	20021231	0.71	OSTM	20151223	1.36
Jason	20030110	0.71	OSTM	20160102	1.3
Jason	20030120	0.57	OSTM	20160112	1.19
Jason	20030130	0.47	OSTM	20160122	1.13
Jason	20030209	0.44	OSTM	20160201	1.02
Jason	20030219	0.29	OSTM	20160211	0.83
Jason	20030301	0.22	OSTM	20160221	0.82
Jason	20030311	0.17	OSTM	20160301	0.78
Jason	20030321	0.1	OSTM	20160311	0.65
Jason	20030331	0.01	OSTM	20160321	0.59
Jason	20030410	-0.16	OSTM	20160331	0.53
Jason	20030419	-0.21	OSTM	20160410	0.45
Jason	20030429	-0.28	OSTM	20160420	0.37
Jason	20030509	-0.41	OSTM	20160430	0.23
Jason	20030519	-0.47	OSTM	20160510	0.28
Jason	20030529	-0.59	OSTM	20160520	0.19
Jason	20030608	-0.65	OSTM	20160530	0.17
Jason	20030618	-0.56	OSTM	20160609	0.04
Jason	20030628	-0.57	OSTM	20160619	0.01
Jason	20030708	-0.38	OSTM	20160628	0.12
Jason	20030718	-0.13	OSTM	20160708	0.25
Jason	20030728	0.02	OSTM	20160718	0.5
Jason	20030807	0.33	OSTM	20160728	0.75
Jason	20030816	0.68	OSTM	20160807	1.08
Jason	20030826	0.94	OSTM	20160817	1.4
Jason	20030905	1.12	OSTM	20160827	1.68
Jason	20030915	1.48	OSTM	20160906	1.9
Jason	20030925	1.53	OSTM	20160916	1.97
Jason	20031005	1.59	OSTM	20160926	2.04
Jason	20031015	1.59	JASN3	20160221	0.83
Jason	20031025	1.62	JASN3	20160301	0.76
Jason	20031104	1.52	JASN3	20160311	0.68
Jason	20031114	1.48	JASN3	20160321	0.63
Jason	99999999	99.99 9	JASN3	20160331	0.57
Jason	20031204	1.4	JASN3	20160410	0.49
Jason	20031213	1.32	JASN3	20160420	0.34
Jason	20031223	1.18	JASN3	20160430	0.23
Jason	20040102	1.14	JASN3	20160510	0.25
Jason	20040112	1.05	JASN3	20160520	0.22
Jason	20040122	99.99 9	JASN3	20160530	0.15
Jason	20040201	0.91	JASN3	20160609	0.06
Jason	20040211	0.89	JASN3	20160619	0.02
Jason	20040221	0.79	JASN3	20160628	0.14
Jason	20040302	0.69	JASN3	20160708	0.25
Jason	20040312	0.62	JASN3	20160718	0.49

Jason	20040322	0.56	JASN3	20160728	0.74
Jason	20040401	0.45	JASN3	20160807	99.99 9
Jason	20040410	0.38	JASN3	20160817	1.38
Jason	20040420	0.26	JASN3	20160827	1.65
Jason	20040430	0.22	JASN3	20160906	1.9
Jason	20040510	0.12	JASN3	20160916	1.99
Jason	20040520	0.04	JASN3	20160926	2
Jason	20040530	-0.02	JASN3	20161006	2.04
Jason	20040609	-0.08	JASN3	20161016	2.07
Jason	20040619	-0.14	JASN3	20161025	2.05
Jason	20040629	-0.01	JASN3	20161104	1.98
Jason	20040709	0.09	JASN3	20161114	1.97
Jason	20040719	0.32	JASN3	20161124	1.87
Jason	20040729	0.52	JASN3	20161204	1.83
Jason	20040807	0.82	JASN3	20161214	1.75
Jason	20040817	1.06	JASN3	20161224	1.68
Jason	20040827	1.2	JASN3	20170103	99.99 9
Jason	20040906	1.35	JASN3	20170113	1.54
Jason	20040916	1.46	JASN3	20170123	1.43
Jason	20040926	1.59	JASN3	20170202	1.42
Jason	20041006	1.62	JASN3	20170212	1.39
Jason	20041016	1.71	JASN3	20170221	1.34
Jason	20041026	1.55	JASN3	20170303	99.99 9
Jason	20041105	1.58	JASN3	20170313	1.14
Jason	20041115	1.54	JASN3	20170323	0.94
Jason	20041125	1.45	JASN3	20170402	0.99
Jason	20041204	1.47	JASN3	20170412	0.96
Jason	20041214	1.35	JASN3	20170422	0.84
Jason	20041224	1.28	JASN3	20170502	0.76
Jason	20050103	1.25	JASN3	20170512	0.69
Jason	20050113	1.19	JASN3	20170522	0.74
Jason	20050123	1.15	JASN3	20170601	0.64
Jason	20050202	1.08	JASN3	20170611	0.68
Jason	20050212	0.89	JASN3	20170620	0.62
Jason	20050222	0.92	JASN3	20170630	0.7
Jason	20050304	0.86	JASN3	20170710	0.83
Jason	20050314	0.87	JASN3	20170720	1.1
Jason	20050323	0.73	JASN3	20170730	1.32
Jason	20050402	0.66	JASN3	20170809	1.6
Jason	20050412	0.56	JASN3	20170819	1.95
Jason	20050422	0.52	JASN3	20170829	2.18
Jason	20050502	0.36	JASN3	20170908	2.39
Jason	20050512	0.24	JASN3	20170918	99.99 9
Jason	20050522	0.21	JASN3	20170928	2.54
Jason	20050601	0.12	JASN3	20171008	2.34
Jason	20050611	0.07	JASN3	20171017	2.51
Jason	20050621	-0.04	JASN3	20171027	2.49
Jason	20050701	0.14	JASN3	20171106	2.44
Jason	20050711	0.29	JASN3	20171116	2.34
Jason	20050720	0.36	JASN3	20171126	2.3
Jason	20050730	0.62	JASN3	20171206	2.1
Jason	20050809	0.8	JASN3	20171216	2.11
Jason	20050819	0.92	JASN3	20171226	2.03
Jason	20050829	1.11			

Appendix D: spectrally analyzed GRACE gravity anomaly for Lake Tana Basin

Data(monthly)	Gravity anomaly (mm)	Stdv.	MSE
aug_2002_CNES-apr_2003_CNES.grd:	0.003835	0.000352563	0.0038485
sep_2002_CNES-apr_2003_CNES.grd:	0.004272	0.000322968	0.0042826
oct_2002_CNES-apr_2003_CNES.grd:	0.003805	0.000272046	0.0038126
nov_2002_CNES-apr_2003_CNES.grd:	0.002909	0.000280142	0.0029206
jan_2003_CNES-apr_2003_CNES.grd:	0.003428	4.59E-05	0.0034284
feb_2003_CNES-apr_2003_CNES.grd:	0.001302	3.15E-05	0.0013024
mar_2003_CNES-apr_2003_CNES.grd:	0.001078	3.15E-05	0.0010787
apr_2003_CNES-apr_2003_CNES.grd:	0	0.00E+00	0
may_2003_CNES-apr_2003_CNES.grd:	0.000183	8.63E-05	0.0001993
jul_2003_CNES-apr_2003_CNES.grd:	0.003286	0.000328495	0.0032994
aug_2003_CNES-apr_2003_CNES.grd:	0.004801	0.000393034	0.0048148
sep_2003_CNES-apr_2003_CNES.grd:	0.005341	0.000451413	0.0053565
oct_2003_CNES-apr_2003_CNES.grd:	0.004506	0.000381002	0.0045198
nov_2003_CNES-apr_2003_CNES.grd:	0.00352	0.000227283	0.0035258
dec_2003_CNES-apr_2003_CNES.grd:	0.003571	0.000167152	0.0035738
jan_2004_CNES-apr_2003_CNES.grd:	0.00297	7.39E-05	0.0029711
feb_2004_CNES-apr_2003_CNES.grd:	0.001923	9.26E-05	0.0019245
apr_2004_CNES-apr_2003_CNES.grd:	0.002126	4.59E-05	0.0021265
may_2004_CNES-apr_2003_CNES.grd:	0.001933	0.000120019	0.0019359
jun_2004_CNES-apr_2003_CNES.grd:	0.001516	0.000161099	0.0015228
jul_2004_CNES-apr_2003_CNES.grd:	0.003133	0.0002827889	0.0031438
aug_2004_CNES-apr_2003_CNES.grd:	0.004445	0.000365022	0.0044579
sep_2004_CNES-apr_2003_CNES.grd:	0.005015	0.000392559	0.0050278
oct_2004_CNES-apr_2003_CNES.grd:	0.004801	0.000363488	0.0048129
nov_2004_CNES-apr_2003_CNES.grd:	0.003601	0.00024107	0.0036078
dec_2004_CNES-apr_2003_CNES.grd:	0.002848	0.000142706	0.0028513
jan_2005_CNES-apr_2003_CNES.grd:	0.001607	8.34E-05	0.0016091
feb_2005_CNES-apr_2003_CNES.grd:	0.001872	3.15E-05	0.001872
mar_2005_CNES-apr_2003_CNES.grd:	0.001516	2.49E-05	0.0015159
apr_2005_CNES-apr_2003_CNES.grd:	0.000946	3.34E-05	0.0009465
may_2005_CNES-apr_2003_CNES.grd:	0.00178	0.000105127	0.0017828
jun_2005_CNES-apr_2003_CNES.grd:	0.001984	0.00025823	0.0019976
jul_2005_CNES-apr_2003_CNES.grd:	0.00351	0.000353267	0.0035243
aug_2005_CNES-apr_2003_CNES.grd:	0.00472	0.000409739	0.0047348
sep_2005_CNES-apr_2003_CNES.grd:	0.005839	0.000504295	0.0058571
oct_2005_CNES-apr_2003_CNES.grd:	0.004964	0.000462688	0.0049821
nov_2005_CNES-apr_2003_CNES.grd:	0.003906	3.51681E+11	9.194E+10
dec_2005_CNES-apr_2003_CNES.grd:	0.003092	0.000147834	0.0030954
jan_2006_CNES-apr_2003_CNES.grd:	0.002635	7.14E-05	0.0026355
feb_2006_CNES-apr_2003_CNES.grd:	0.00234	8.34E-05	0.0023409
mar_2006_CNES-apr_2003_CNES.grd:	0.001729	3.15E-05	0.0017296
apr_2006_CNES-apr_2003_CNES.grd:	0.00174	5.11E-05	0.0017401
may_2006_CNES-apr_2003_CNES.grd:	0.001821	0.000170097	0.0018275
jun_2006_CNES-apr_2003_CNES.grd:	0.002543	0.000257989	0.002554
jul_2006_CNES-apr_2003_CNES.grd:	0.004171	0.000379532	0.0041851
aug_2006_CNES-apr_2003_CNES.grd:	0.005493	0.000488281	5.511E+11
sep_2006_CNES-apr_2003_CNES.grd:	0.005788	0.000491955	0.0058056
oct_2006_CNES-apr_2003_CNES.grd:	0.005341	0.000449759	0.0053563
nov_2006_CNES-apr_2003_CNES.grd:	0.005493	0.000479038	0.0055105
dec_2006_CNES-apr_2003_CNES.grd:	0.003713	0.000297553	0.0037229
jan_2007_CNES-apr_2003_CNES.grd:	0.003469	0.000161099	0.0034719
feb_2007_CNES-apr_2003_CNES.grd:	0.002848	0.000120019	0.0028504
mar_2007_CNES-apr_2003_CNES.grd:	0.002635	7.14E-05	0.0026355
apr_2007_CNES-apr_2003_CNES.grd:	0.001994	9.19E-05	0.0019956
may_2007_CNES-apr_2003_CNES.grd:	0.002431	0.000161099	0.0024357

jun_2007_CNES-apr_2003_CNES.grd:	0.002411	0.000290799	0.0024255
jul_2007_CNES-apr_2003_CNES.grd:	0.004578	0.000422864	0.0045939
aug_2007_CNES-apr_2003_CNES.grd:	0.006256	0.000451413	0.0062697
sep_2007_CNES-apr_2003_CNES.grd:	0.00709	0.000550558	0.007108
oct_2007_CNES-apr_2003_CNES.grd:	0.006042	0.000509196	0.0060603
nov_2007_CNES-apr_2003_CNES.grd:	0.004974	0.000396963	0.0049875
dec_2007_CNES-apr_2003_CNES.grd:	0.003998	0.000210549	0.0040024
jan_2008_CNES-apr_2003_CNES.grd:	0.003215	0.000126074	0.0032166
feb_2008_CNES-apr_2003_CNES.grd:	0.002584	9.97E-05	0.0025854
mar_2008_CNES-apr_2003_CNES.grd:	0.002299	3.15E-05	0.0022992
apr_2008_CNES-apr_2003_CNES.grd:	0.000966	2.49E+00	0.0009667
may_2008_CNES-apr_2003_CNES.grd:	0.00237	0.000161099	0.0023748
jun_2008_CNES-apr_2003_CNES.grd:	0.003326	0.00025823	0.0033348
jul_2008_CNES-apr_2003_CNES.grd:	0.004486	0.000342559	0.004497
aug_2008_CNES-apr_2003_CNES.grd:	0.005585	0.000480204	0.0056019
sep_2008_CNES-apr_2003_CNES.grd:	0.006795	0.000515979	0.0068116
oct_2008_CNES-apr_2003_CNES.grd:	0.006114	0.00052987	0.0061328
nov_2008_CNES-apr_2003_CNES.grd:	0.005219	0.000369754	0.0052294
dec_2008_CNES-apr_2003_CNES.grd:	0.003632	0.000217511	0.003637
jan_2009_CNES-apr_2003_CNES.grd:	0.004232	0.000142706	0.0042338
feb_2009_CNES-apr_2003_CNES.grd:	0.004272	7.72E-05	0.004273
mar_2009_CNES-apr_2003_CNES.grd:	0.002909	4.98E-05	0.0029097
apr_2009_CNES-apr_2003_CNES.grd:	0.00234	7.39E-05	0.0023407
may_2009_CNES-apr_2003_CNES.grd:	0.002594	0.000132321	0.0025968
jun_2009_CNES-apr_2003_CNES.grd:	0.00177	0.000154408	0.0017756
jul_2009_CNES-apr_2003_CNES.grd:	0.004232	0.000252147	0.004238
aug_2009_CNES-apr_2003_CNES.grd:	0.005147	0.000305582	0.0051549
sep_2009_CNES-apr_2003_CNES.grd:	0.004954	0.000265813	0.00496
oct_2009_CNES-apr_2003_CNES.grd:	0.005473	0.000377564	0.0054837
nov_2009_CNES-apr_2003_CNES.grd:	0.003062	0.000198403	0.0030673
dec_2009_CNES-apr_2003_CNES.grd:	0.004374	7.39E-05	0.0043747
jan_2010_CNES-apr_2003_CNES.grd:	0.002757	2.49E-05	0.0027568
feb_2010_CNES-apr_2003_CNES.grd:	0.002716	3.34E-05	0.0027162
mar_2010_CNES-apr_2003_CNES.grd:	0.002126	2.49E-05	0.0021262
apr_2010_CNES-apr_2003_CNES.grd:	0.00116	5.46E-05	0.0011607
may_2010_CNES-apr_2003_CNES.grd:	0.00179	0.000175487	0.0017975
jun_2010_CNES-apr_2003_CNES.grd:	0.003123	0.000257266	0.0031318
jul_2010_CNES-apr_2003_CNES.grd:	0.003957	0.000292502	0.0039661
aug_2010_CNES-apr_2003_CNES.grd:	0.005656	0.00033356	0.0056641
sep_2010_CNES-apr_2003_CNES.grd:	0.00649	0.000383438	0.0064995
oct_2010_CNES-apr_2003_CNES.grd:	0.00588	0.000357286	0.0058888
nov_2010_CNES-apr_2003_CNES.grd:	0.00473	0.00025823	0.0047361
dec_2010_CNES-apr_2003_CNES.grd:	0.00414	0.000141394	0.0041422
dec_2010_CNES-apr_2003_CNES.grd:	0.00414	0.000141394	0.0041422
feb_2011_CNES-apr_2003_CNES.grd:	0.001912	3.15E-05	0.0019127
mar_2011_CNES-apr_2003_CNES.grd:	0.00178	4.59E-05	0.0017807
apr_2011_CNES-apr_2003_CNES.grd:	0.001943	8.11E-05	0.0019444
may_2011_CNES-apr_2003_CNES.grd:	0.002055	6.30E-05	0.0020557
jun_2011_CNES-apr_2003_CNES.grd:	0.001994	0.000175487	0.0020002
jul_2011_CNES-apr_2003_CNES.grd:	0.004211	0.000288871	0.0042197
aug_2011_CNES-apr_2003_CNES.grd:	0.005737	0.000376246	0.0057476
sep_2011_CNES-apr_2003_CNES.grd:	0.006256	0.000451413	0.0062697
oct_2011_CNES-apr_2003_CNES.grd:	0.005961	0.000394925	0.005972
nov_2011_CNES-apr_2003_CNES.grd:	0.004638671875	0.000399302	4.653E+11
dec_2011_CNES-apr_2003_CNES.grd:	0.002675	0.000161099	0.0026794
jan_2012_CNES-apr_2003_CNES.grd:	0.002736	9.78E-05	0.0027379
feb_2012_CNES-apr_2003_CNES.grd:	0.002909	3.15E-05	0.0029095

mar_2012_CNES-apr_2003_CNES.grd:	0.002452	4.59E-05	0.0024519
apr_2012_CNES-apr_2003_CNES.grd:	0.001526	6.69E-05	0.0015271
may_2012_CNES-apr_2003_CNES.grd:	0.001628	9.19E-05	0.0016298
jun_2012_CNES-apr_2003_CNES.grd:	0.00176	0.000161099	0.001766
jul_2012_CNES-apr_2003_CNES.grd:	0.003743	0.000246167	0.0037502
aug_2012_CNES-apr_2003_CNES.grd:	0.006215	0.000384893	0.0062253
sep_2012_CNES-apr_2003_CNES.grd:	0.007202	0.000475918	0.0072152
sep_2012_CNES-apr_2003_CNES.grd:	0.007202	0.000475918	0.0072152
nov_2012_CNES-apr_2003_CNES.grd:	0.004913	0.00031062	0.0049215
dec_2012_CNES-apr_2003_CNES.grd:	0.003916	0.000251408	0.0039231
jan_2013_CNES-apr_2003_CNES.grd:	0.003357	0.00015916	0.0033601
feb_2013_CNES-apr_2003_CNES.grd:	0.002736	7.14E-05	0.0027372
feb_2013_CNES-apr_2003_CNES.grd:	0.002736	7.14E-05	0.0027372
may_2013_CNES-apr_2003_CNES.grd:	0.001729	0.000137386	0.0017339
jun_2013_CNES-apr_2003_CNES.grd:	0.001892	0.000237959	0.0019045
jul_2013_CNES-apr_2003_CNES.grd:	0.003672	0.000341833	0.0036855
oct_2013_CNES-apr_2003_CNES.grd:	0.005981	0.000446851	0.0059953
nov_2013_CNES-apr_2003_CNES.grd:	0.005229	0.00033356	0.0052375
dec_2013_CNES-apr_2003_CNES.grd:	0.003703	0.000227283	0.0037086
jan_2014_CNES-apr_2003_CNES.grd:	0.003723	0.000144436	0.0037255
mar_2014_CNES-apr_2003_CNES.grd:	0.003215	3.15E-05	0.0032146
apr_2014_CNES-apr_2003_CNES.grd:	0.002207	7.14E-05	0.0022084
may_2014_CNES-apr_2003_CNES.grd:	0.002767	0.000195567	0.0027727
jun_2014_CNES-apr_2003_CNES.grd:	0.002584	0.000266512	0.0025953
aug_2014_CNES-apr_2003_CNES.grd:	0.006134	0.000406239	0.0061452
sep_2014_CNES-apr_2003_CNES.grd:	0.006978	0.000493844	0.0069929
oct_2014_CNES-apr_2003_CNES.grd:	0.007579	0.000550558	0.0075952
nov_2014_CNES-apr_2003_CNES.grd:	0.005107	0.000437868	0.0051222
jan_2015_CNES-apr_2003_CNES.grd:	0.003876	0.000132321	0.0038776
feb_2015_CNES-apr_2003_CNES.grd:	0.003428	7.14E-05	0.0034288
mar_2015_CNES-apr_2003_CNES.grd:	0.002431	7.14E-05	0.0024321
apr_2015_CNES-apr_2003_CNES.grd:	0.002136	7.72E-05	0.0021374
may_2015_CNES-apr_2003_CNES.grd:	0.002258	8.63E-05	0.0022597
jun_2015_CNES-apr_2003_CNES.grd:	0.002563	0.000345267	0.0025828
jul_2015_CNES-apr_2003_CNES.grd:	0.004527	0.000341833	0.0045375
aug_2015_CNES-apr_2003_CNES.grd:	0.005514	0.000357286	0.0055231
sep_2015_CNES-apr_2003_CNES.grd:	0.007131	0.000439142	0.0071422
sep_2015_CNES-apr_2003_CNES.grd:	0.007131	0.000439142	0.0071422
dec_2015_CNES-apr_2003_CNES.grd:	0.003581	0.000203043	0.0035855
jan_2016_CNES-apr_2003_CNES.grd:	0.003825	9.97E-05	0.003826
feb_2016_CNES-apr_2003_CNES.grd:	0.004150	8.60E-06	0.0041505
mar_2016_CNES-apr_2003_CNES.grd:	0.002207	2.49E-05	0.0022076
may_2016_CNES-apr_2003_CNES.grd:	0.002319	0.000228373	0.0023287